



Calhoun: The NPS Institutional Archive
DSpace Repository

Theses and Dissertations

1. Thesis and Dissertation Collection, all items

1993-12

Direct time resolution of sonoluminescence

Abel, Gary R.

Monterey, California. Naval Postgraduate School

<http://hdl.handle.net/10945/39652>

This publication is a work of the U.S. Government as defined in Title 17, United States Code, Section 101. Copyright protection is not available for this work in the United States.

Downloaded from NPS Archive: Calhoun



Calhoun is the Naval Postgraduate School's public access digital repository for research materials and institutional publications created by the NPS community. Calhoun is named for Professor of Mathematics Guy K. Calhoun, NPS's first appointed -- and published -- scholarly author.

Dudley Knox Library / Naval Postgraduate School
411 Dyer Road / 1 University Circle
Monterey, California USA 93943

<http://www.nps.edu/library>

2

NAVAL POSTGRADUATE SCHOOL
Monterey, California

AD-A276 157



DTIC
ELECTE
MAR 02 1994
S F D



THESIS

DIRECT TIME RESOLUTION OF SONOLUMINESCENCE

by

Gary R. Abel

December, 1993

Thesis Advisor:

X. K. Maruyama

Co-Advisor:

A. A. Atchley

Approved for public release; distribution is unlimited.

94-06804



01 023

REPORT DOCUMENTATION PAGE			Form Approved OMB No. 0704
Public reporting burden for this collection of information is estimated to average 1 hour per response, including the time for reviewing instruction, searching existing data sources, gathering and maintaining the data needed, and completing and reviewing the collection of information. Send comments regarding this burden estimate or any other aspect of this collection of information, including suggestions for reducing this burden, to Washington Headquarters Services, Directorate for Information Operations and Reports, 1215 Jefferson Davis Highway, Suite 1204, Arlington, VA 22202-4302, and to the Office of Management and Budget, Paperwork Reduction Project (0704-0188) Washington DC 20503.			
1. AGENCY USE ONLY (Leave blank)	2. REPORT DATE 01 December 1993.	3. REPORT TYPE AND DATES COVERED Master's Thesis	
4. TITLE AND SUBTITLE DIRECT TIME RESOLUTION OF SONOLUMINESCENCE		5. FUNDING NUMBERS	
6. AUTHOR(S) Gary R. Abel			
7. PERFORMING ORGANIZATION NAME(S) AND ADDRESS(ES) Naval Postgraduate School Monterey CA 93943-5000		8. PERFORMING ORGANIZATION REPORT NUMBER	
9. SPONSORING/MONITORING AGENCY NAME(S) AND ADDRESS(ES)		10. SPONSORING/MONITORING AGENCY REPORT NUMBER	
11. SUPPLEMENTARY NOTES The views expressed in this thesis are those of the author and do not reflect the official policy or position of the Department of Defense or the U.S. Government.			
12a. DISTRIBUTION/AVAILABILITY STATEMENT Approved for public release; distribution is unlimited.		12b. DISTRIBUTION CODE A	
13. ABSTRACT (maximum 200 words) Sonoluminescence is the synchronous emissions of pulses of light that are observed to originate from a gas bubble trapped at the pressure antinode of a resonant sound field in a liquid. The duration of the pulse has been directly measured by launching the light through an optical fiber into a streak camera equipped with a linear array CCD detector. Questions regarding dispersion in the fiber and the fundamental limitations imposed by it are addressed. The resulting direct measurements show that the duration of the emission is less than 8 picoseconds.			
14. SUBJECT TERMS Sonoluminescence		15. NUMBER OF PAGES 100	
		16. PRICE CODE	
17. SECURITY CLASSIFICATION OF REPORT Unclassified	18. SECURITY CLASSIFICATION OF THIS PAGE Unclassified	19. SECURITY CLASSIFICATION OF ABSTRACT Unclassified	20. LIMITATION OF ABSTRACT UL

NSN 7540-01-280-5500

Standard Form 298 (Rev. 2-89)

Prescribed by ANSI Std. Z39-18

Accession For	
NTIS GRA&I	<input checked="" type="checkbox"/>
DTIC TAB	<input type="checkbox"/>
Unannounced	<input type="checkbox"/>
Justification	
By	
Distribution	
Availability	
Dist	Availability
A-1	

Approved for public release: distribution is unlimited.

DIRECT TIME RESOLUTION OF SONOLUMINESCENCE

by

G. R. Abel

Lieutenant, United States Navy

B. S., Towson State University, 1984

Submitted in partial fulfillment of the
requirements for the degree of

MASTER OF SCIENCE IN PHYSICS

from the

NAVAL POSTGRADUATE SCHOOL

December 1993

Author:

Gary R. Abel

Approved by:

Xavier K. Maruyama, Thesis Advisor

Anthony A. Atchley, Thesis Co-Advisor

William B. Colson, Chairman,

Department of Physics

ABSTRACT

Sonoluminescence is the synchronous emissions of pulses of light that are observed to originate from a gas bubble trapped at the pressure antinode of a resonant sound field in a liquid. The duration of the pulse has been directly measured by launching the light through an optical fiber into a streak camera equipped with a linear array CCD detector. Questions regarding dispersion in the fiber and the fundamental limitations imposed by it are addressed. The resulting direct measurements show that the duration of the emission is less than 8 picoseconds.

Table of Contents

I. INTRODUCTION	1
A. HISTORY	1
B. OVERVIEW	1
II. THE EXPERIMENT	3
A. SETUP	3
B. CALIBRATION	7
1. 10 ns Sweep, 17.4 ps/pixel Speed Calibration	7
2. 2.3 ns Sweep, 4 ps/pixel Speed Calibration	7
C. MEASURING TECHNIQUES	8
III. DATA RESULTS AND CONCLUSIONS	11
A. 10 ns SWEEP, 17.4 ps/pixel SPEED	11
1. Procedure	11
2. Results and Conclusions	13
B. 2.3 ns SWEEP, 4 ps/pixel SPEED	15
1. Procedure	15
2. Verification	16
3. Results and Conclusions	17
IV. DISPERSION	20
A. CALCULATION	20
1. Modal Dispersion	20
2. Material Dispersion	22

B. DISPERSION MEASUREMENTS	23
1. Modal Dispersion	24
2. Material Dispersion	25
V. SYSTEM RESPONSE	31
A. CALCULATION	31
B. MEASUREMENT	32
C. DISPERSION CALCULATION	33
VI. INTENSITY CALCULATIONS	38
VII. CONCLUSIONS	42
APPENDIX A. 10 ns SWEEP, 17.4 ps/pixel SPEED DATA	
STREAK CAMERA IMAGES AND PLOTS	44
APPENDIX B. 2.3 ns SWEEP, 4 ps/pixel SPEED DATA	
STREAK CAMERA IMAGES AND PLOTS	55
APPENDIX C. STREAK CAMERA IMAGES AND PLOTS OF	
ALL DATA USED PRIOR TO ANALYSIS	68
APPENDIX D. DATA SHEETS FOR EQUIPMENT	84
LIST OF REFERENCES	88
INITIAL DISTRIBUTION LIST	90

ACKNOWLEDGEMENT

The work done here was a follow on to a previous study of the sonoluminescence spectrum in an effort to answer new questions that arose. Discussions and new ideas from the numerous people involved helped out tremendously and hopefully all names can be accredited here.

It started when I was introduced to the thesis work of Joe Carlson on the *Visible Spectrum of Stable Sonoluminescence*. Most of Joe's work was done at Lawrence Livermore National Lab (LLNL) in Livermore, California so we went on a tour of the facility and this is when I learned of the need to time resolve the sonoluminescence.

Professor Xavier K. Maruyama became my thesis advisor and we decided that my research would also have to be done at LLNL. I would like to thank Dr. Michael J. Moran who graciously arranged for me to use the lab facilities. Ronald E. Haigh provided a work space, equipment, and encouragement. Others at the Electro Optics Calibration Facility such as Philip M. Armatis and Thomas R. Crabtree also provided assistance. Also Henry E. Garrett who helped with the fiber optics.

Finally, special thanks to Daren R. Sweider and John E. Flatley, both of whom I worked with on a daily basis, and provided assistance, insights, and expertise in the setup, operation, and analysis. Our many discussions always provided new ideas and enlightenment.

DISCLAIMER

The specific experiment equipment described in this work in no way constitutes an endorsement of these products.

I. INTRODUCTION

A. HISTORY

Sonoluminescence (SL) is the phenomenon of light emission from acoustically driven gas bubbles. It was first discovered in 1933 when darkening of photographic plates immersed in ultrasonically irradiated water was observed [Ref. 1]. In 1939 it was discovered that the light intensity increased with decreasing temperature and also with increasing water pressure. It was also determined that the SL was strictly related to the acoustic field since SL was not observed in cavitation caused by boiling or flow [Ref. 2].

In 1990, SL emission from a single bubble levitated at the pressure antinode of an acoustic standing wave was observed by Felipe Gaitan [Ref. 3]. In 1991 Bradley P. Barber *et al* attempted to resolve the time characteristics of single bubble SL. Using the fastest available photomultiplier tube, they measured the rise and fall time caused by a 34 ps laser pulser and SL. Comparison of the two signals led to the conclusion that the width of the SL flashes is conservatively less than 50 ps [Ref. 4].

B. OVERVIEW

This work is a measurement of the duration of a single SL event giving a more direct time resolution than has ever been achieved. The duration is measured with a streak camera.

Chapter II describes the experiment setup and calibration procedure for both 10 ns and 2.3 ns streak camera sweeps. It also describes the measuring techniques used. Chapter III provides the results and conclusions for the 10 ns streak camera sweep and results, verification, and conclusions for the 2.3 ns streak camera sweep. Chapter IV discusses dispersion and calculates the material and modal dispersion

caused by the optical fiber used in the measurements. It also includes dispersion measurements. Chapter V contains system response calculations and measurements. Chapter VI gives intensity calculations to determine the number of photons being emitted by and the peak power of the SL. Chapter VII gives final conclusions. Appendix A presents 10 ns sweep streak camera images and intensity plots. Appendix B presents 2.3 ns streak camera images and intensity plots. Appendix C presents blown up images and intensity plots of all the data used prior to computer analysis. Appendix D provides all available data sheets for the equipment used.

II. THE EXPERIMENT

A. SETUP

Figure 2 is a schematic of the experimental setup [Ref 5]. A function generator produces a sine wave signal that goes to an amplifier. This amplified signal is used as the driver for the acoustic field. The amplifier signal is fed through a coaxial cable to a junction box where it is split into four separate leads to individual hollow, cylindrical piezoelectric transducers which transfer acoustic energy to the water in the flask. The transducers are epoxied to a 150 ml spherical flask and arranged in a tetrahedral configuration. The flask is filled with an 80 % distilled water and 20 % glycerine mixture solution that has been degassed. The flask is probed with a miniature hydrophone to find its resonance frequency. A nominal resonance frequency of 31690 Hz produced a radially symmetric standing sound wave. A small amount of air is injected into the flask using a hypodermic needle. This injected air evolves into a single bubble which becomes trapped at the pressure antinode, centered in the flask. With proper adjustment of the driving amplitude, the levitated bubble emits SL.

The entire flask is enclosed in an insulated "chill box" which is cooled to an inside temperature of approximately 12° C as measured with a digital Fluke thermocouple thermometer. The cooling is done to increase the intensity of the SL. It is observed that cooling the solution improves the stability of the bubble. At room temperature, the bubble has a tendency to jitter around the antinode location. At cooler temperatures, it is observed that the jitter decreases substantially. A photomultiplier tube (PMT), also enclosed in the chill box, is used to detect the SL. The PMT high voltage is supplied by a Power Designs (model 3K10B) High Voltage

Supply set at 2500 V. The PMT output signal is amplified using a Sonoma Instrument 310 Amplifier with a bandwidth of 10 kHz - 1 GHz and 32 dB gain. The signal then goes to the events input of a Tektronix 501 Digital Delay (DD) before being used as the external trigger input of a Stanford Digital Delay/Pulse Generator (PG). One output of the PG is used to trigger an EG&G L-CA-24 Streak Camera with a Microchannel Plate Intensifier (MCPI) attached. The MCPI is triggered by a second output from the PG. The SL is launched into the streak camera through an optical fiber that is lowered into the flask to within a few hundred microns of the SL bubble. The output of the MCPI is focused with a Tinsley 2.5:1 lens into a Photometrics LTD Series 200 Charged Coupled Device (CCD) which interfaces with an Apple Macintosh computer using the OMA V.1.2c program [Ref. 6]. The trigger for the CCD is connected to the start output of the DD. This configuration enables all the equipment to be phase locked to the SL event. The PMT signal and the signal for the streak camera are simultaneously monitored on a Tektronix 7104 1-GHz Oscilloscope. A video monitor is also connected to the CCD output so data can be viewed as it is taken without having to wait for analysis. The CCD is 576 by 576 pixels which are all displayed on the monitor.

The streak camera works by taking a light source input through a slit onto a photocathode plate which converts the photon beam into an electron beam. This conversion occurs at the front of the streak camera where a cathode is located. There is an anode at the rear. A high voltage potential between the cathode and anode accelerates the electron beam towards the rear of the camera where it strikes a phosphorous plate which changes the electron beam into a monochromatic photon beam. The attached MCPI amplifies the new photon beam which is then directed into the CCD and captured by the computer. In the non-streaked mode, the electron beam travels straight through the camera and strikes the phosphorous plate in one spot. In the streaked mode, the electron beam is deflected from one side of the camera to the other side. The deflection is caused by a cathode/anode pair on opposite sides of the

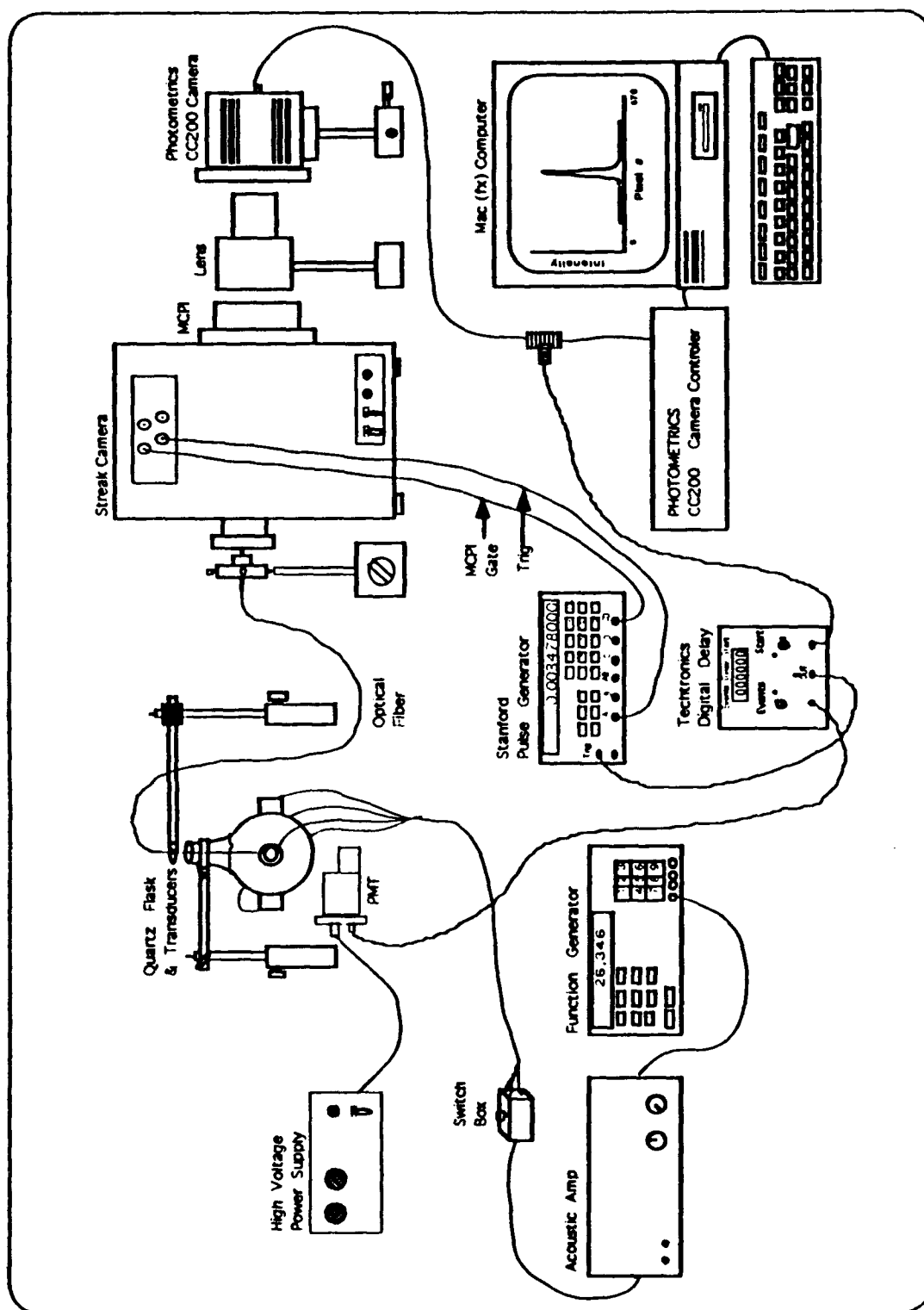


Figure 1 Schematic of Streak Camera Setup

camera and is controlled by a ramp charge. The ramp creates a high voltage potential across the electrodes and deflects the electron beam all the way to one side so that the beam strikes the edge of the phosphorous plate. When the camera is triggered, the potential across the electrodes is reversed deflecting the electron beam to the other side of the camera causing it to create a streak across the phosphorous plate. The rate at which this potential is reversed gives the time duration of the entire sweep. The speed resolution of the sweep is calculated by taking the duration of the sweep and dividing by the number of pixels in the sweep. This speed resolution allows for calculating the duration of the SL. The duration of the initial light signal is found from measuring the length of the streak created by the source and multiplying by the speed of the sweep.

The entire system is triggered by the SL event and sends a signal through the DD, which has been armed to start by the computer, to the PG. A delay has been set to trigger the streak camera and MCPI to record the next SL event. Figure 2 shows how the triggers are set with respect to each other and the SL event. The figure is not to scale. Note that the SL event measured occurs after the SL event which triggered the system.

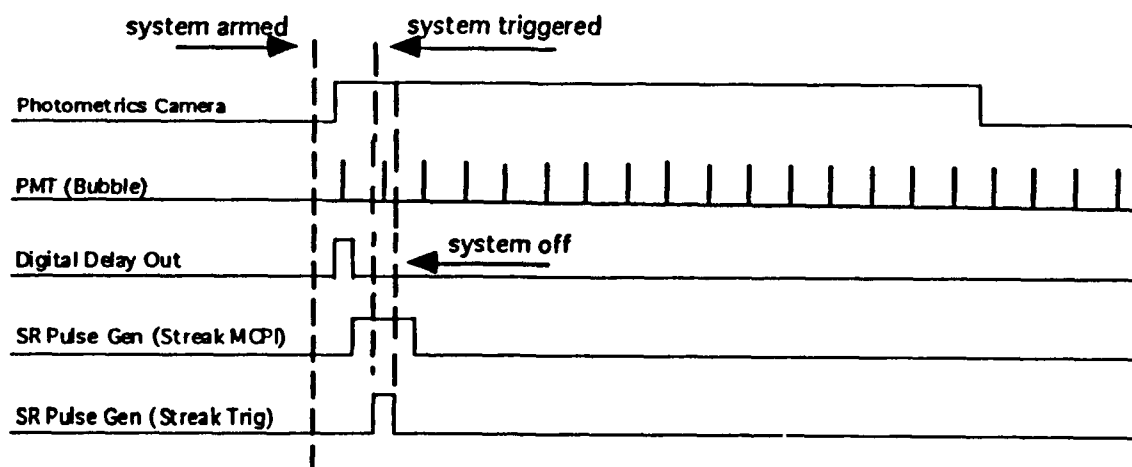


Figure 2 System Timing Showing Relative Position and Duration of All Signals

B. CALIBRATION

1. 10 ns Sweep, 17.4 ps/pixel Speed Calibration

The ramp speed of the streak camera is set at 10 ns. This means that the streak will cover the entire 576 pixels in 10 ns. Verification is done using a pulsed laser source called a "comb."

A 3 GHz comb is used. This gives a burst of photons, referred to as a cycle, every 0.33 ns. The result is

$$3 \times 10^9 \frac{\text{cycles}}{\text{sec}} (10 \times 10^{-9} \text{ sec}) = 30 \text{ cycles}$$

or 30 peaks on the screen during the 10 ns sweep. Figure 3 is the 3 GHz comb streak camera image and associated intensity plot. Time starts at the left and advances to the right. The entire streak is 10 ns long and dividing by the number of pixels in the streak gives a speed of

$$10 \times 10^{-9} \text{ sec} (576 \text{ pixels})^{-1} = 17.4 \times 10^{-12} \frac{\text{sec}}{\text{pixel}} = 17.4 \frac{\text{ps}}{\text{pixel}}$$

2. 2.3 ns Sweep, 4 ps/pixel Speed Calibration

The ramp speed of the streak camera is set at 2.3 ns which is its fastest setting. Verification is done using a 6 GHz comb. This gives a pulse of photons every 0.16 ns. The result is

$$6 \times 10^9 \frac{\text{cycles}}{\text{sec}} (2.3 \times 10^{-9} \text{ sec}) = 13.8 \text{ cycles}$$

or 13.8 peaks on the screen during the 2.3 ns sweep. Figure 4 is the 6 GHz comb streak camera image and associated intensity plot. Again time starts at the left and advances to the right. The entire streak is 2.3 ns long and dividing by the number of pixels in the streak gives a speed of $4 \frac{\text{ps}}{\text{pixel}}$.

C. MEASURING TECHNIQUES

The streak camera is first run in the non-streaked mode in order to locate the SL event on the sweep image. Once the SL event is located, the computer is used to construct a rectangular box on the digital image with the SL event centered in it. The length of the box matches the sweep length and the width is on the order of 30 pixels which will give a little extra room on both top and bottom of the SL event display. The box is constructed in order to eliminate the extra video display where the SL event cannot be located. The optical fiber is in a fixed position at the entrance slit of the streak camera and since the beam is not deflected vertically, the SL event display will occur at the same vertical position throughout the sweep and only the horizontal position will change. The camera is then switched to the streak mode and data is taken. Due to the electronic nature of the CCD, there is a background signal and scintillation signals also occur. The background signal is due to "dark current" in the camera circuitry and generally has a level of approximately 300 counts/pixel for every data run. The entire chill box and streak camera are covered to isolate them from any external light. Scintillations are false signals due to "thermal blooming" and generally give a few counts above background and are confined to one or two pixels. A signal is determined to be an SL event by the vertical position in the box, by the intensity of the signal display, and by the horizontal position in the box which corresponds to the signal position on the oscilloscope. The position of the SL in the streak camera signal corresponds to its position on the sweep. Any signal not meeting these criteria is determined to be a scintillation.

Using the OMA V.1.2c program, a smaller rectangle is constructed to just enclose the SL event vertically and includes almost the entire original box horizontally. The data in this new rectangle is integrated vertically to change the 2-D image into a 1-D intensity plot which is made using the Kaleidegraph program [Ref. 7]. This method eliminates any scintillations that are outside the chosen vertical position from skewing the data. Each plot is background subtracted and normalized.

Sonoluminescence - Streak Camera Image and Plot

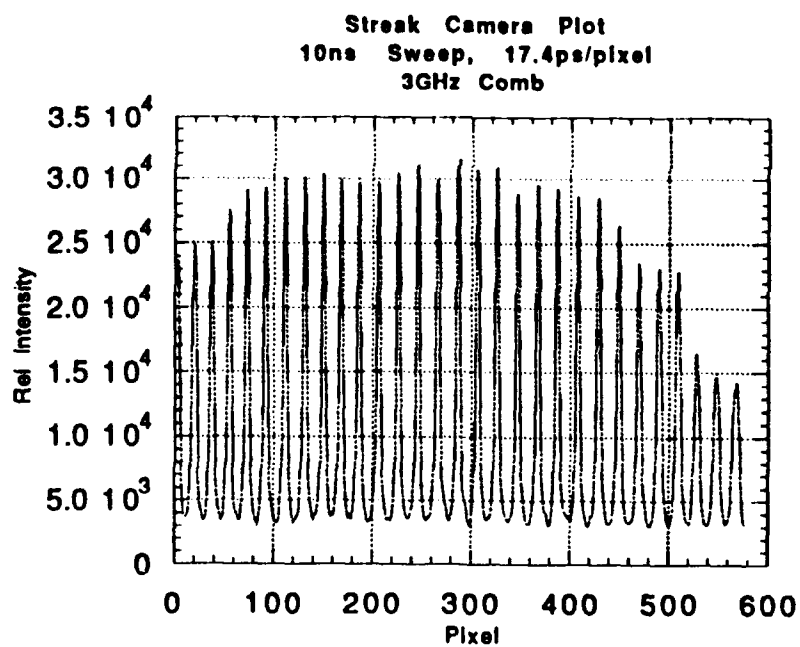
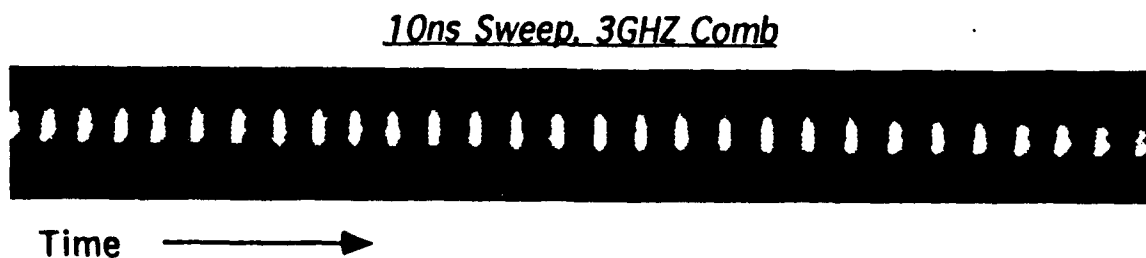


Figure 3 3 GHz Comb Streak Camera Image and Intensity Plot, File #3GHz

Sonoluminescence - Streak Camera Image and Plot

2.3ns Seep. 6GHz Comb



Time →

Streak Camera Plot
2.3ns Sweep, 4ps/pixel Speed
6GHz Comb

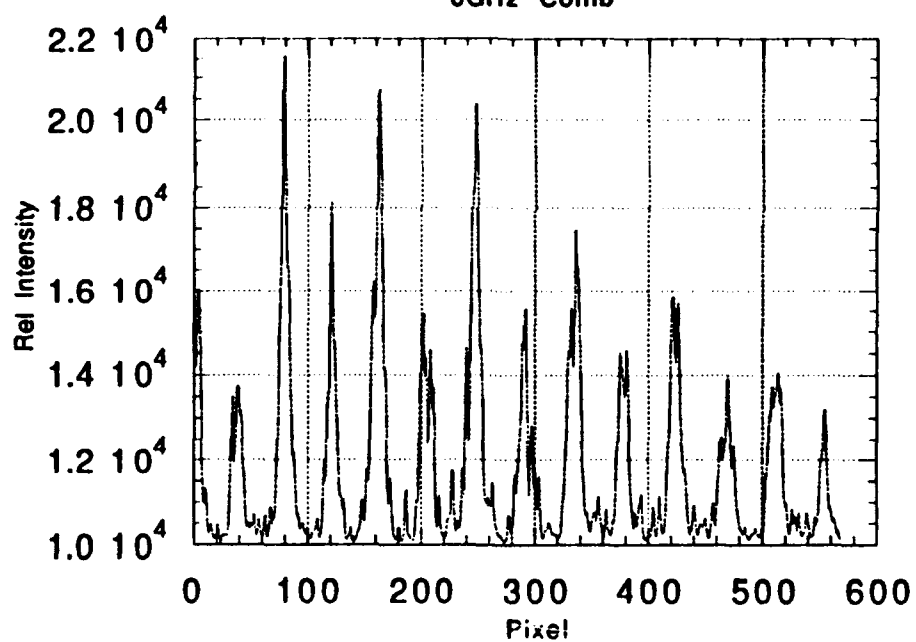


Figure 4 6 GHz Comb Streak Camera Image and Intensity Plot, File #6GHz

III. DATA RESULTS AND CONCLUSIONS

A. 10 ns SWEEP, 17.4 ps/pixel SPEED

1. Procedure

A driving frequency of 31690 Hz is used to generate the SL. This frequency gives a calculated SL event cycle time of 31.556 μ s. Next a 3M FP-1.0-UHT 1000 micron core optic fiber, 30.48 cm in length, is lowered into the flask to within approximately 500 microns of the SL bubble. The distance between the fiber and the SL bubble is visually estimated by comparison with the fiber core diameter. Calculations for placing the SL event signal in the middle of the MCPI gate signal gives a delay of 31.306 μ s for the streak camera to activate after the system arming. The MCPI has a set trigger that will activate 10 μ s prior to the streak camera trigger and the MCPI will stay active for 1 ms.

Following the measurement techniques previously given, data is taken adjusting the streak camera trigger delay from 31.2863 to 31.3130 μ s. Monitoring of the signals on the oscilloscope allows the streak camera delay to be changed to vary the position of the SL event signal within the MCPI gate signal in order to ensure that none of the SL has been cut out of the measurement. A shorter delay gives a SL event display late in the sweep and a longer delay gives a SL event display early in the sweep. The SL event can be seen as it moves across the sweep as the delay is changed. Jitter in the system is approximately less than 100 ps. Table I gives the streak camera settings.

TABLE I
STREAK CAMERA SETTINGS FOR 10 ns SWEEP

SETTING	READOUT	SETTING	READOUT
S-TUBE	- 1.8279	+15V	1.4849
GATE	0.8045	+5V	0.4912
MCPI OUT	0.7947	-15V	- 1.4790
+ RAMP	- 2.4752	-5V	- 0.4905
- RAMP	2.4932	+28V	2.8056

Once all the data has been stored in memory, it is analyzed and an individual intensity plot of each measurement is constructed. The full width half maximum (FWHM) of the plot is measured to give the duration of the event. Table II gives the results after analysis. Figure 5 shows the streak camera image, the intensity plot of the display, and a blown up intensity plot of the pulse to show the FWHM that most closely resembles the average of the data. Appendix A gives streak camera images and intensity plots for all the data used in Table II. All streak camera images are a section of the entire sweep that is centered as much as possible around the SL event display. Time starts at the top and advances downward meaning that the top of the image is the earlier portion and the bottom is the later portion in time of the sweep. Note: Some additional data was taken but not presented due to scintillations from the MCPI that do not make the SL event display clear.

2. Results and Conclusions

The average of the data gives a streak length of 2.3 pixels with an averaged SL event duration of 40.0 ps. This is less than the duration previously reported [Ref. 4]. The resolution of the CCD is 2 pixels so further time resolution is equipment limited. This is when it was decided that the SL event duration is possibly shorter than the 40.0 ps measured and that the measurements had met the limitations of the equipment. Better time resolution of the SL event requires an increased ramp speed.

TABLE II
DATA ANALYSIS FOR 10 ns SWEEP

FILE #	FIGURE #	FWHM (pixels)
10s2	A-1	2.3
10s3	A-2	2.2
10s5	A-3	2.3
1s2	A-4	2.3
5s1	A-5	2.1
6s1	A-6	2.8
7s4	A-7	2.4
9s1	A-8	2.2
9s4	A-9	2.2
9s5	A-10	2.2
AVERAGE		2.3

Sonoluminescence - Streak Camera Image and Plots

10ns Sweep

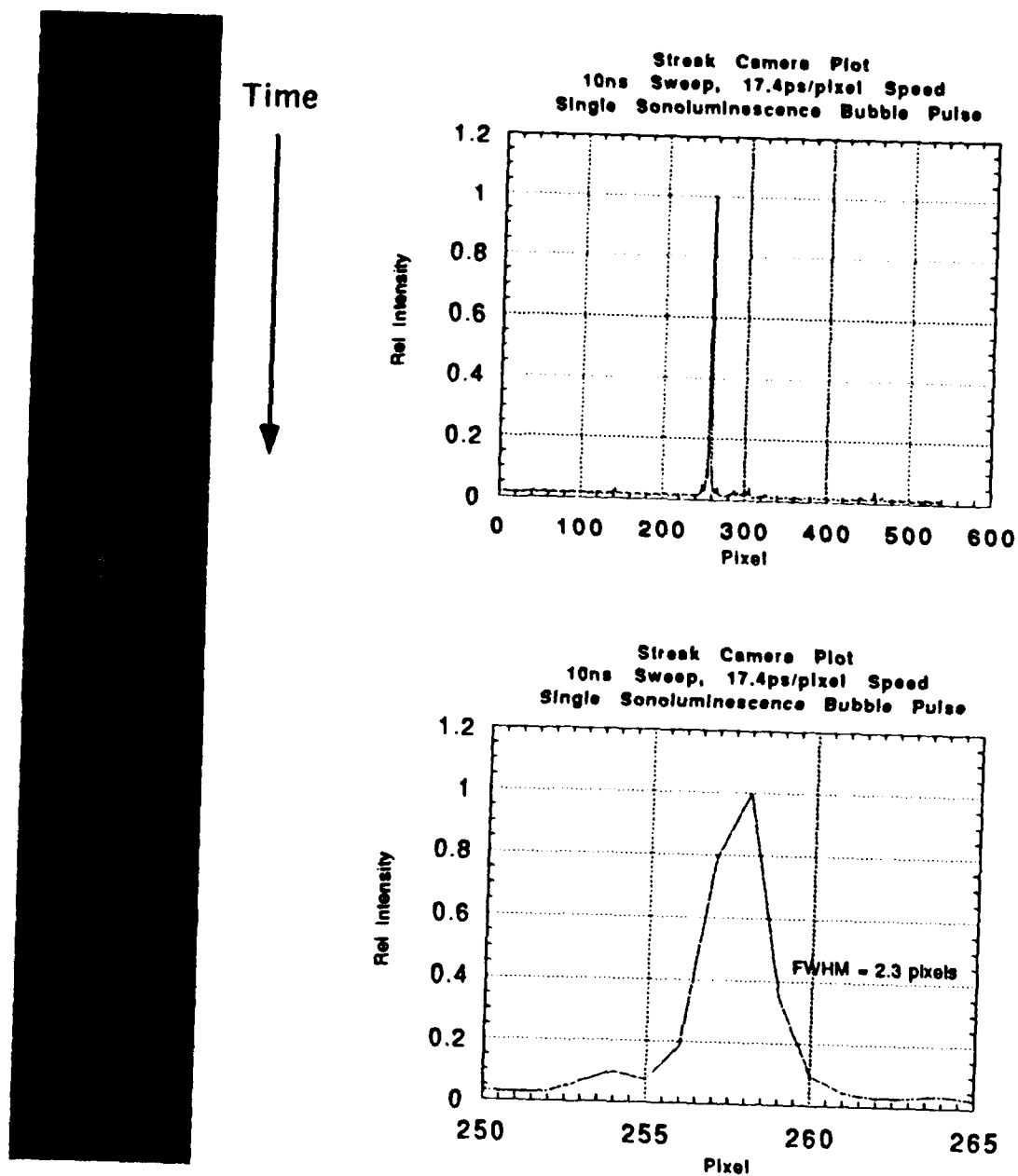


Figure 5 Single Sonoluminescence Event Streak Camera Image and Intensity Plots, File #10s2

B. 2.3 ns SWEEP, 4 ps/pixel SPEED

1. Procedure

The streak camera ramp speed is increased to 2.3 ns which is the fastest it will go. Speed calibration and verification is done as previously discussed. A driving frequency of 31700 Hz is used to generate the SL which gives an event cycle time of 31.545 μ s. Next a 3M FP-1.0-UHT 600 micron core optic fiber, 43.18 cm in length, is lowered into the flask to within approximately 300 microns of the SL bubble. Again the distance between the fiber and the SL bubble is visually estimated by comparison with the fiber core diameter. A smaller core fiber is used to allow the fiber to be placed closer to the SL bubble. Calculations for placing the SL event signal in the middle of the MCPI gate signal gives a delay of 31.295 μ s for the streak camera to activate after the system arming.

Following the measurement techniques previously given, data is taken adjusting the streak camera trigger delay from 31.2863 to 31.3030 μ s. The same SL event display movement is seen to occur as in the previous data set. Jitter in the system is approximately less than 100 ps. Table III gives the streak camera settings.

Once all the data has been stored in memory, it is analyzed and an individual intensity plot of each measurement is constructed. Table IV gives the results of the data analysis. Figure 6 shows the the streak camera image, the intensity plot of the display, and a blown up intensity plot of the pulse to show the FWHM that most closely resembles the average of the data. Appendix B gives streak camera images and intensity plots for all the data used in Table IV. All streak camera images are a section of the entire sweep that is centered as much as possible around the SL event display. As before, time starts at the top and advances downward. Note: Some additional data was taken but not presented due to scintillations from the MCPI that do not make the SL event display clear.

TABLE III
STREAK CAMERA SETTINGS FOR 2.3 ns SWEEP

SETTING	READOUT	SETTING	READOUT
S-TUBE	- 1.8265	+15V	1.4855
GATE	0.8061	+5V	0.4918
MCPI OUT	0.7950	-15V	- 1.4796
+ RAMP	- 2.4764	-5V	- 0.4913
- RAMP	2.4462	+28V	2.8171

2. Verification

Streak camera speed and CCD resolution is verified using a source of known duration under the same conditions. A model PLK-820 picosecond laser pulser with a known FWHM of 13 ps as measured by an autocontroller is used. The pulser, launched through the same fiber, gives a streak length of 3.6 pixels at FWHM which corresponds to 14.4 ps which is in agreement with the calibration data. The size of the fiber attached to the pulser is 50 microns and coupling between the two fibers is poor, thus making the pulser essentially a point source. Figure 7 is the streak camera image and associated intensity plot of the pulser. The streak camera image is a section of the entire sweep that is centered as much as possible around the SL event display.

3. Results and Conclusions

The averaged data gives a streak length of 2.05 pixels with an averaged SL event duration of 8.13 ps. The data are consistent throughout but since the CCD resolution is 2 pixels, the measurement is equipment limited and establishes an upper limit for the SL duration. This upper limit measurement implies a shorter SL duration than previously reported elsewhere.

TABLE IV
DATA ANALYSIS FOR 2.3 ns SWEEP

FILE #	FIGURE #	FWHM (pixels)	FWHM (ps)
95s1	B-1	2.3	9.2
96s1	B-2	2.2	8.8
96s2	B-3	2.5	10.0
97s1	B-4	1.4	5.6
97s2	B-5	2.1	8.4
97s3	B-6	2.4	8.8
98s1	B-7	1.8	7.2
98s2	B-8	2.0	8.0
98s3	B-9	1.9	7.6
99s1	B-10	1.8	7.2
99s3	B-11	1.9	7.6
99s4	B-12	2.3	9.2
AVERAGE		2.05	8.13

Sonoluminescence - Streak Camera Image and Plots

2.3ns Sweep

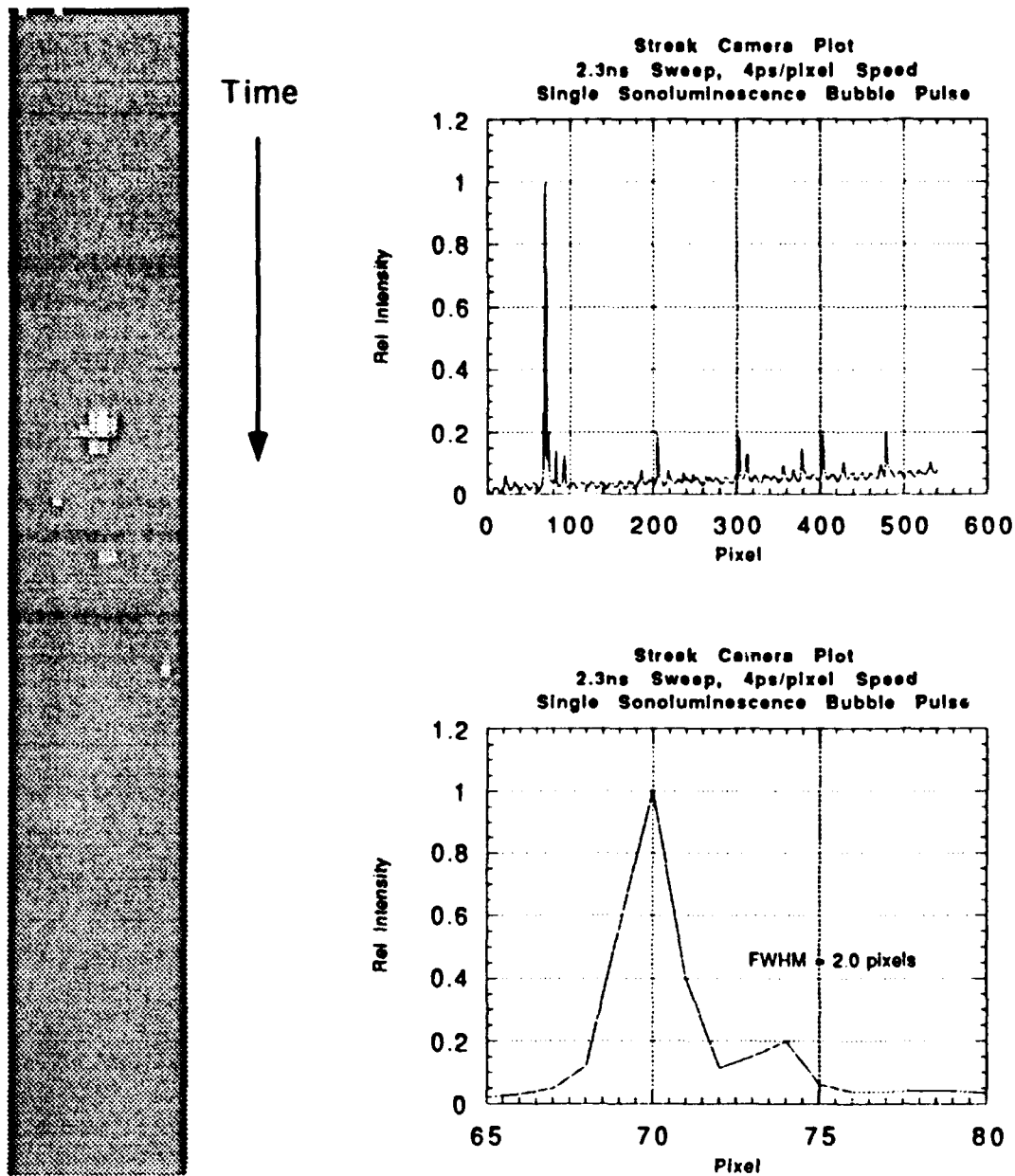


Figure 6 Single Sonoluminescence Event Streak Camera Image
and Intensity Plots, File #98s2

Sonoluminescence - Streak Camera Image and Plots

2.3ns Sweep

13ps Pulser



Time

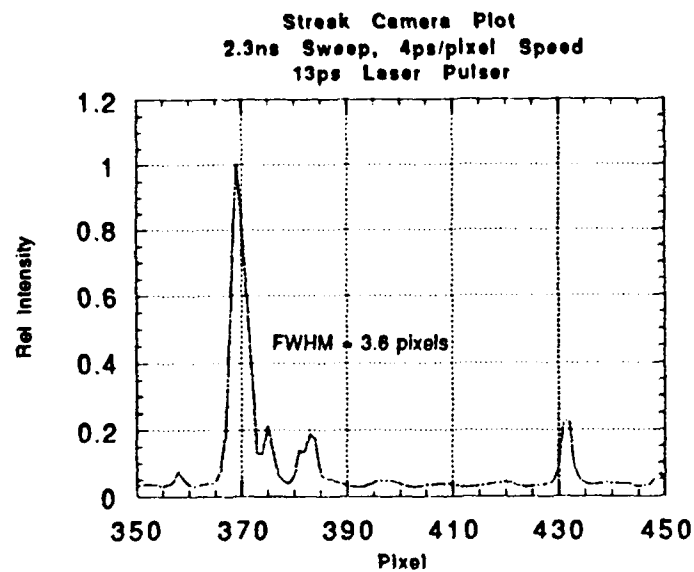
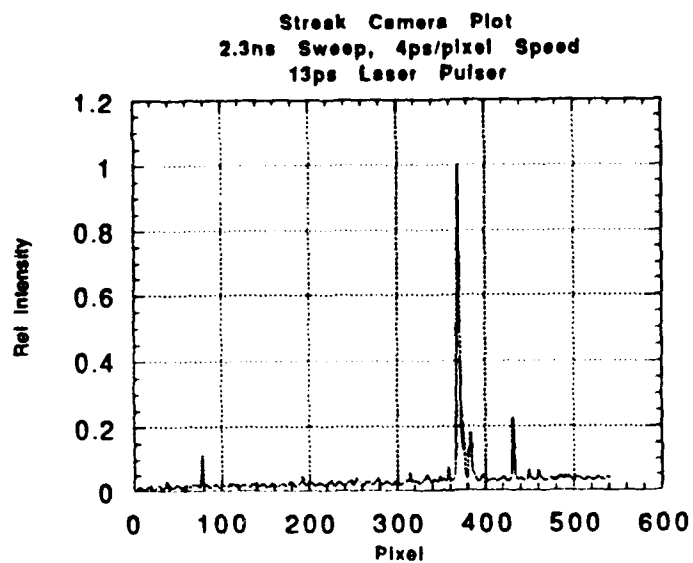


Figure 7 13 ps Laser Pulser Streak Camera Image and Intensity Plots, File #p8

IV. DISPERSION

A. CALCULATION

There are two type of dispersion, modal and material. In an optical fiber, modal dispersion will cause broadening of a monochromatic pulse due to different transmission paths, or "modes", through the fiber. The different modes give different transmission times due to different path lengths. Material dispersion causes the lower wavelengths (higher frequencies) to travel slower than the longer wavelengths (lower frequencies). This means that if the entire SL spectrum is emitted at the same time, the red portion (longer wavelength) of the spectrum travels faster and arrives before the blue portion (shorter wavelength) of the spectrum.

1. Modal Dispersion

Modal dispersion is due to the type of fiber used, either multi-mode or single mode, and is dependent on the difference in the index of refraction between the fiber core and the cladding. The numerical aperture (NA) of the fiber is dependent on the index of refraction for the fiber cladding. A larger NA will allow more modes or paths for the incident light to travel through the fiber. The shortest mode is the path that travels straight through the fiber and the longest mode is the path that enters the fiber at the largest allowable angle and is reflected the most as it travels through the fiber. Modal dispersion will cause a broadening of a monochromatic signal from a light source. The equation for maximum modal dispersion is

$$\Delta t = \frac{Ln_f}{c} \left[\frac{n_f}{n_c} - 1 \right]$$

where Δt is the time delay for the different modes, L is the length of the fiber, c is the speed of light in vacuum, n_f is the index of refraction for the fiber core, and n_c is the

index of refraction for the fiber cladding [Ref. 8]. The fiber used in the experiment is multi-mode with a silica core and a silicone resin cladding. The index of refraction for the fiber core is $n_f = 1.475$ at $\lambda = 365 \text{ nm}$. The index of refraction for the cladding is given by

$$n_c = \left[n_f^2 - NA^2 \right]^{\frac{1}{2}} \quad [\text{Ref. 8}].$$

Using $NA = 0.40$ [Ref. 10] gives $n_c = 1.420$. Substituting these values in the modal dispersion equation and using $L = 0.4318 \text{ m}$ gives for a wavelength of 365 nm a maximum delay time of

$$\Delta t = \frac{0.4318 (1.475)}{2.998 \times 10^8} \left[\frac{1.475}{1.420} - 1 \right] = 82.3 \times 10^{-12} \text{ sec} = 82.3 \text{ ps} .$$

The index of refraction for the fiber core is $n_f = 1.455$ at $\lambda = 707 \text{ nm}$. Using $NA = 0.40$ gives $n_c = 1.399$. Substituting these values in the modal dispersion equation and using $L = 0.4318 \text{ m}$ gives for a wavelength of 707 nm a maximum delay time of

$$\Delta t = \frac{0.4318 (1.455)}{2.998 \times 10^8} \left[\frac{1.455}{1.399} - 1 \right] = 83.9 \times 10^{-12} \text{ sec} = 83.9 \text{ ps} .$$

Thus when the incident light is launched into all modes of the fiber, there will be a maximum average delay of 83.1 ps between the lowest and the highest modes of the fiber if the fiber is completely filled by the incident light. If the fiber is "underfilled" then not all the transmission modes of the fiber are excited. The maximum modal dispersion is less because the difference between transmission times of the lowest and highest modes is less. The time difference due to modal dispersion is greater than the measured duration of the SL event.

2. Material Dispersion

Material dispersion is due to the frequency dependence of the index of refraction of the fiber core. The equation for group velocity due to material dispersion is

$$v_g = \frac{c}{n} + \frac{\lambda c}{n^2} \frac{dn}{d\lambda}$$

where v_g is the group velocity, c is the speed of light in vacuum, n is the index of refraction at wavelength λ , and $\frac{dn}{d\lambda}$ is how the index of refraction changes with wavelength [Ref 11]. Material dispersion will cause a separation of pulses of different wavelength from a light source. Using the fiber characteristics, the following calculations are performed: The transmission time through the fiber is calculated for the lower end and the higher end of the streak camera response curve. At the lower end

$$\lambda_1 = 365 \text{ nm} \quad n_1 = 1.475 \quad [\text{Ref 12}]$$

$$\lambda_2 = 405 \text{ nm} \quad n_2 = 1.470$$

$$\frac{dn}{d\lambda} = \frac{(n_1 - n_2)}{(\lambda_1 - \lambda_2)} = \frac{(1.475 - 1.470)}{(365 \times 10^{-9} - 405 \times 10^{-9})} = - \frac{0.005}{40 \times 10^{-9}} = - 1.25 \times 10^5 \text{ m}^{-1}$$

The group velocity for the 365 nm wavelength is

$$v_{g1} = \frac{2.998 \times 10^8}{1.475} - \frac{365 \times 10^{-9} (2.998 \times 10^8)}{(1.475)^2} (1.25 \times 10^5) = 1.970 \times 10^8 \frac{\text{m}}{\text{s}}$$

Inverting gives

$$\frac{1}{v_{g1}} = 5.077 \times 10^{-9} \frac{\text{s}}{\text{m}}$$

For a 0.4318 m length of fiber, the transmission times are

$$t_1 = 5.077 \times 10^{-9} \frac{\text{s}}{\text{m}} (0.4318 \text{ m}) = 2.192 \times 10^{-9} \text{ s} = 2.192 \text{ ns}$$

$$t_2 = 2.193 \text{ ns}$$

The same calculations are performed for the higher end of the SL spectrum using

$$\lambda_3 = 707 \text{ nm} \quad n_3 = 1.455$$

$$\lambda_4 = 852 \text{ nm} \quad n_4 = 1.452$$

The corresponding $\frac{dn}{d\lambda} = -2.07 \times 10^4 \text{ m}^{-1}$ and the transmission times are

$$t_3 = 2.117 \text{ ns}$$

$$t_4 = 2.117 \text{ ns}$$

The difference in the transmission times due to material dispersion for the lower and higher ends of the SL spectrum (487 nm bandwidth) is

$$\Delta t = t_1 - t_4 = 2.192 \text{ ns} - 2.117 \text{ ns} = 0.075 \text{ ns} = 75 \text{ ps}$$

The time difference due to material dispersion has a length of 19 pixels which is greater than the SL measurement.

B. DISPERSION MEASUREMENTS

Fiber dispersion testing is done using a 100 fs pulse Tsunami laser with a wavelength of 760 nm which is at the high end of the response window for the streak camera, and a KDP crystal for frequency doubling. The crystal will produce a second pulse at double the frequency, half the wavelength, of the original pulse and will be at the low end of the response window. This gives two synchronous, coherent pulses of different known wavelength. The two pulses are then filtered to a lower intensity and focused into the fiber and the experiment is performed [Ref 12]. Figure 8 is a schematic of the fiber dispersion test layout [Ref 13].

During the test, the streak camera MCPI out setting was lower than the setting used for the SL measurements. A lower setting gives a broader sweep image and decreases the system resolution. The amount of dispersion will be different under the

same SL measurement conditions. Therefore the dispersion measurements are not under the same SL measurement conditions and are only used to determine the dispersion characteristics of the fiber.

Figure 9 shows the streak camera plot of the two pulses without going through the fiber [Ref 15]. The FWHM = 4 pixels = 16 ps and this is the new system resolution for the lower MCPI out setting.

1. Modal Dispersion

The laser is launched into the fiber with the lower wavelength blue pulse filtered out and the experiment is run. Figure 10 is the streak camera plot of the red pulse at 760 nm with and without the fiber present [Ref 16]. The FWHM = 15 pixels = 60 ps with the fiber present. The measured modal dispersion at a wavelength of 760 nm is

$$15 \text{ pixels} - 4 \text{ pixels} = 11 \text{ pixels} = 44 \text{ ps} .$$

The red pulse is filtered out and the experiment is run again on the blue pulse. Figure 11 is the streak camera plot of the blue pulse at 380 nm with and without the fiber present [Ref 17]. The FWHM = 10 pixels = 40 ps with the fiber present. The measured modal dispersion at a wavelength of 380 nm is

$$10 \text{ pixels} - 4 \text{ pixels} = 6 \text{ pixels} = 24 \text{ ps} .$$

The average measured modal dispersion is 9 pixels = 36 ps which is less than half the calculated value. This difference is probably due to the actual index of refraction of the cladding is different from that calculated. Due to the nature of the cladding, it is not possible to measure its index of refraction [Ref 18].

2. Material Dispersion

Both pulses are used and the experiment is run again. Figure 12 is the streak camera plot of both pulses through the fiber [Ref 19]. The difference in the peaks is

$$120.5 \text{ pixels} - 92.5 \text{ pixels} = 28 \text{ pixels} = 112 \text{ ps}$$

for the measured maximum material dispersion for a 380 nm bandwidth. Using previous calculations, the calculated maximum material dispersion for a 380 nm bandwidth is

$$\Delta t = t_1 - t_3 = 2.192 \text{ ns} - 2.117 \text{ ns} = 0.075 \text{ ns} = 75 \text{ ps} = 19 \text{ pixels}.$$

The difference in the delay is possibly due to the worst case scenario of one beam taking the shortest mode and the other beam taking the longest mode due to the launching conditions therefor the modal dispersion must be taken into account. Subtracting the total dispersion by the modal dispersion gives

$$28 \text{ pixels} - 9 \text{ pixels} = 19 \text{ pixels} = 76 \text{ ps}$$

for the measured material dispersion.

Fiber Dispersion - Test Layout

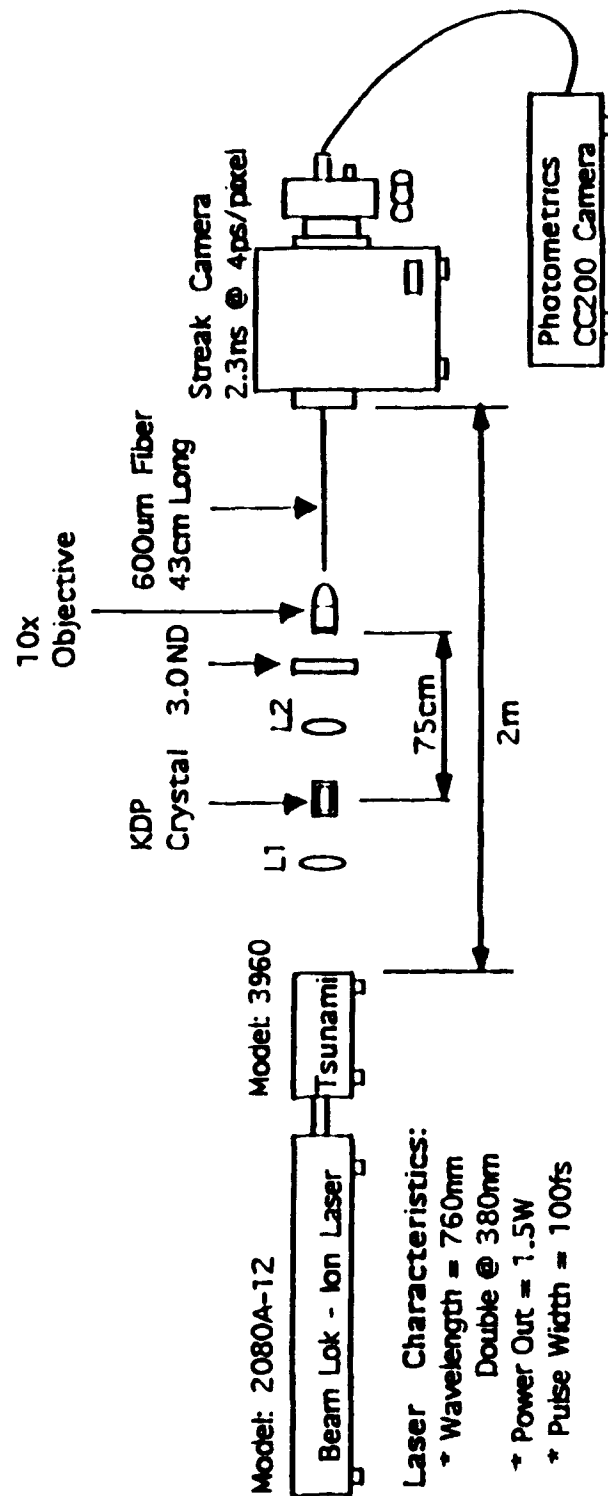


Figure 8 Schematic of Fiber Dispersion Test Layout

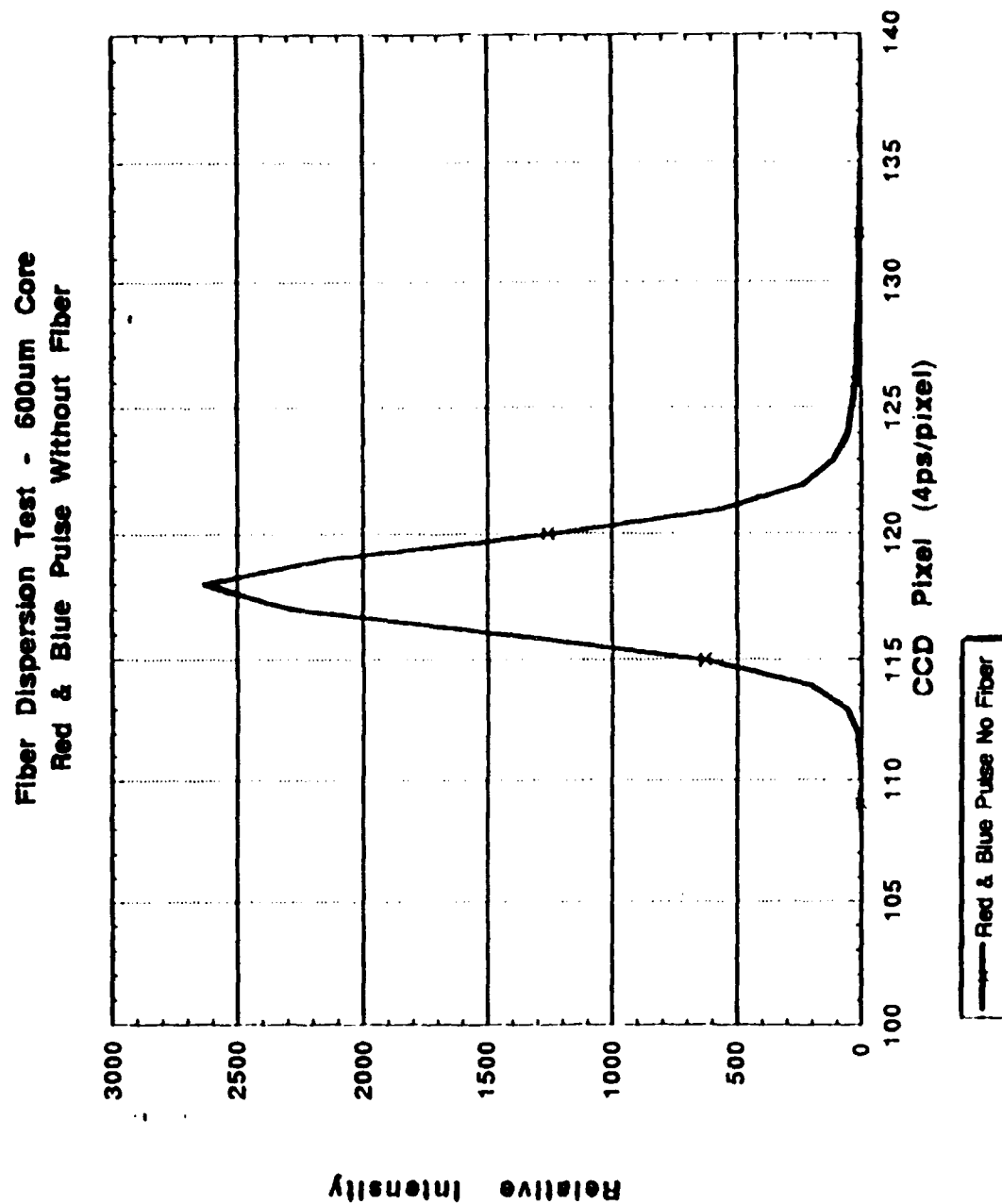


Figure 9 Intensity Plot of Red and Blue Pulse Without Fiber

Fiber Dispersion Test - 600um Core
Red Pulse @ 750nm

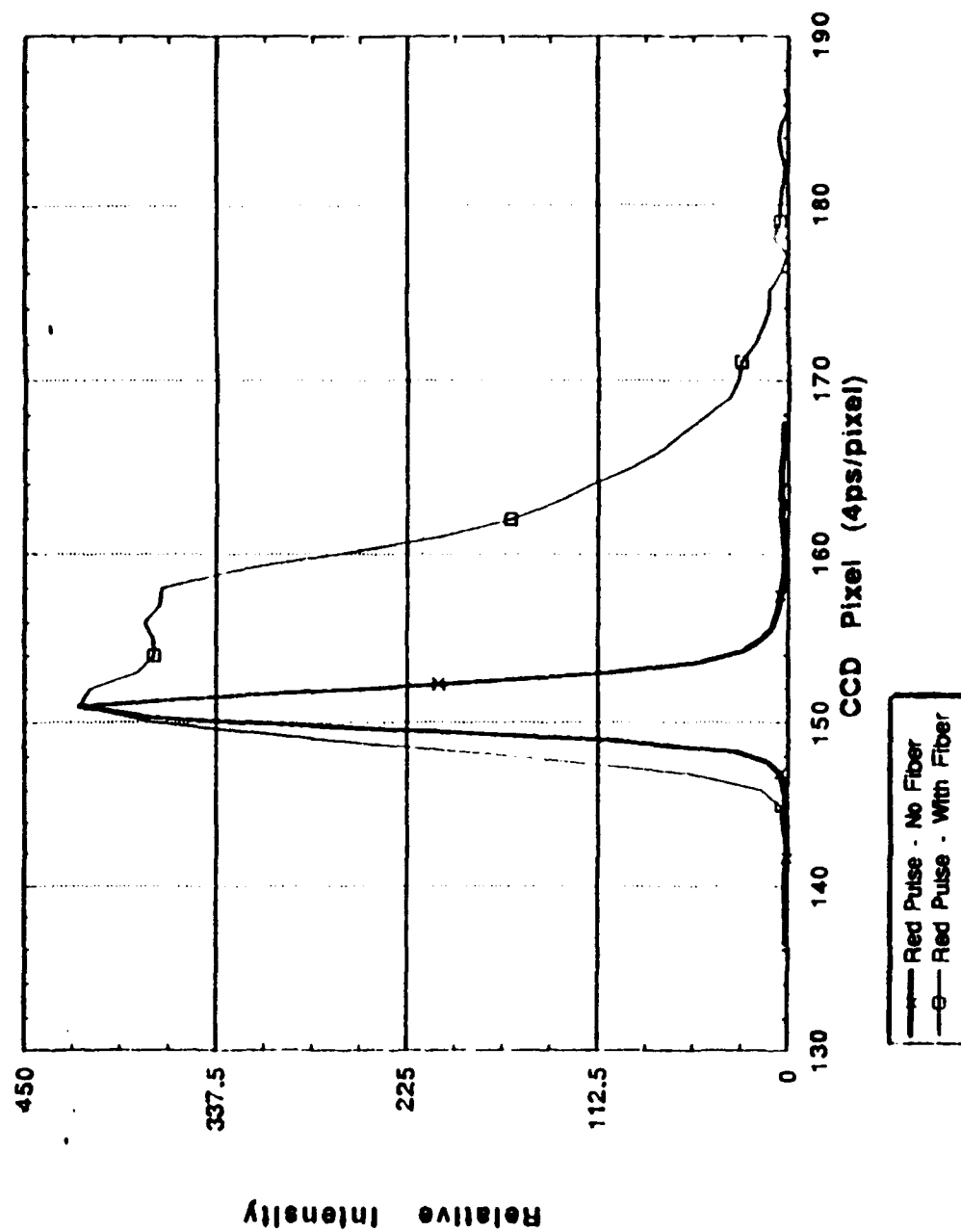


Figure 10 Intensity Plot of Red Pulse With and Without Fiber

Fiber Dispersion Test - 600um Core
Blue Pulse @ 380nm

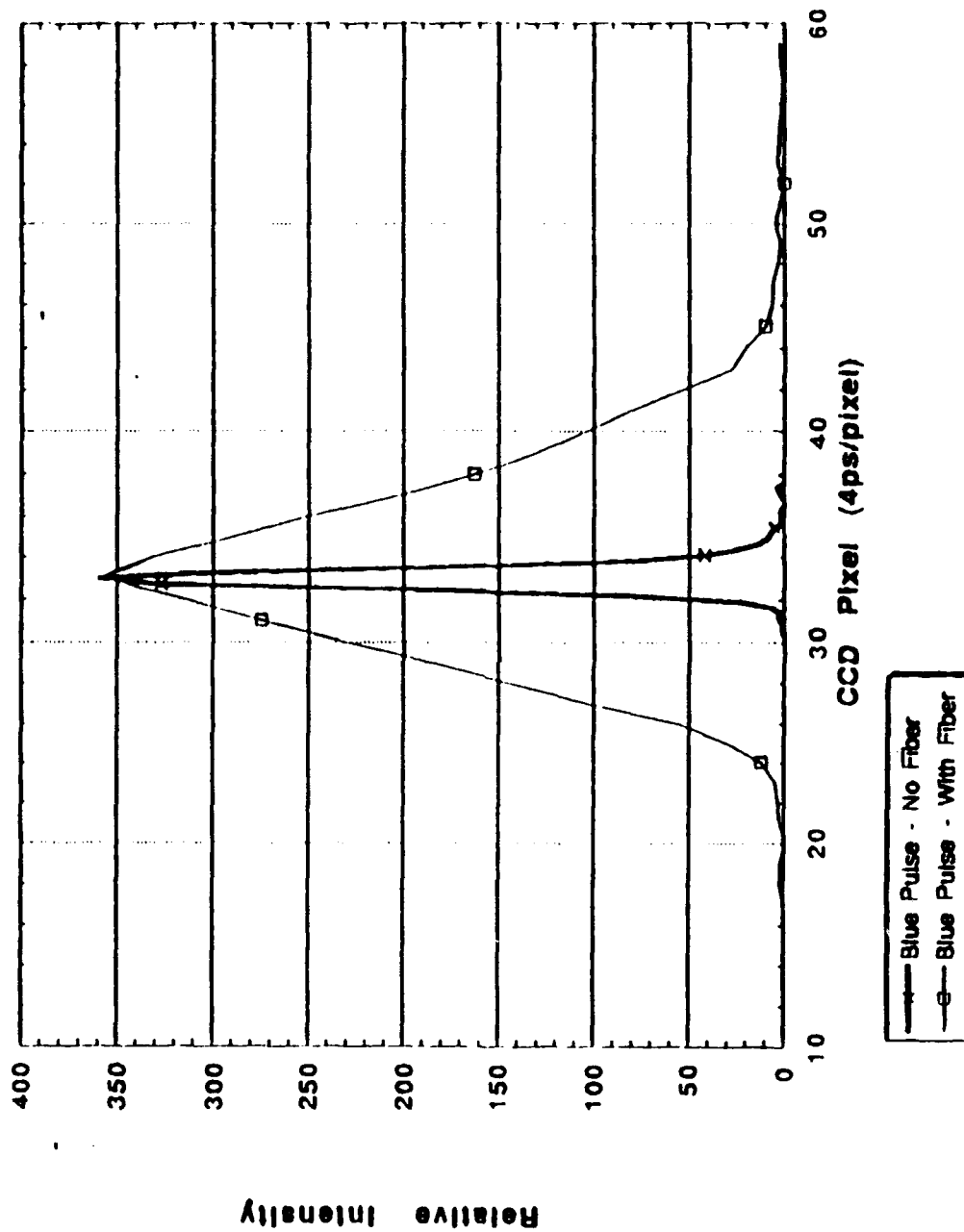


Figure 11 Intensity Plot of Blue Pulse With and Without Fiber

Fiber Dispersion Test - 600um Core Red & Blue Pulse Through Fiber

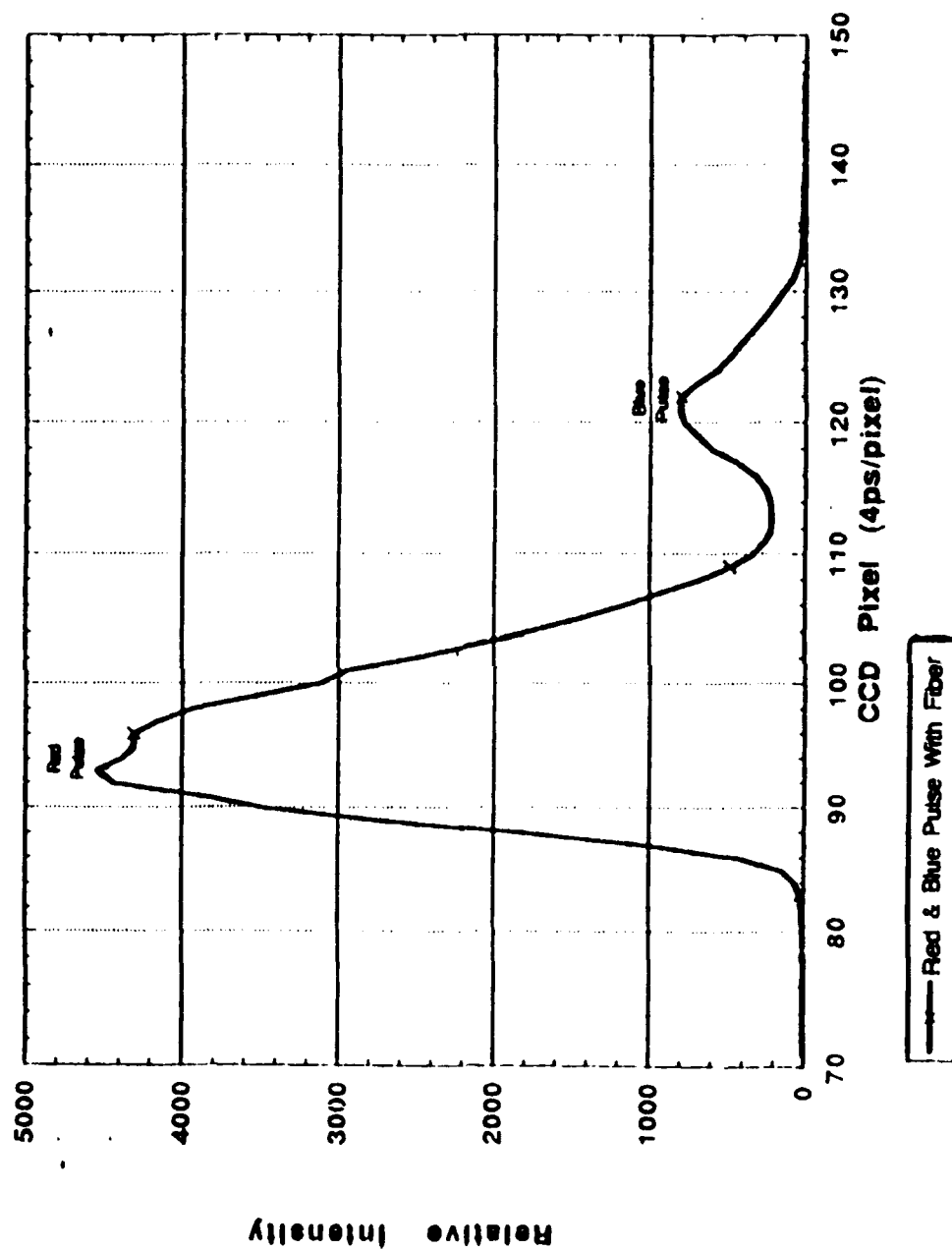


Figure 12 Intensity Plot of Red and Blue Pulse With Fiber

V. SYSTEM RESPONSE

The measured duration of the SL event is 2.05 pixels but there should also be 19 pixels of material dispersion for the 425 nm bandwidth that the streak camera is capable of detecting plus 9 pixels of modal dispersion for a total of 28 pixels due to dispersion. The short duration of the actual measurement suggests that a bandwidth smaller than 425 nm is actually being measured and that the fiber is being underfilled. The effective response of the system must be calculated and verified to determine the bandwidth that is being measured.

A. CALCULATION

Each part of the system has its own characteristic response curve. These curves must be multiplied together, in a method termed "folding", to get the response of the entire system. Figure 13 is the quantum efficiency (QE) curve for the streak camera. Figure 14 is the transmission curve for the fiber [Ref 20]. The SL spectrum previously done by Joseph T. Carlson [Ref 21] is adjusted for a different glycerine concentration and a more intense bubble due to decreased solution temperature. The adjustment evenly shifts the entire SL spectrum up by a factor of 10. The amount of the shift is determined by a visual comparison between the two different SL sources. Using these, a characteristic curve for the SL can be determined.

Figure 15 shows all 3 curves on the same plot before being multiplied together. Folding all 3 curves together determines the response curve of the system and is shown in Figure 16. The peak of the curve occurs at 470 nm and the curve has a FWHM of 154 nm which is the effective bandwidth of the system response.

B. MEASUREMENT

A deuterium light source (D2 lamp) closely resembles the SL curve for a non-cooled solution [Ref 22] and using neutral density (ND) filters to lower the lamp intensity to match the SL intensity of a cooled solution, the response of the system is checked. Other ND bandpass filters with a 10 nm bandwidth are used to limit the bandwidth and the light signal is lensed into the streak camera input. After measuring the intensity at the input of the streak camera, the experiment is run to check for either a response or no response on the video display. The DT lamp has a broadband intensity of $80 \mu W$ and at $\lambda = 400 \text{ nm}$ the intensity is 383 nW for a continuous wave (CW). The results are given in Table V.

TABLE V
DATA ANALYSIS FOR SYSTEM RESPONSE

ND FILTER (nm)	RESPONSE
None	Yes
400	No
450	Yes
500	Yes
550	Yes
600	Yes
630	No

These results show a response bandwidth of 150 nm for non-cooled SL which agrees with the calculated response curve for the cooled SL. It was also observed that there is a minimum CW power response of 500 nW for the lens setup. A fiber optic will deliver more power to the streak camera so the minimum power response for the fiber optic setup will be lower. The response bandwidth is smaller at lower power.

C. DISPERSION CALCULATION

Dispersion calculations are performed for a 141 nm bandwidth centered at the 470 nm peak system response. The lower end of the system response curve has from previous calculations, a transmission time for a 405 nm wavelength as $t_2 = 2.19275$ ns. Calculations for the higher end of the system response curve use

$$\lambda_5 = 508 \text{ nm} \quad n_5 = 1.462$$

$$\lambda_6 = 546 \text{ nm} \quad n_6 = 1.460$$

The corresponding

$$\frac{dn}{d\lambda} = -5.26 \times 10^4 \text{ m}^{-1}$$

and the transmission time is

$$t_6 = 2.145 \text{ ns}$$

The difference in the transmission times due to material dispersion for the lower and higher ends of the system response spectrum (141 nm bandwidth) is

$$\Delta t = t_2 - t_6 = 2.193 \text{ ns} - 2.145 \text{ ns} = 0.048 \text{ ns} = 48 \text{ ps}$$

The time difference due to material dispersion has a length of 12 pixels which is longer than the SL measurement.

STA51FF0992

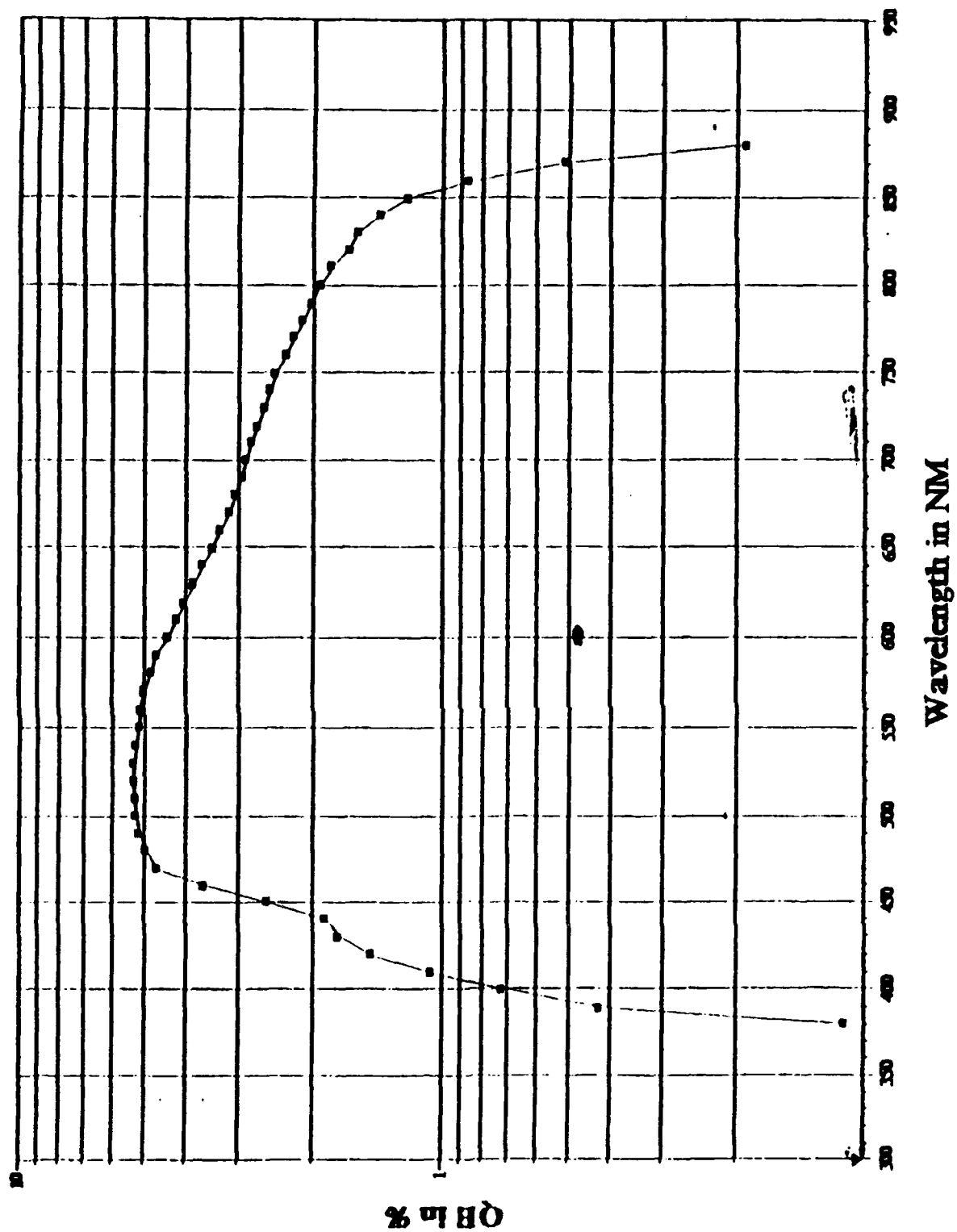


Figure 13 Streak Camera Quantum Efficiency Curve

**Relative Plot Of
Sonoluminescence Spectrum,
Streak Camera Quantum Efficiency,
And Fiber Transmission**

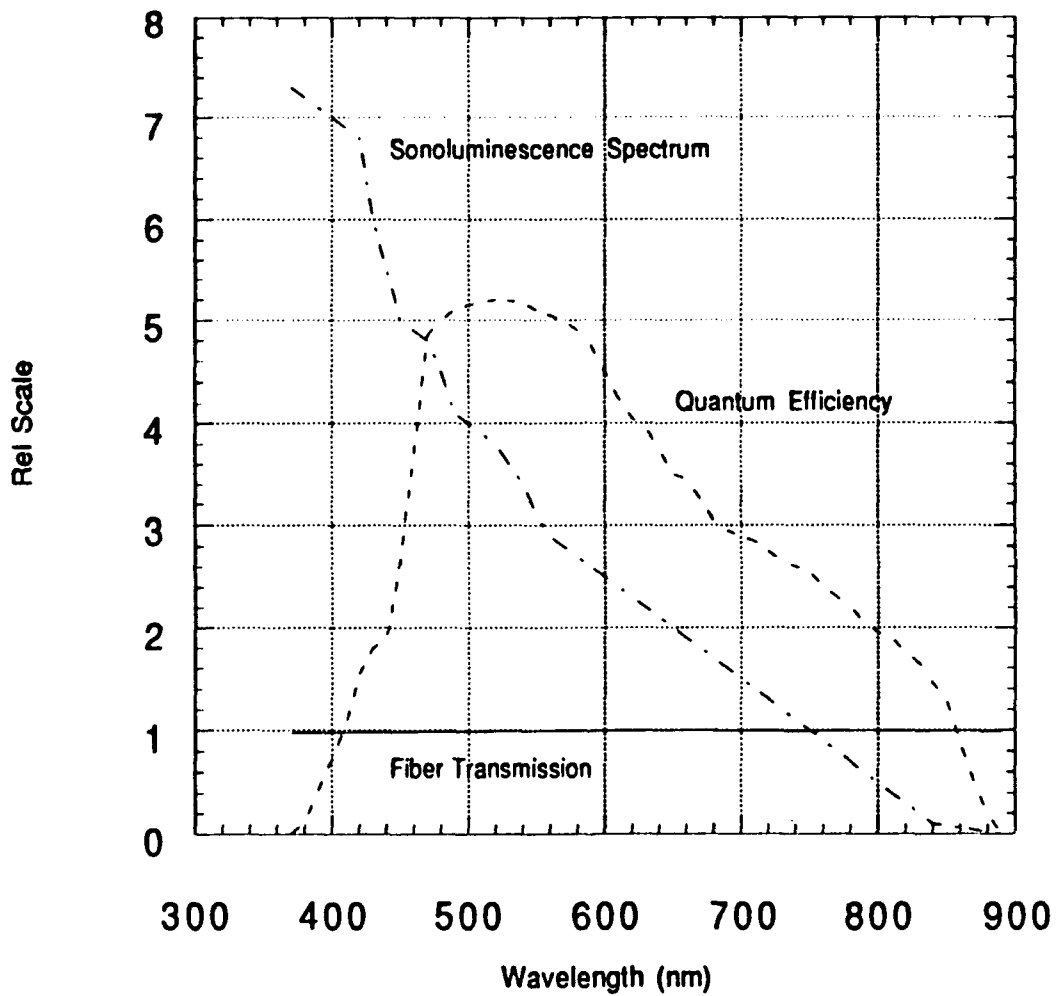
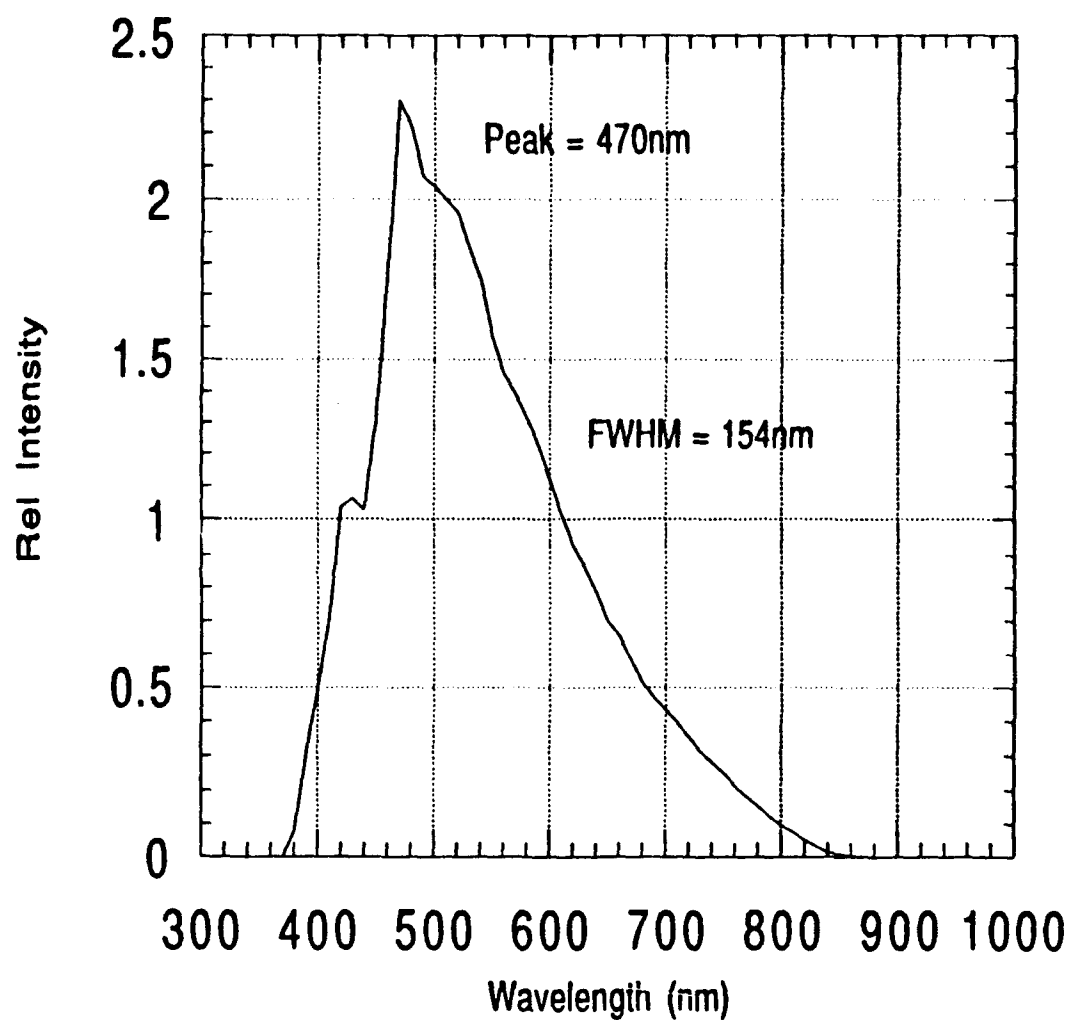


Figure 15 Relative Plot of Sonoluminescence Spectrum, Streak Camera Quantum Efficiency, and Fiber Transmission Curves

**Streak Camera System
Effective Response Curve For
Chilled Solution Sonoluminescence**



**Figure 16 Streak Camera System Effective Response Curve For
Chilled Solution Sonoluminescence**

VI. INTENSITY CALCULATIONS

A HeNe laser is used to determine how many counts are generated by each streak camera electron and ultimately the number of photons emitted by the SL. The HeNe has a wavelength of 545.3 nm and a CW intensity of $32 \frac{\mu W}{cm^2}$ as measured through the 600 micron core fiber with an EG&G photometer. The HeNe replaces the SL and the experiment is performed. A representative section of the streak is picked, digitally boxed and analyzed to give an average number of counts/pixel. After subtracting the average background, the average is 685.31 counts/pixel for a 100 pixel long section which gives 685.31 counts/pixel for 400 ps. The following calculations are performed:

$$E = \frac{hc}{\lambda} \quad \lambda = 545.3 \text{ nm}$$

$$E = 3.64 \times 10^{-19} \text{ J} \quad \text{photon energy}$$

$$1 \text{ mW} = 1 \times 10^{-3} \frac{\text{J}}{\text{s}} = 1 \times 10^{-15} \frac{\text{J}}{\text{ps}}$$

at 545.3 nm

$$1 \text{ mW} = 1 \times 10^{-15} \frac{\text{J}}{\text{ps}} \left[2.75 \times 10^{18} \frac{\text{photon}}{\text{J}} \right] = 2747 \frac{\text{photons}}{\text{ps}}$$

gives a laser intensity of

$$32 \times 10^{-3} \text{ mW} \left[2747 \frac{\text{photons}}{\text{ps}} \right] = 87.9 \frac{\text{photons}}{\text{ps}}$$

The 400 ps streak was made by 35165 photons. At 545 nm the QE of the streak camera is $5.3 \frac{\text{electrons}}{\text{photon}}$ [Ref. 23]. The new digital representative box has a total of 1212 pixels, there are

$$685.31 \frac{\text{counts}}{\text{pixel}} (1212 \text{ pixels}) = 8.306 \times 10^5 \text{ counts}$$

This is produced by

$$3.516 \times 10^4 \text{ photons} \left[5.3 \frac{\text{electrons}}{\text{photon}} \right] = 1.863 \times 10^5 \text{ electrons} .$$

This results in

$$\frac{1.863 \times 10^5 \text{ electrons}}{8.306 \times 10^5 \text{ counts}} = 0.2243 \frac{\text{electrons}}{\text{CCD count}} \quad \text{or} \quad 4.458 \frac{\text{CCD counts}}{\text{electron}} .$$

Or in terms of photons

$$\frac{3.516 \times 10^4 \text{ photons}}{8.306 \times 10^5 \text{ counts}} = 4.233 \times 10^{-2} \frac{\text{photons}}{\text{CCD count}}$$

when inverted gives

$$23.62 \frac{\text{CCD counts}}{\text{photon}} .$$

The average 2.3 ns sweep SL event is picked to construct a box around the SL. The box is averaged to get a total number of counts/pixel and multiplied by the total number of pixels to give the average number of counts. The average background count of 300 counts/pixel must be subtracted out to give the actual number of counts for each SL event. The average number of counts for the SL is 1550. Appendix C presents blown up images and intensity plots of all the data used prior to computer analysis. Each plot shows FWHM and is superimposed over the SL event display. The plot also shows the number of counts.

Using the 1550 average number of counts and the above calculations gives

$$1550 \text{ counts} \left[4.233 \times 10^{-2} \frac{\text{photons}}{\text{count}} \right] = 65.6 \text{ photons}$$

being collected by the optical fiber. The total number of detectable photons emitted (TNDPE) by the SL can be calculated by

$$(\text{TNDPE}) = (\# \text{ photons detected}) \frac{4}{\Delta\theta^2}$$

where $\Delta\theta$ is the solid angle that launches into the fiber. The maximum incident angle for transmission through the longest mode of the fiber is given by

$$\theta_{\max} = \sin^{-1} \left[\frac{NA}{n_0} \right]$$

where n_0 is the index of refraction for the glycerine solution [Ref 24]. Using $n_0 = 1.357$ for $\lambda = 589 \text{ nm}$ [Ref 25] and $NA = 0.40$ gives $\theta_{\max} = 17^\circ$. Any light incident at an angle greater than θ_{\max} will not be transmitted through the fiber. The effective area of the fiber being filled is only the inner 30.6 % of the core. This gives a $\Delta\theta$ of

$$\Delta\theta = \tan^{-1} \left[\frac{(0.306) 300 \mu\text{m fiber core radius}}{300 \mu\text{m distance SL}} \right] = 0.2970 \text{ str}$$

which gives

$$(TNDPE) = 65.6 \text{ photons detected} \left[\frac{4}{(0.2970)^2} \right] = 2975 \text{ photons}$$

that can be emitted from the SL during one pulse and that are in the detectable wavelength of the system.

The peak wavelength is assumed to be 470 nm which gives a photon energy $E = 4.22 \times 10^{-19} \text{ J}$. The number of photons emitted at this wavelength can be estimated as

$$\frac{2975 \text{ photons}}{154 \text{ nm bandwidth}} = 19 \text{ photons at } 470 \text{ nm} .$$

The duration of the pulse is assumed to be 8.00 ps because dispersion is not evident. This gives a detected peak power of

$$P_{\text{det}} = 4.22 \times 10^{-19} \frac{\text{J}}{\text{photon}} \left[\frac{19 \text{ photons}}{8.00 \text{ ps}} \right] = 10.0 \times 10^{-19} \frac{\text{J}}{\text{ps}} = 10.0 \mu\text{W}$$

and a maximum total detectable peak power of

$$P_{\text{mtd}} = 10.0 \mu\text{W} \left[\frac{4}{\Delta\theta^2} \right] = 453 \mu\text{W}$$

that can be emitted from the SL during one pulse and that is in the detectable wavelength of the system. Using the blackbody radiation theory for the SL spectrum, the peak of the SL spectrum is calculated to be 265 nm which gives a photon energy $E = 7.49 \times 10^{-19} \text{ J}$. The number of photons emitted at this wavelength can be estimated as 38. This estimate is based on the SL spectrum and that it has twice the height at 265 nm than at 470 nm. This gives a peak power of

$$P_{peak} = 7.49 \times 10^{-19} \frac{\text{J}}{\text{photon}} \left[\frac{38 \text{ photons}}{8.00 \text{ ps}} \right] = 35.6 \times 10^{-19} \frac{\text{J}}{\text{ps}} = 35.6 \text{ } \mu\text{W}$$

and a maximum total peak power of

$$P_{max \text{ peak}} = 35.6 \text{ } \mu\text{W} \left[\frac{4}{\Delta\theta^2} \right] = 1614 \text{ } \mu\text{W} = 1.614 \text{ mW}$$

that can be emitted from the SL during one pulse.

VII. CONCLUSIONS

Measurements of a single sonoluminescence (SL) event are performed using a streak camera system. Dispersion measurements on the fiber show that dispersion is evident at a 4 ps/pixel sweep speed. A 100 fs pulse is used for the measurements and has a FWHM = 4 pixels = 16 ps. This establishes a system resolution of 4 pixels. The measured material dispersion of the system is 28 pixels = 112 ps. The calculated material dispersion is 19 pixels = 75 ps. The calculated average modal dispersion is 21 pixels = 80 ps. Modal dispersion for $\lambda = 760 \text{ nm}$ is measured at 15 pixels = 60 ps. Modal dispersion for $\lambda = 380 \text{ nm}$ is measured at 10 pixels = 40 ps. All dispersion measurements are done at a lower MCPI out setting which causes a low system resolution.

At the optimum MCPI out setting, SL measurements at a 17.4 ps/pixel sweep speed show a duration upper limit of 2 pixels = 35 ps which is believed to be the system resolution limit. At a 4 ps/pixel sweep speed, measurements of a 13 ps pulser show 4 pixels = 16 ps and verify the system resolution of 2 pixels. Measurements of a single SL event at the 4 ps/pixels sweep speed show a duration of 2 pixels = 8 ps.

All the data are consistent however there are inconsistencies between measurement trials. The first inconsistency is in the 100 fs pulse having a FWHM = 4 pixels which is longer than the SL measurements. This could be due to the difference in the MCPI out settings. Other inconsistencies occur in all the dispersion measurements and calculations being longer than the SL measurements. Modal dispersion is not observed in either the pulser or the SL measurement because both sources act as point sources and do not excite all the possible transmission modes in the fiber. Material dispersion is not observed in the pulser because it has a small bandwidth and the dispersion is smaller than the camera resolution. Material dispersion should be evident in the SL measurement because of the effective system response bandwidth but it is not observed. This leads to the conclusion that a smaller

effective system response bandwidth is being measured. This could be due to the computer system interface and the program used, neither of which can be taken into account for a measurement. The lack of identifiable dispersion warrants the assumption that the dispersion in the measurement is zero otherwise the SL duration goes into the femtosecond region which is not predicted by hydrodynamic modeling [Ref 23]. Based on this assumption, calculations are performed to give a peak power of 1.614 *mW* emitted by the SL. All measurements lead to the conclusion that the time resolution of a single sonoluminescence event is less than 2 pixels = 8 ps.

Recommendations for future measurements are to use a single mode fiber that has a core size on the order of the SL bubble size. This will eliminate any modal dispersion and will ensure that the fiber is "filled" by the SL. In order to eliminate any material dispersion, the fiber should also have a small transmission bandwidth. This would mean that many measurements with different transmission bandwidth fibers would need to be done to have a measurement of the entire SL spectrum.

APPENDIX A. 10 ns SWEEP, 17.4 ps/pixel SPEED DATA STREAK CAMERA IMAGES AND PLOTS

Figures A-1 through A-10 show the streak camera images and plots of all the data used for analysis given in Table II. The greyscale for the images varies to give the best contrast between the SL event and the background. The top intensity plot is over the entire sweep length and the bottom intensity plot is on blown up to show FWHM.

Sonoluminescence - Streak Camera Image and Plots

10ns Sweep

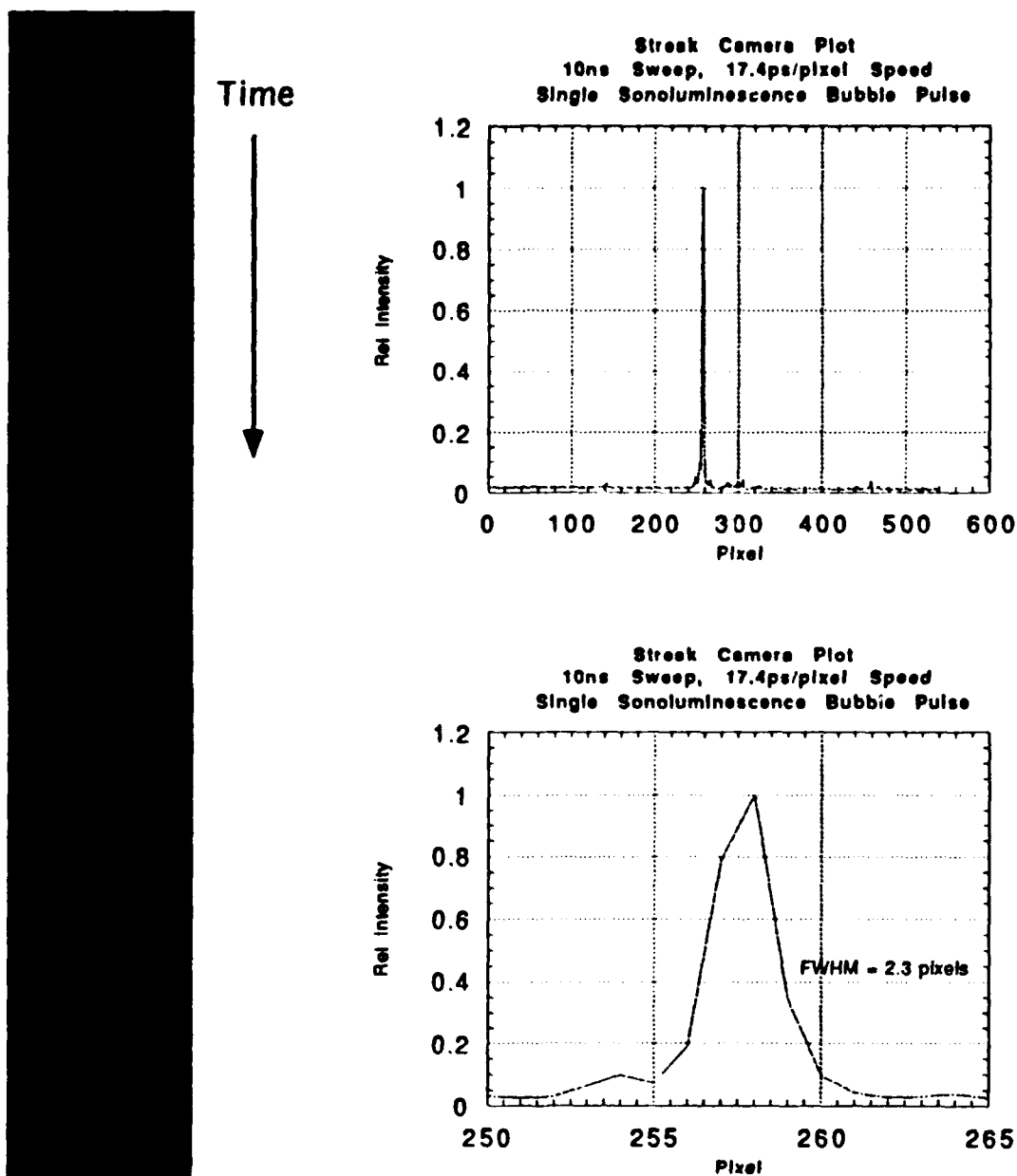


Figure A-1 Single Sonoluminescence Event Streak Camera Image
and Intensity Plots, File #10s2

Sonoluminescence - Streak Camera Image and Plots

10ns Sweep

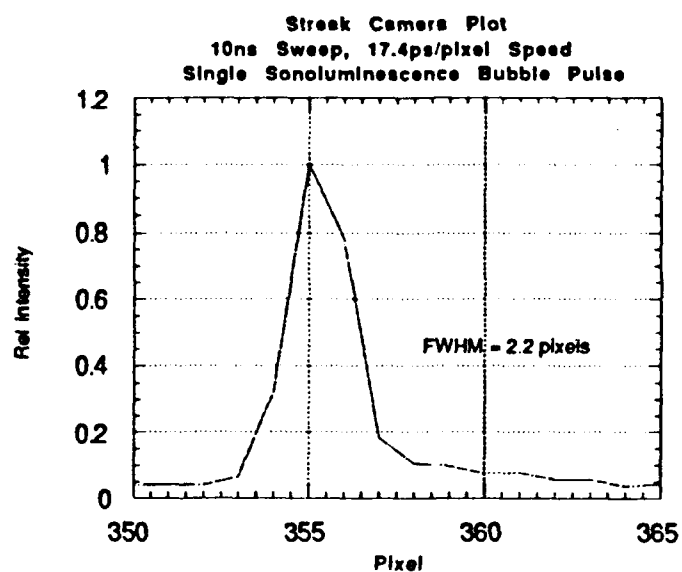
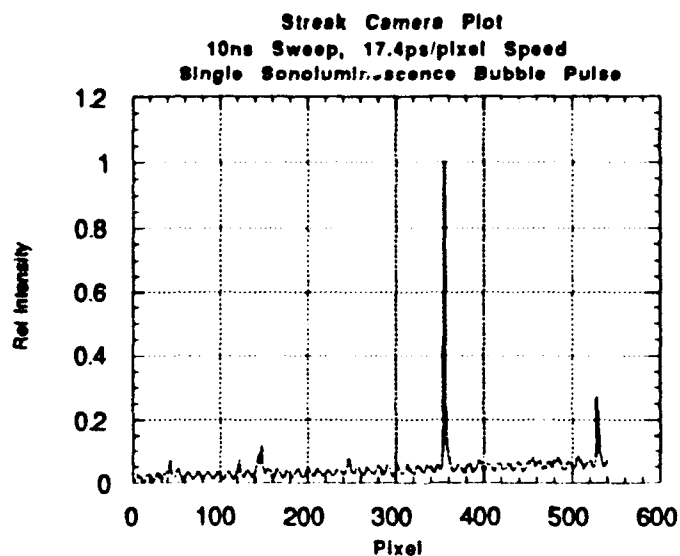


Figure A-2 Single Sonoluminescence Event Streak Camera Image
and Intensity Plots, File #10s3

Sonoluminescence - Streak Camera Image and Plots

10ns Sweep

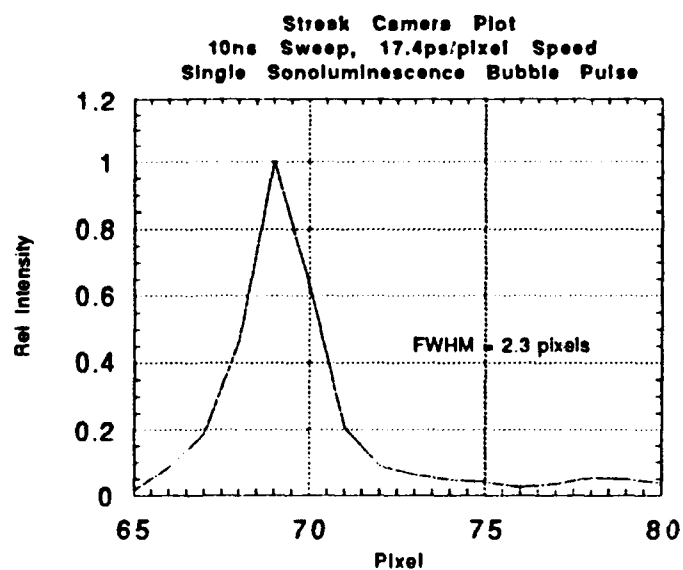
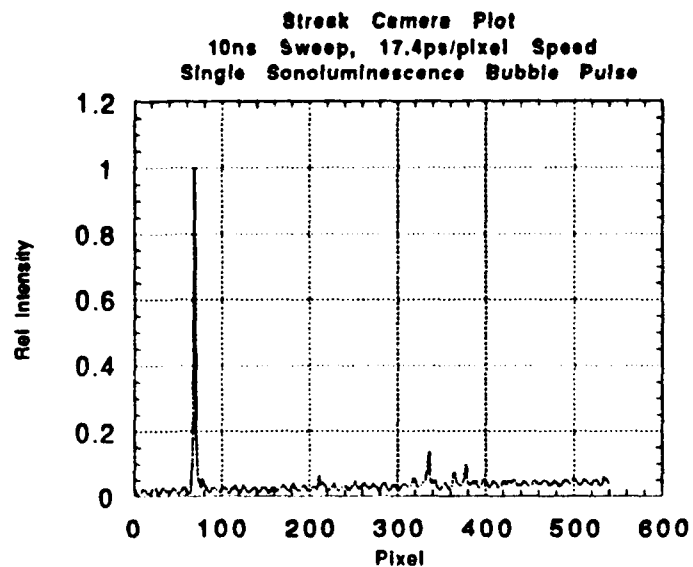


Figure A-3 Single Sonoluminescence Event Streak Camera Image
and Intensity Plots, File #10s5

Sonoluminescence - Streak Camera Image and Plots

10ns Sweep

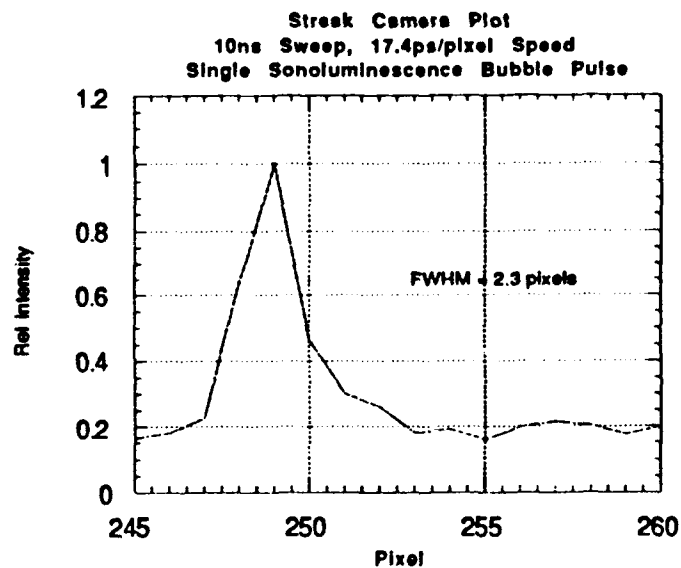
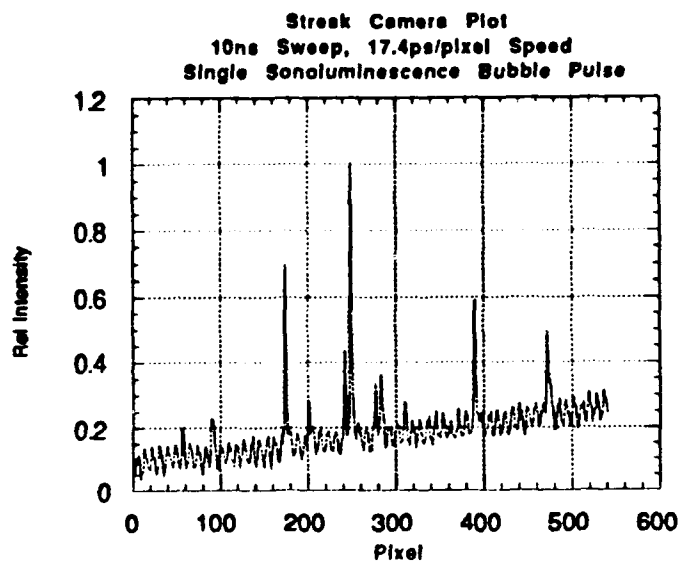
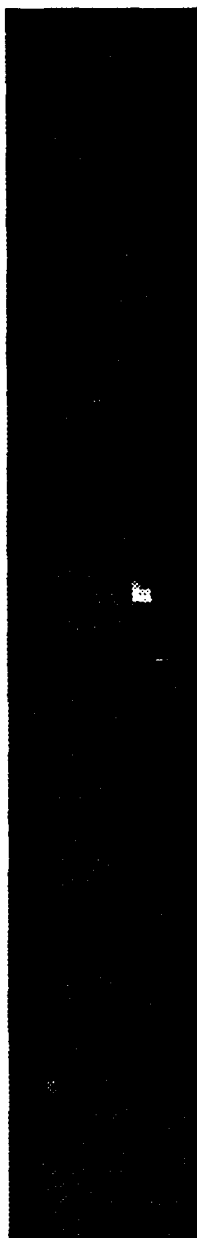


Figure A-4 Single Sonoluminescence Event Streak Camera Image
and Intensity Plots, File #1s2

Sonoluminescence - Streak Camera Image and Plots

10ns Sweep

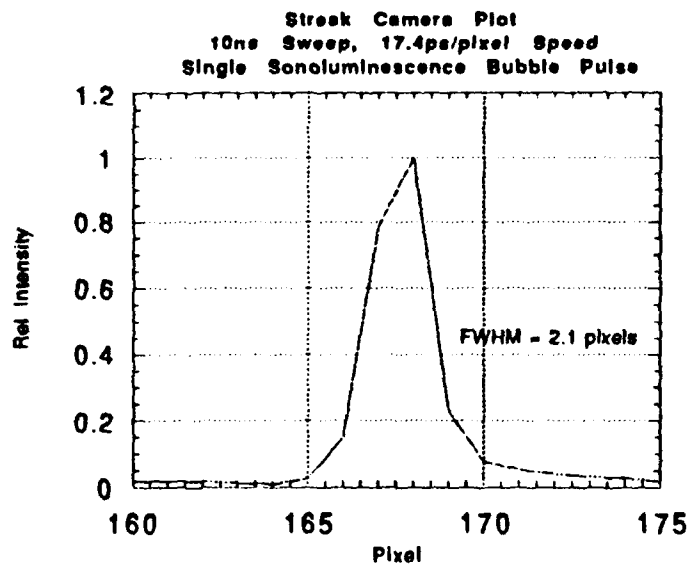
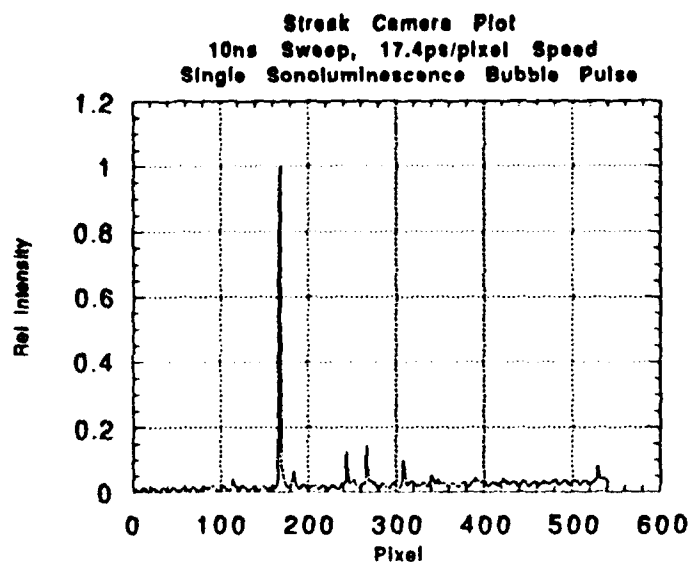


Figure A-5 Single Sonoluminescence Event Streak Camera Image
and Intensity Plots, File #5s1

Sonoluminescence - Streak Camera Image and Plots

10ns Sweep

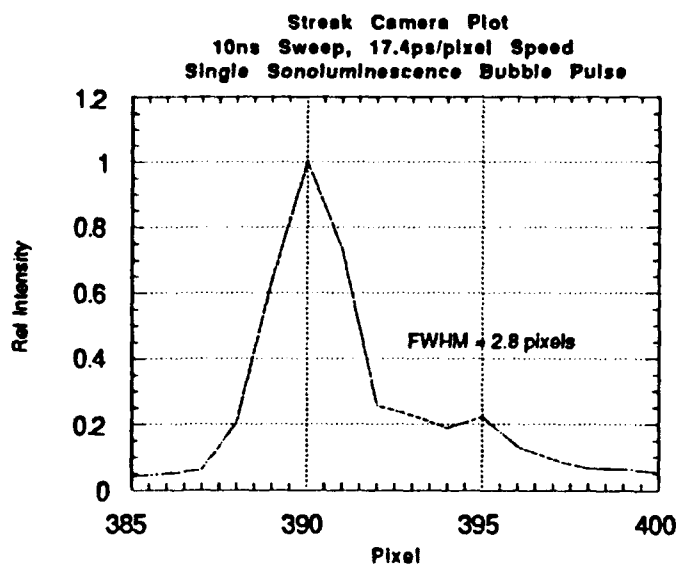
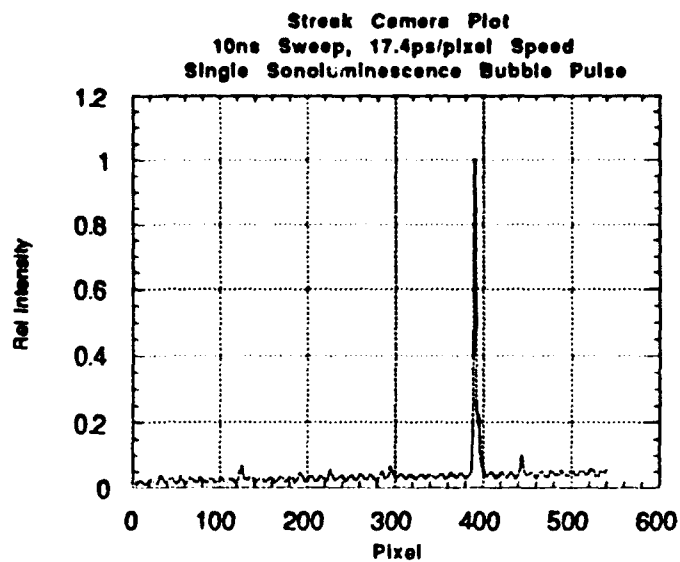


Figure A-6 Single Sonoluminescence Event Streak Camera Image
and Intensity Plots, File #6s1

Sonoluminescence - Streak Camera Image and Plots

10ns Sweep

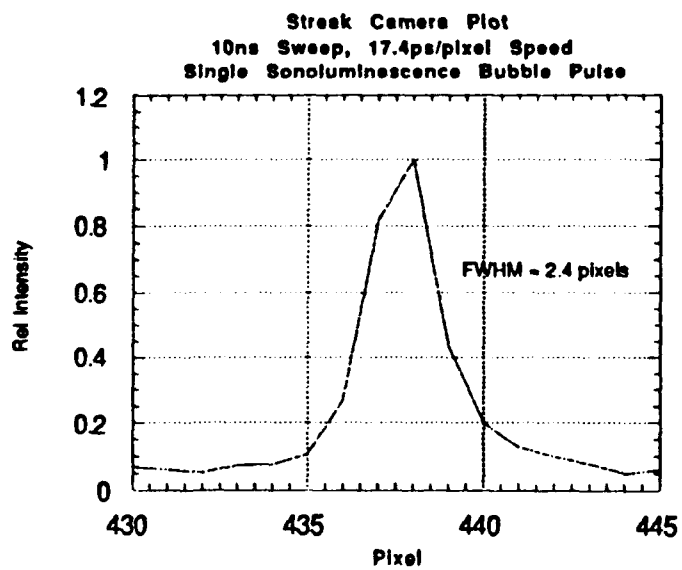
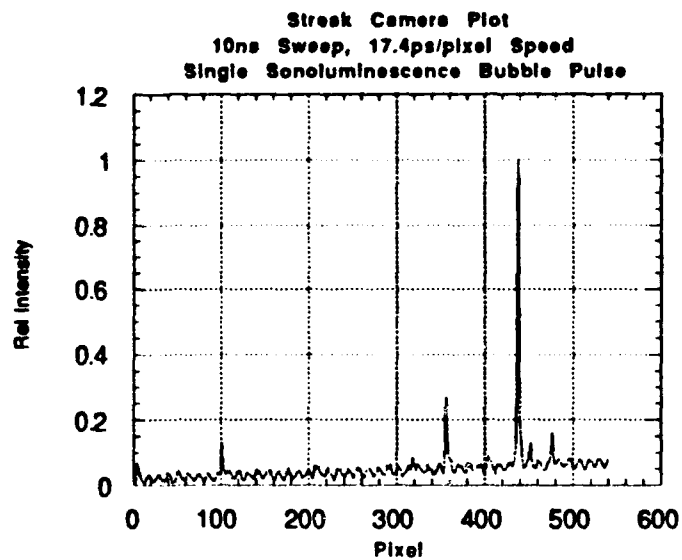
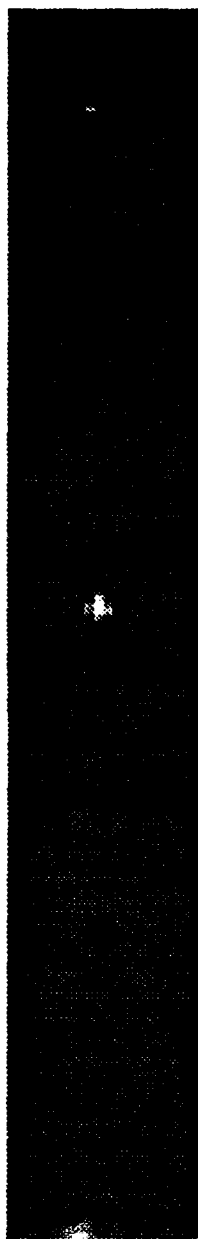


Figure A-7 Single Sonoluminescence Event Streak Camera Image
and Intensity Plots, File #7s4

Sonoluminescence - Streak Camera Image and Plots

10ns Sweep

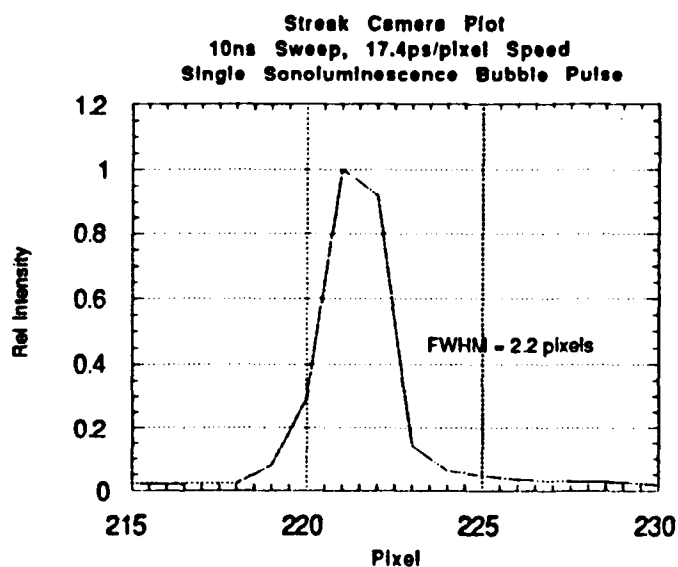
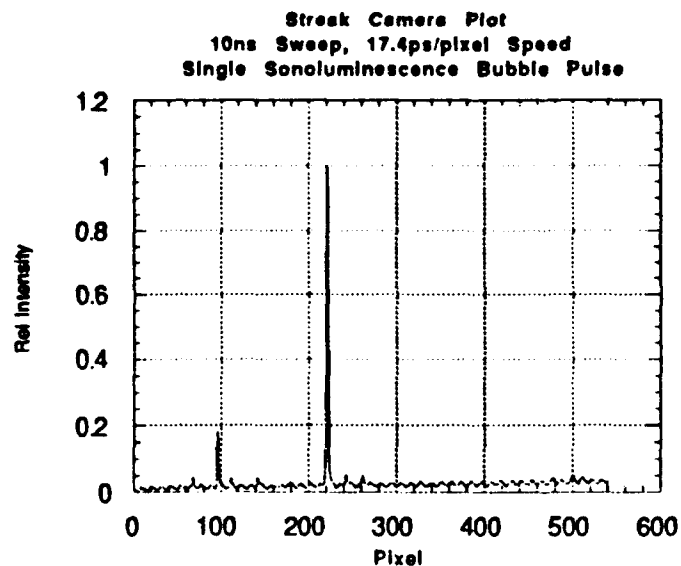
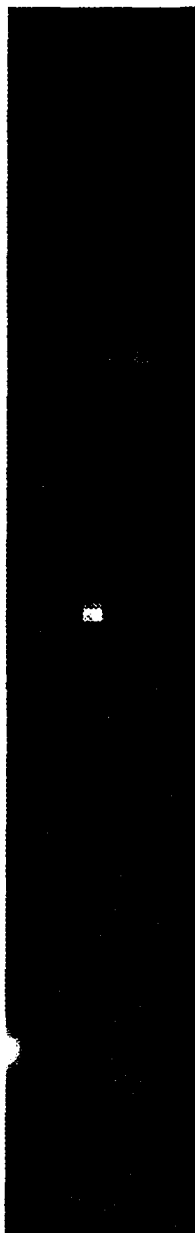


Figure A-8 Single Sonoluminescence Event Streak Camera Image
and Intensity Plots, File #9s1

Sonoluminescence - Streak Camera Image and Plots

10ns Sweep

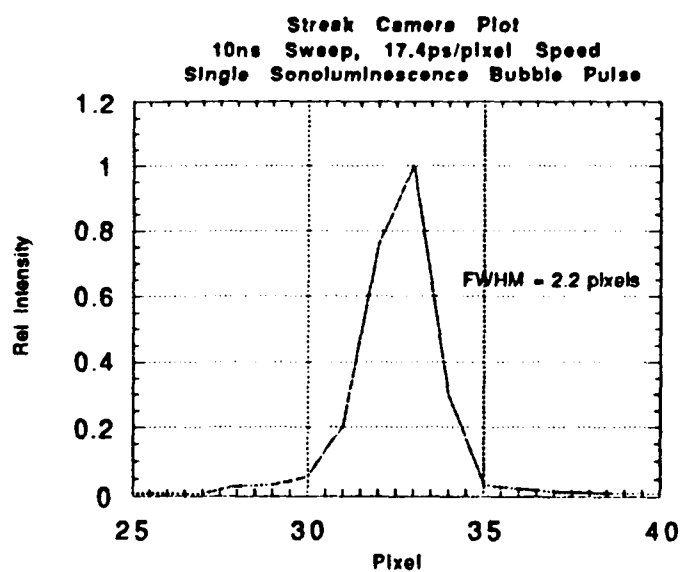
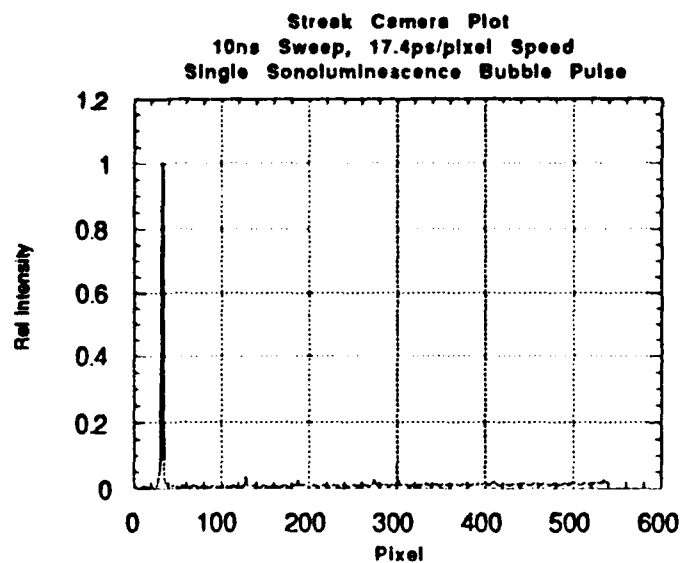


Figure A-9 Single Sonoluminescence Event Streak Camera Image
and Intensity Plots, File #9s4

Sonoluminescence - Streak Camera Image and Plots

10ns Sweep

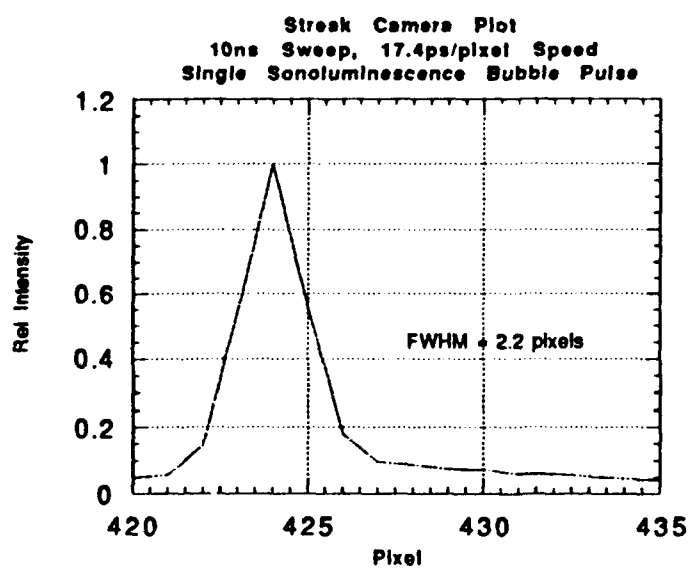
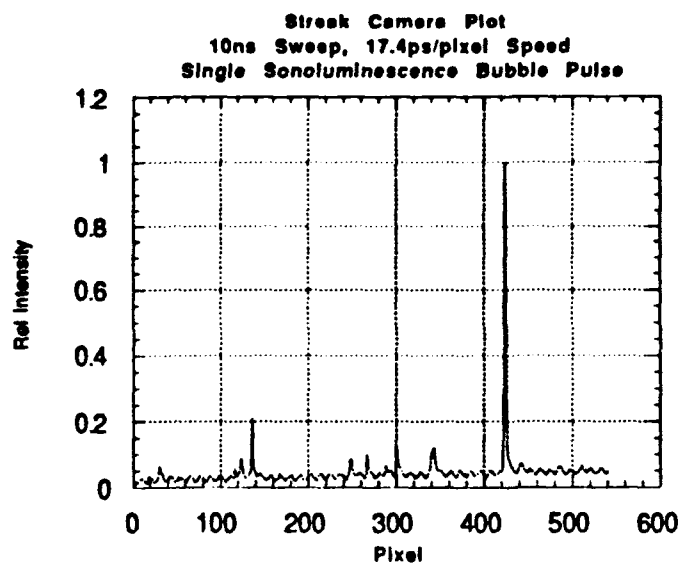


Figure A-10 Single Sonoluminescence Event Streak Camera Image
and Intensity Plots, File #9s5

APPENDIX B. 2.3 ns SWEEP, 4 ps/pixel SPEED DATA STREAK CAMERA IMAGES AND PLOTS

Figures B-1 through B-12 show the streak camera images and plots of all the data used for analysis given in Table IV. The greyscale for the images varies to give the best contrast between the SL event and the background. The top intensity plot is over the entire sweep length and the bottom intensity plot is on blown up to show FWHM.

Sonoluminescence - Streak Camera Image and Plots

2.3ns Sweep

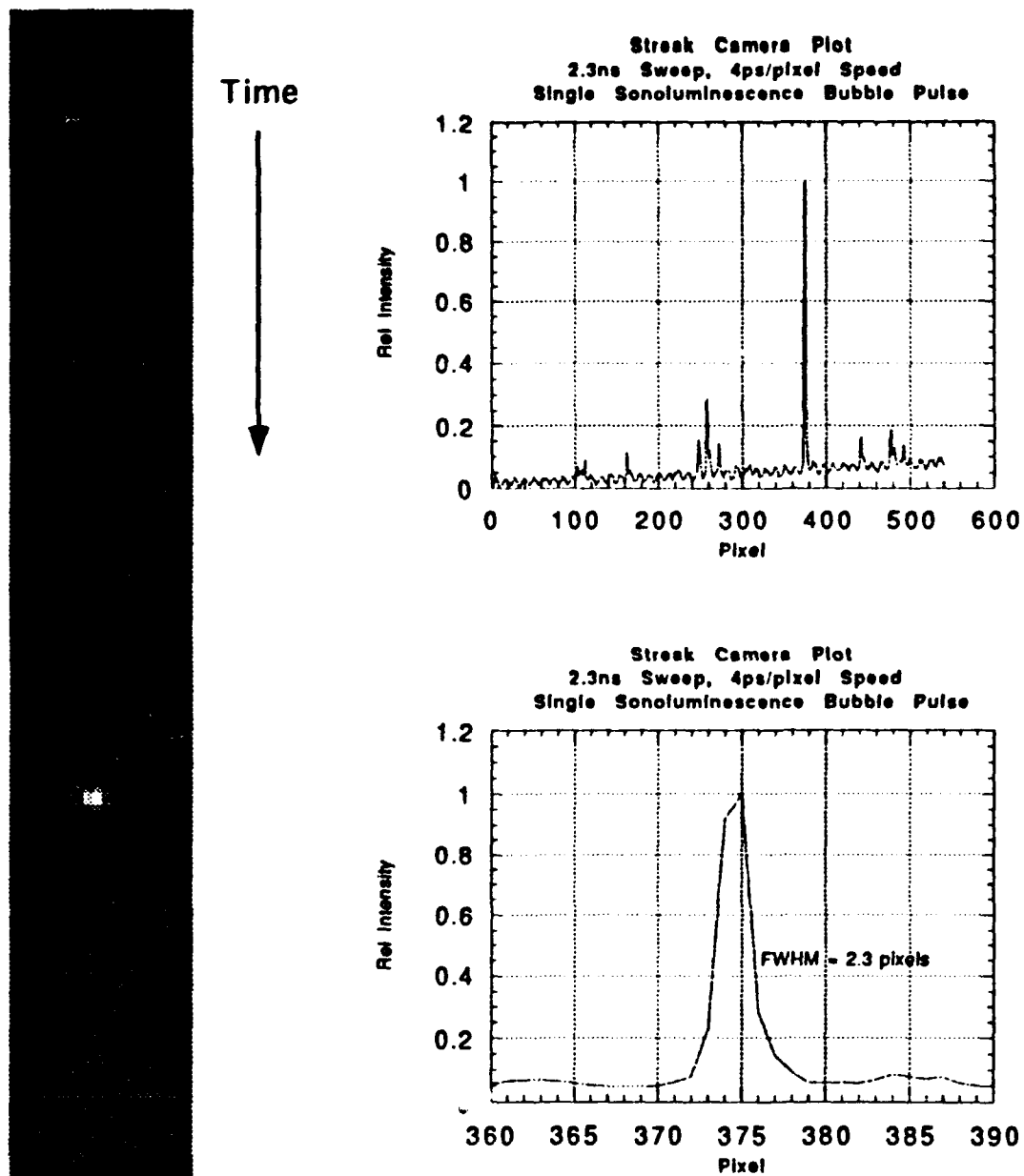


Figure B-1 Single Sonoluminescence Event Streak Camera Image
and Intensity Plots, File #95s1

Sonoluminescence - Streak Camera Image and Plots

2.3ns Sweep

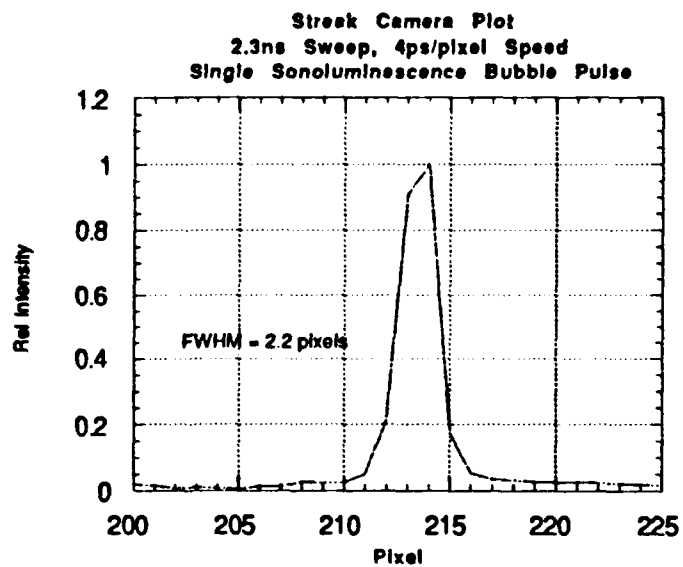
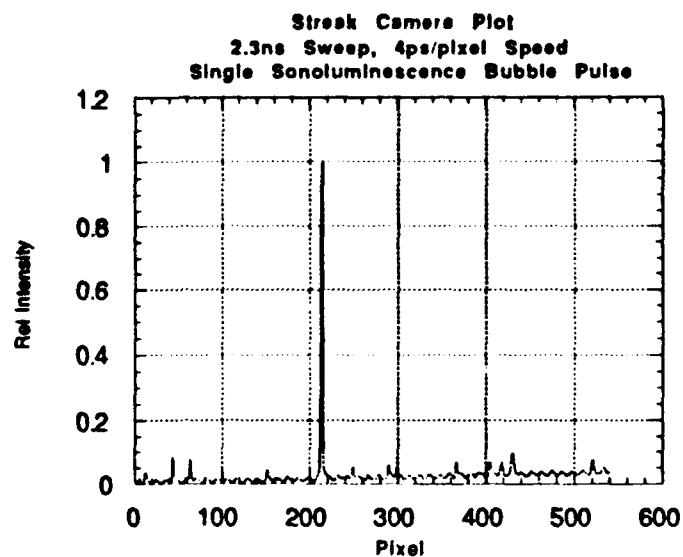
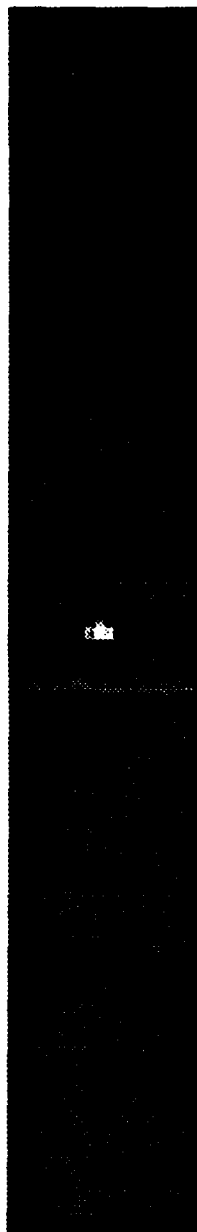


Figure B-2 Single Sonoluminescence Event Streak Camera Image
and Intensity Plots, File #96s1

Sonoluminescence - Streak Camera Image and Plots

2.3ns Sweep

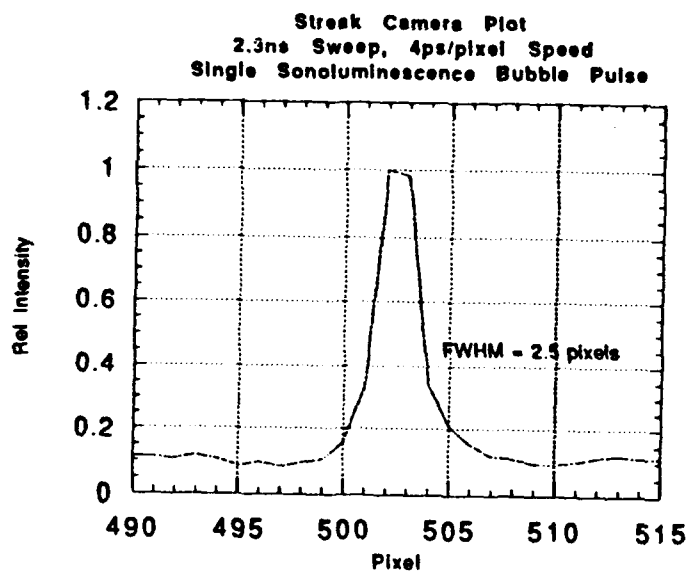
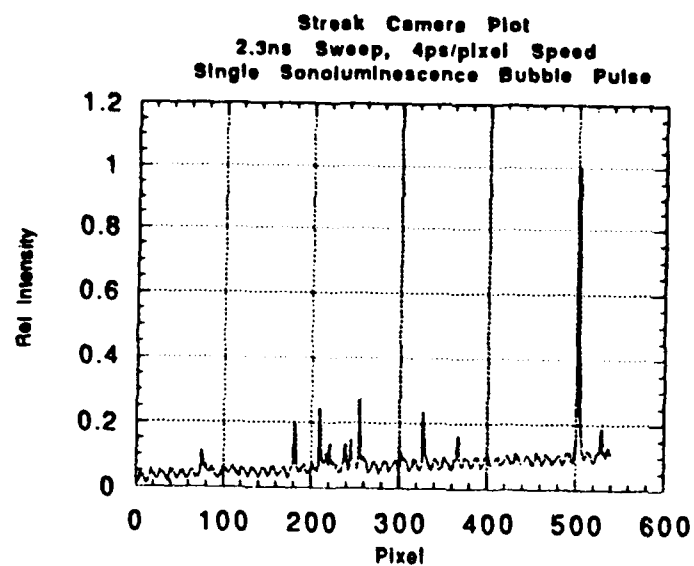
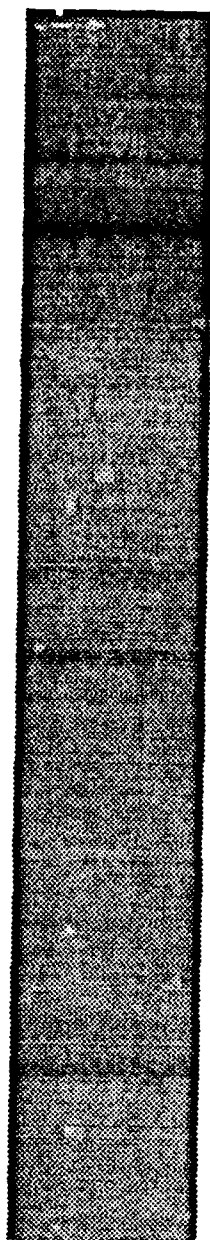


Figure B-3 Single Sonoluminescence Event Streak Camera Image
and Intensity Plots, File #96s2

Sonoluminescence - Streak Camera Image and Plots

2.3ns Sweep

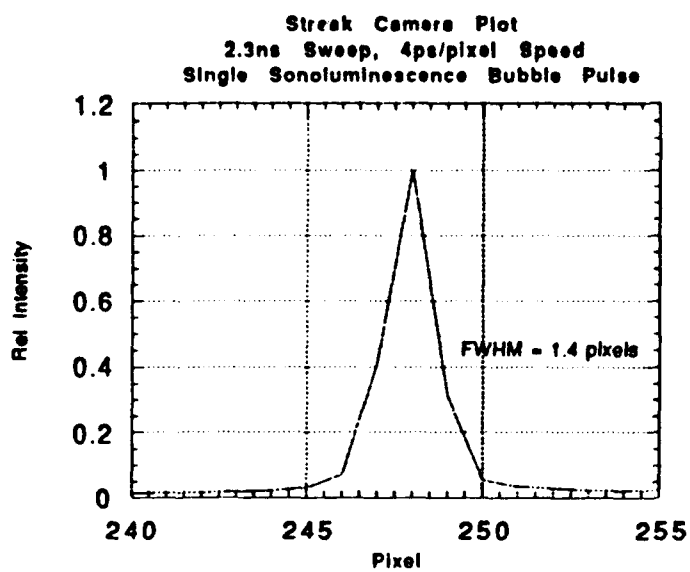
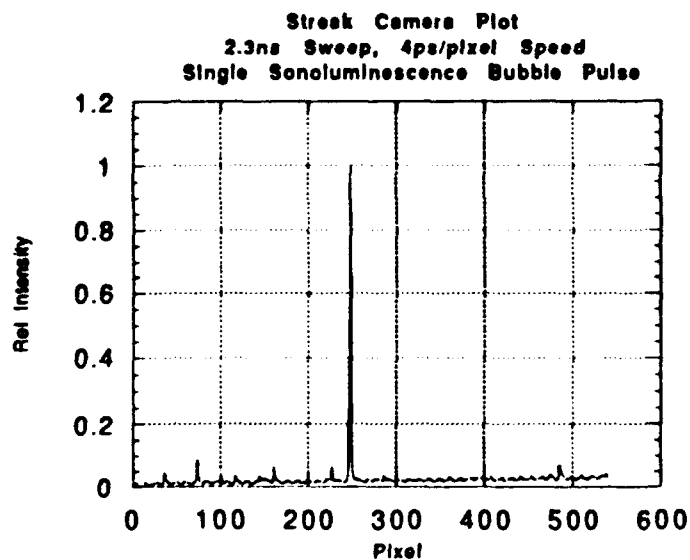


Figure B-4 Single Sonoluminescence Event Streak Camera Image
and Intensity Plots, File #97s1

Sonoluminescence - Streak Camera Image and Plots

2.3ns Sweep

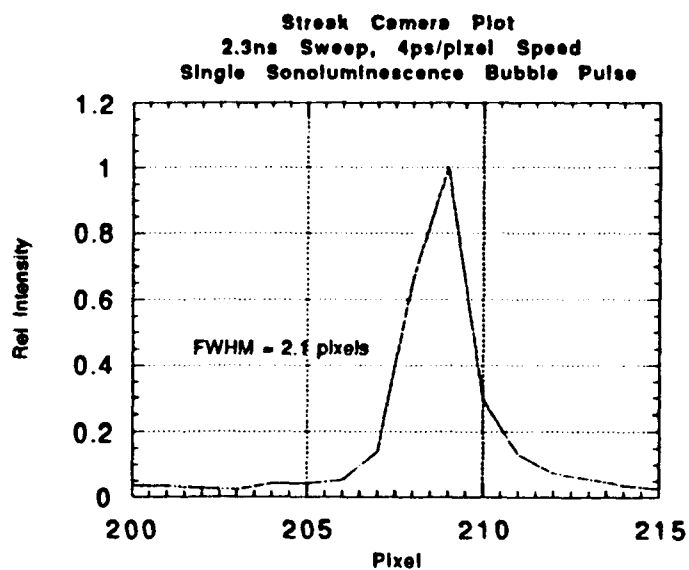
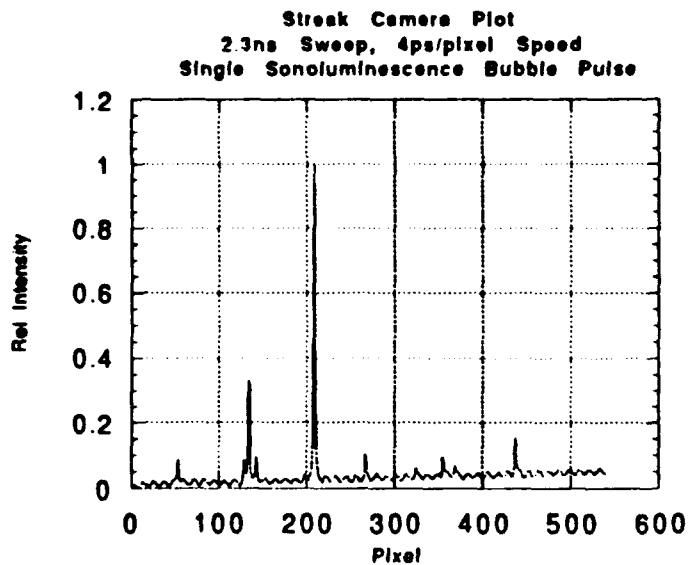


Figure B-5 Single Sonoluminescence Event Streak Camera Image
and Intensity Plots, File #97s2

Sonoluminescence - Streak Camera Image and Plots

2.3ns Sweep

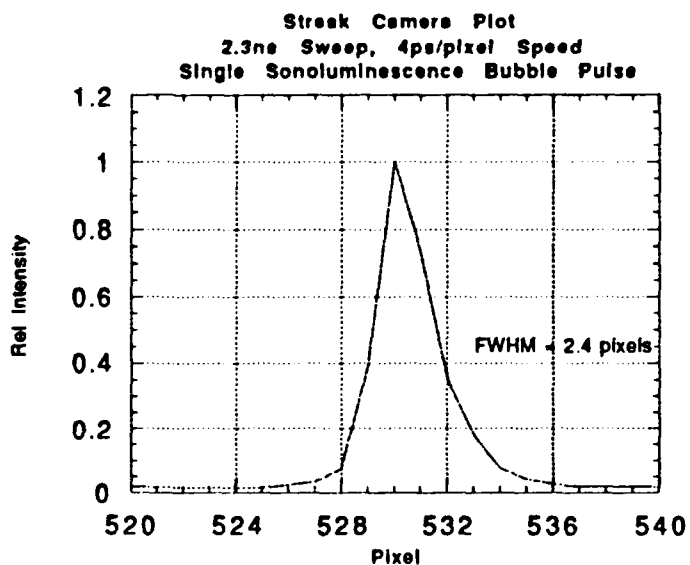
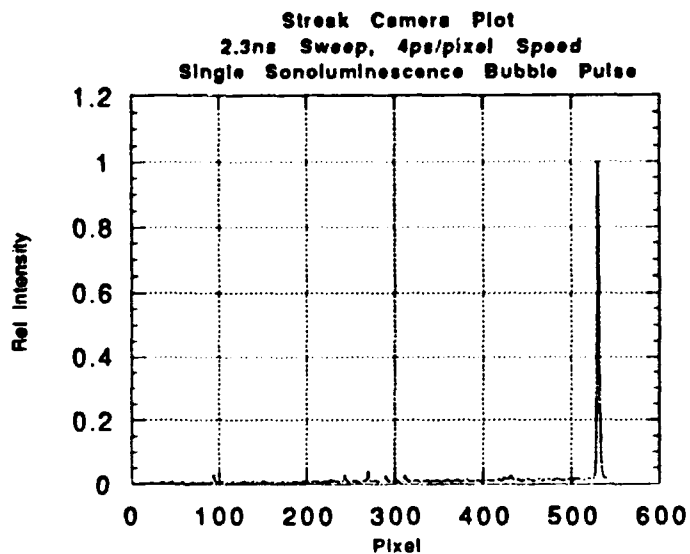


Figure B-6 Single Sonoluminescence Event Streak Camera Image
and Intensity Plots, File #97s3

Sonoluminescence - Streak Camera Image and Plots

2.3ns Sweep

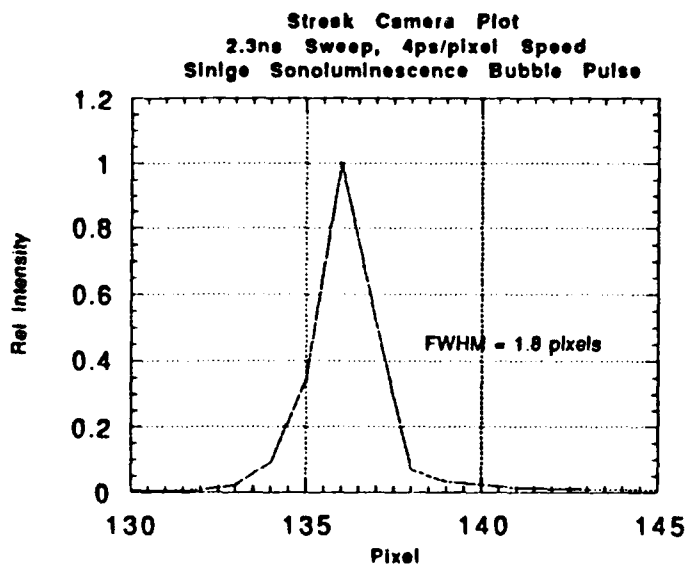
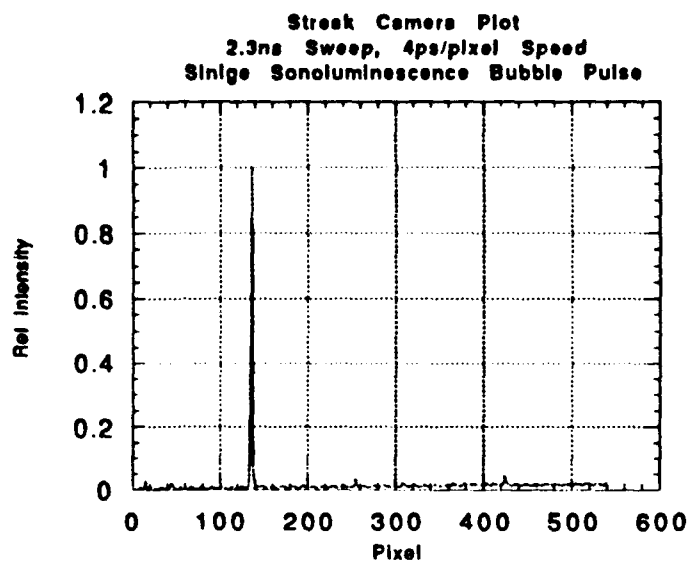
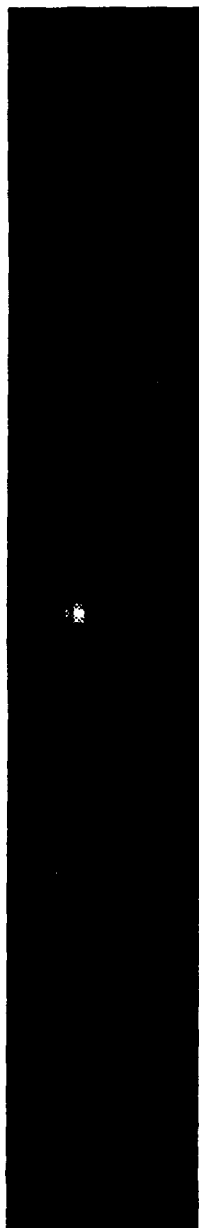


Figure B-7 Single Sonoluminescence Event Streak Camera Image
and Intensity Plots, File #98s1

Sonoluminescence - Streak Camera Image and Plots

2.3ns Sweep

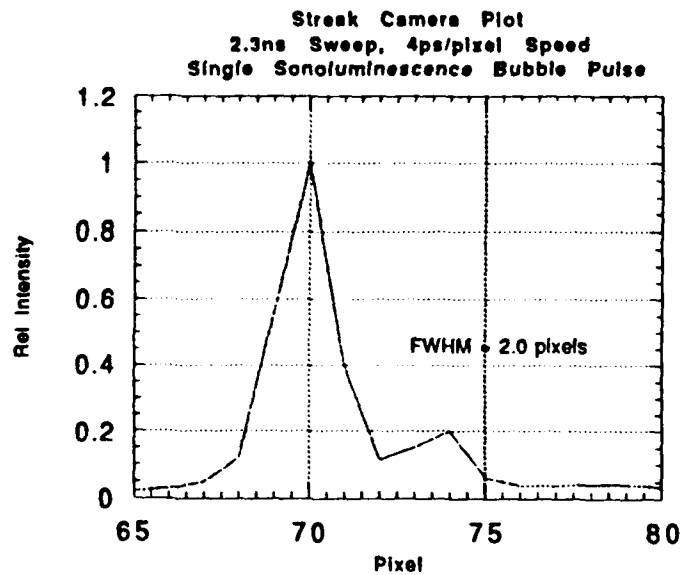
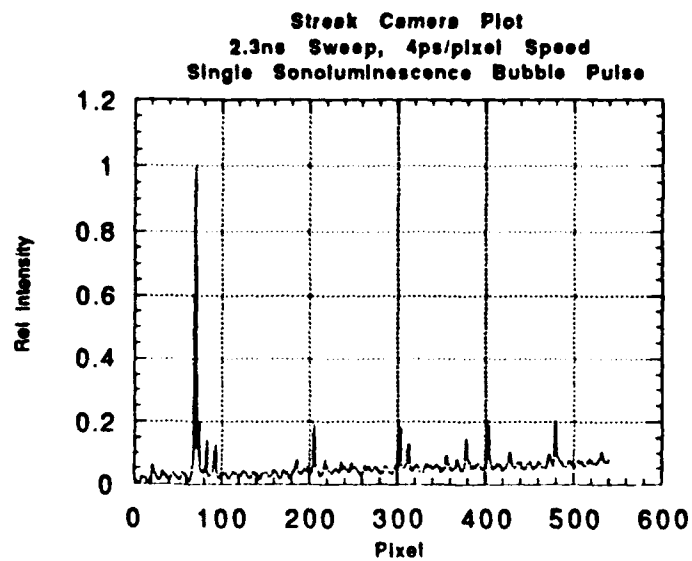
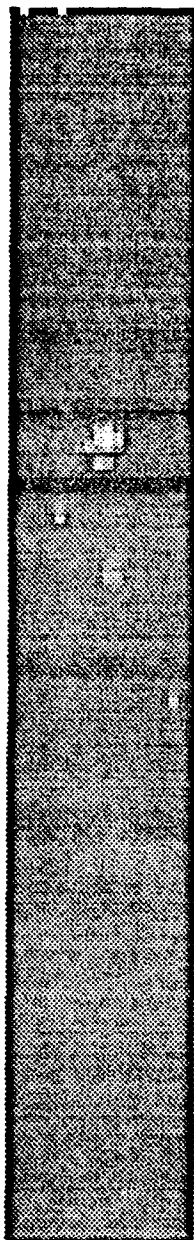


Figure B-8 Single Sonoluminescence Event Streak Camera Image
and Intensity Plots, File #98s2

Sonoluminescence - Streak Camera Image and Plots

2.3ns Sweep

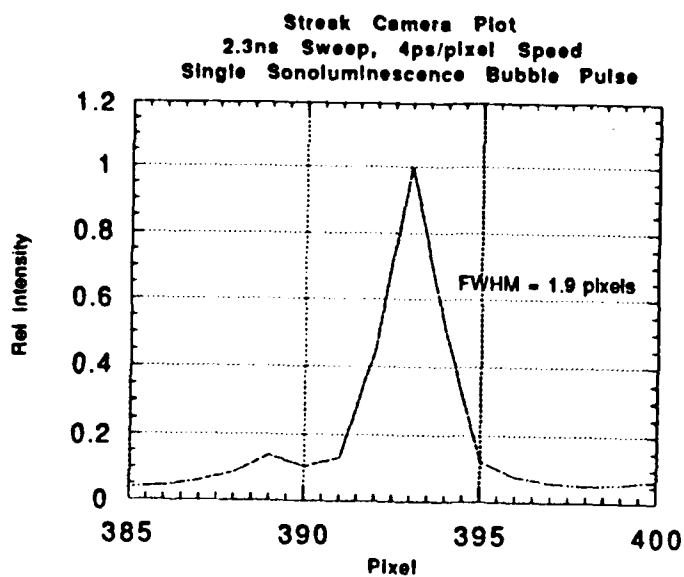
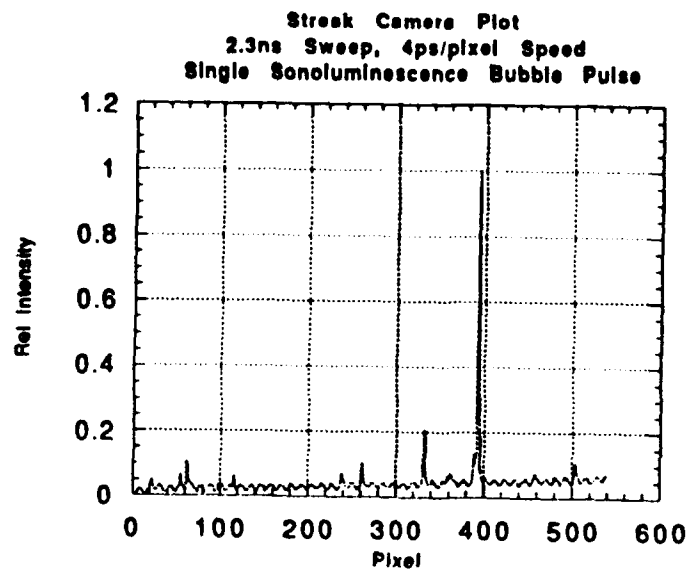
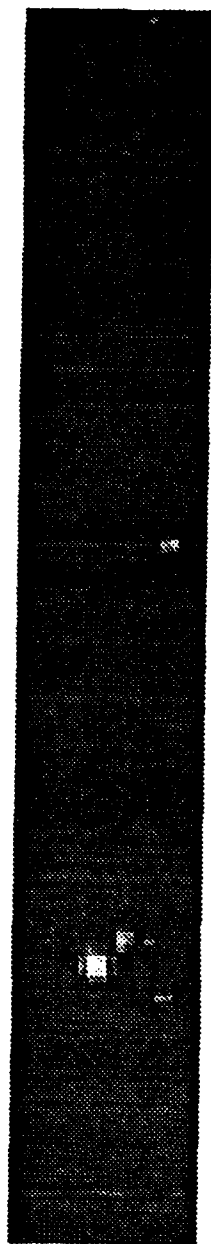


Figure B-9 Single Sonoluminescence Event Streak Camera Image
and Intensity Plots, File #98s3

Sonoluminescence - Streak Camera Image and Plots

2.3ns Sweep

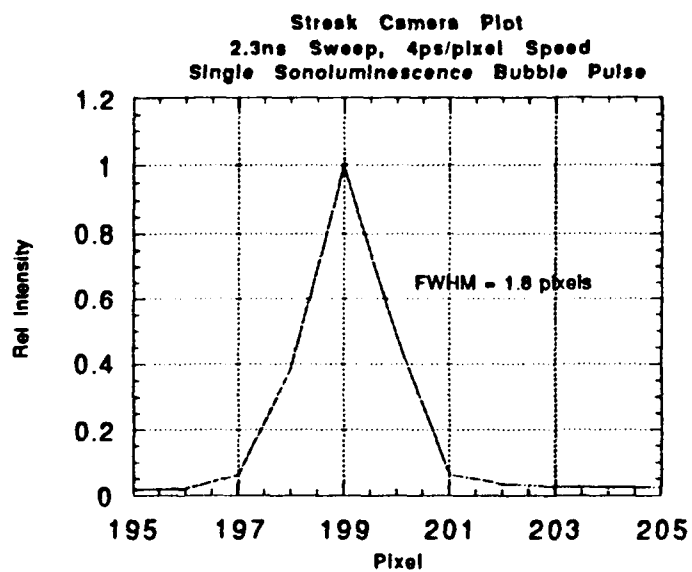
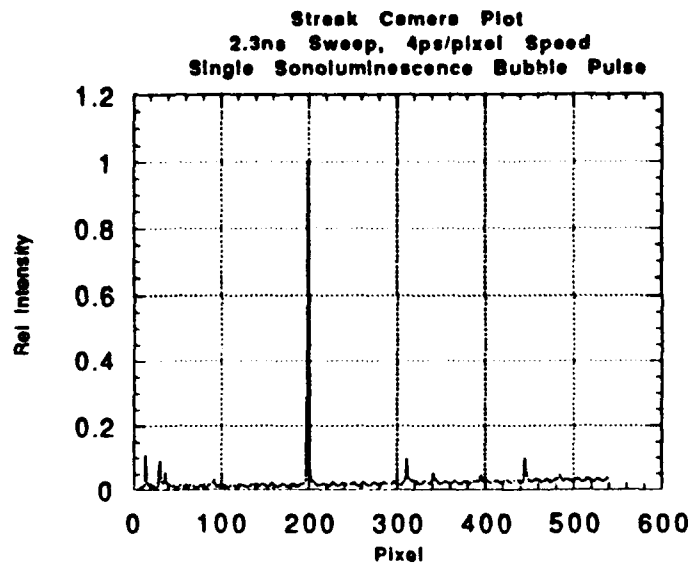


Figure B-10 Single Sonoluminescence Event Streak Camera Image
and Intensity Plots, File #99s1

Sonoluminescence - Streak Camera Image and Plots

2.3ns Sweep

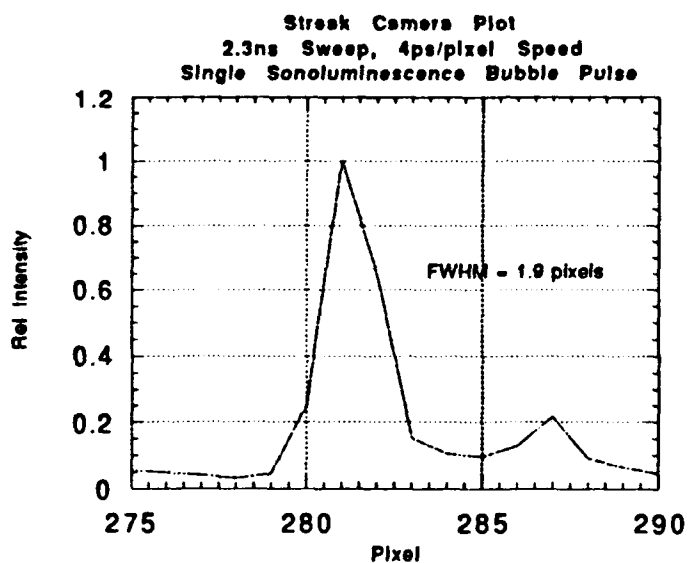
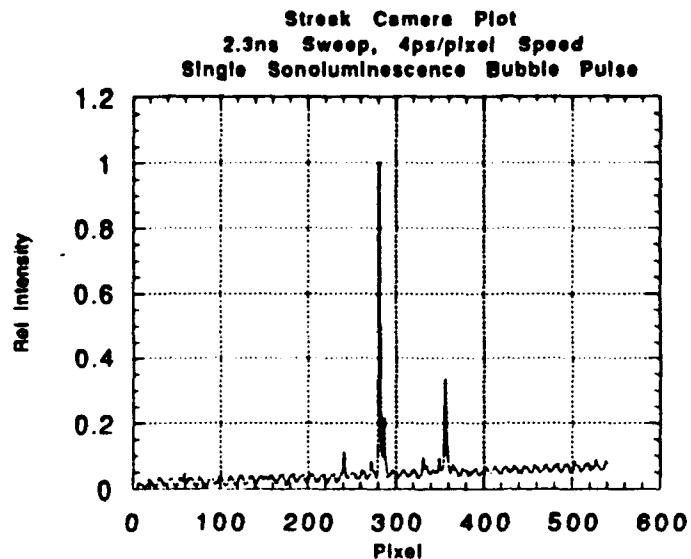
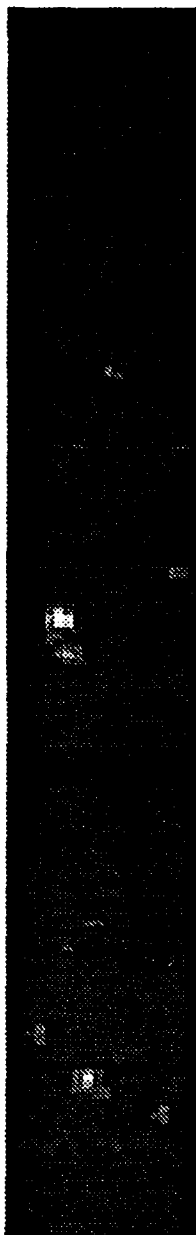


Figure B-11 Single Sonoluminescence Event Streak Camera Image
and Intensity Plots, File #99s3

Sonoluminescence - Streak Camera Image and Plots

2.3ns Sweep

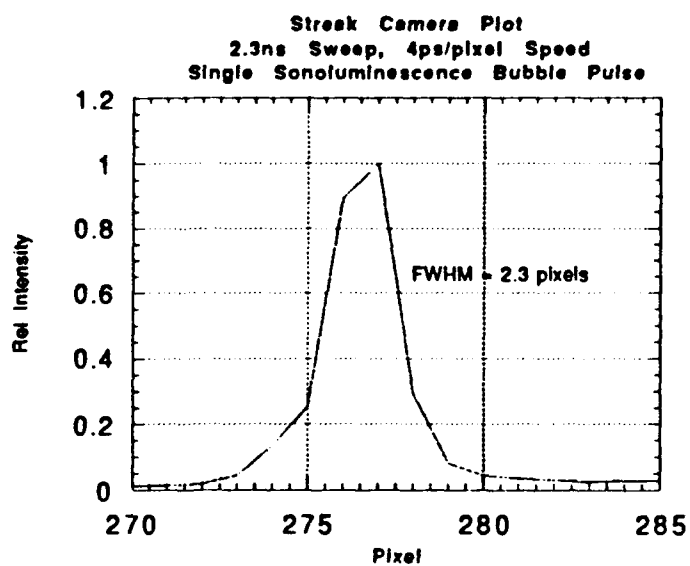
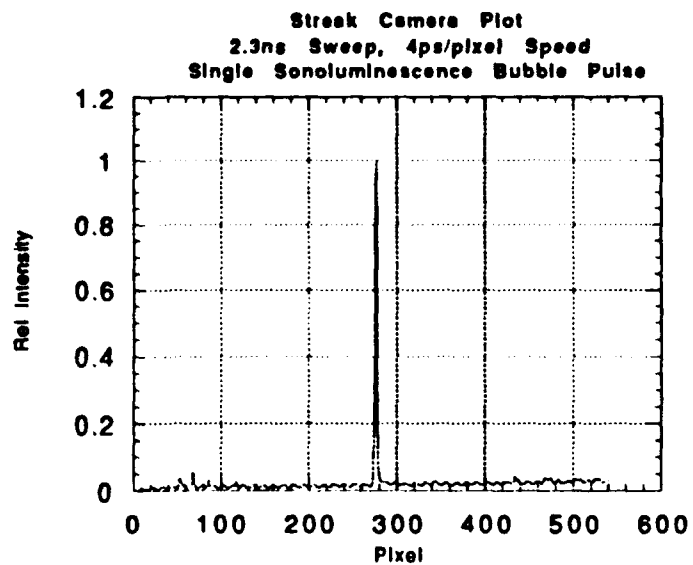


Figure B-12 Single Sonoluminescence Event Streak Camera Image
and Intensity Plots, File #99s4

APPENDIX C. STREAK CAMERA IMAGES AND PLOTS OF ALL DATA USED PRIOR TO ANALYSIS

All figures are reproductions from a video monitor. Figures C-1 through C-10 show the streak camera images and intensity plots of all the data used for analysis given in Table II. Figures C-11 through C-22 show the streak camera images and intensity plots of all the data used for analysis given in Table IV. Figures C-25 through C-27 show the streak camera images and intensity plots of the HeNe laser. Figure C-28 shows the streak camera image and intensity plot of the picosecond pulser. Figures C-29 and C-30 show streak camera images and intensity plots of the SL in the non-streaked mode. All images have been enlarged to show resolution and the graph is a blown up portion of the entire graph to show resolution. The two are not on the same scale. Some images have broad bands through them which are the sides of the rectangular boxes constructed around the SL and that show up on the video monitor.

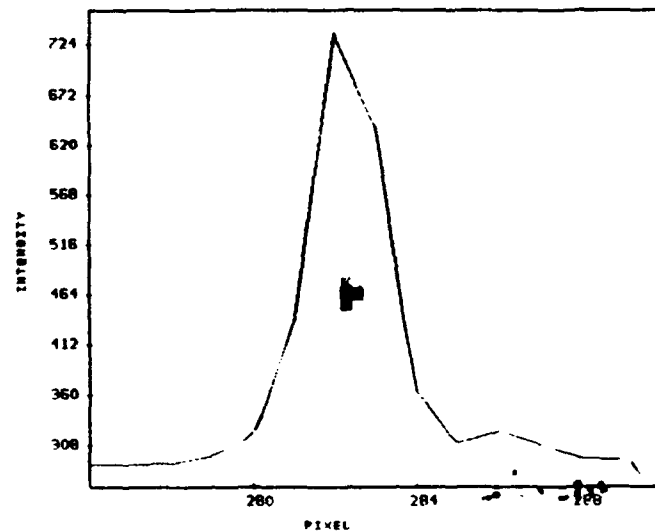


Figure C-1 Single Sonoluminescence Event Streak Camera Image
and Intensity Plot, File #10s2

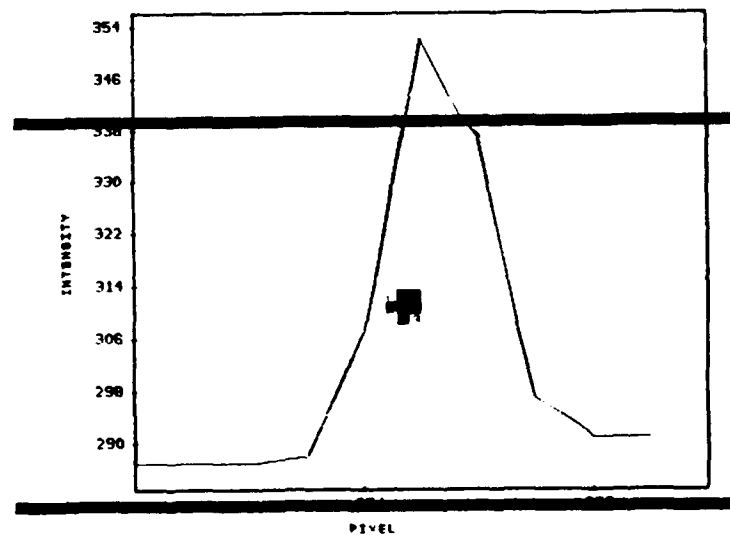


Figure C-2 Single Sonoluminescence Event Streak Camera Image
and Intensity Plot, File #10s3

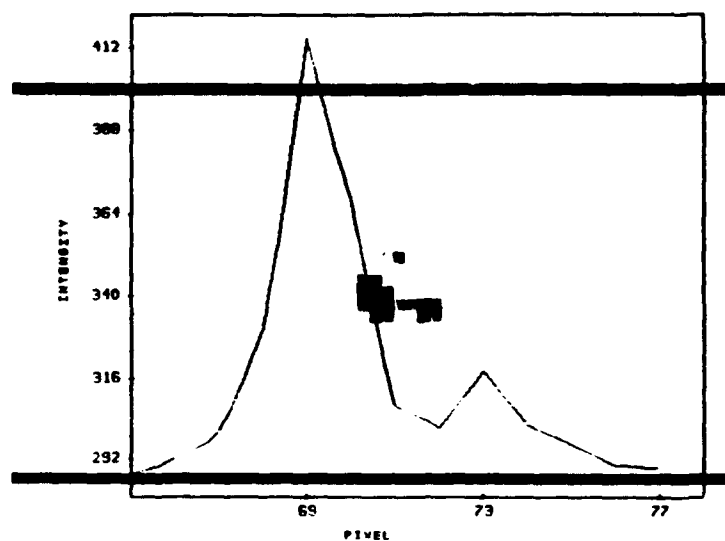


Figure C-3 Single Sonoluminescence Event Streak Camera Image
and Intensity Plot, File #10s5

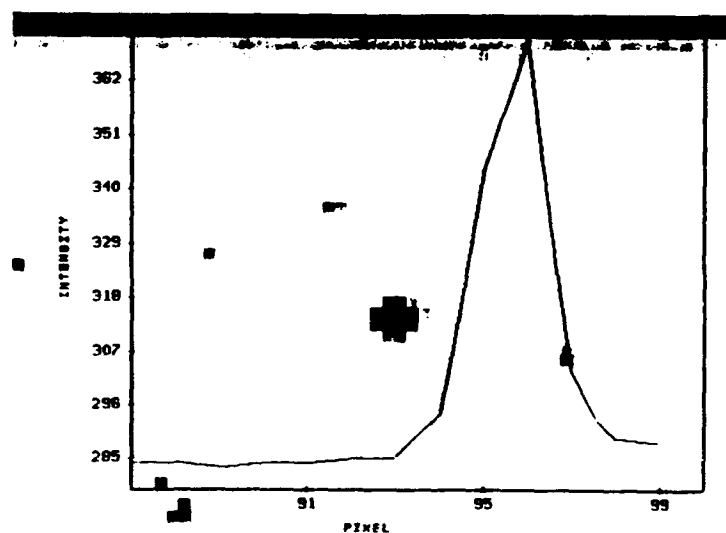


Figure C-4 Single Sonoluminescence Event Streak Camera Image
and Intensity Plot, File #1s2

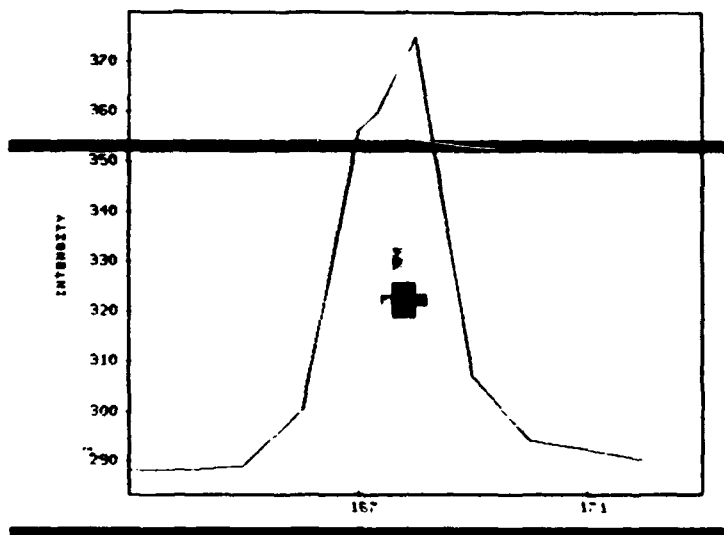


Figure C-5 Single Sonoluminescence Event Streak Camera Image
and Intensity Plot, File #5s1

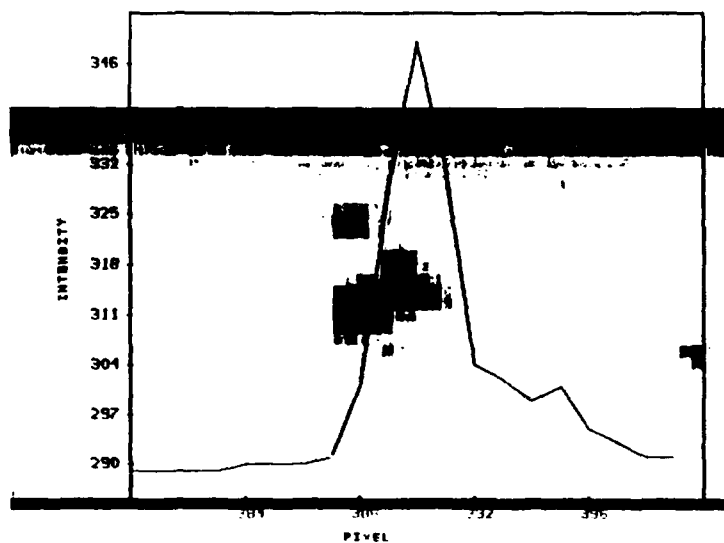


Figure C-6 Single Sonoluminescence Event Streak Camera Image
and Intensity Plot, File #6s1

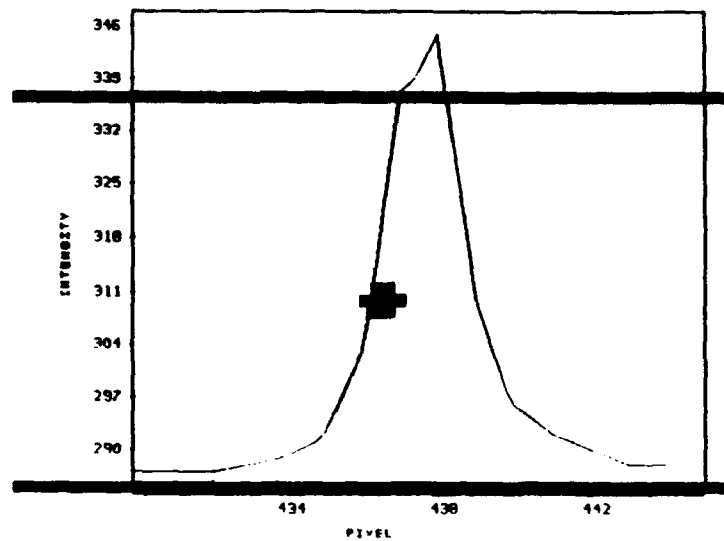


Figure C-7 Single Sonoluminescence Event Streak Camera Image
and Intensity Plot, File #7s4

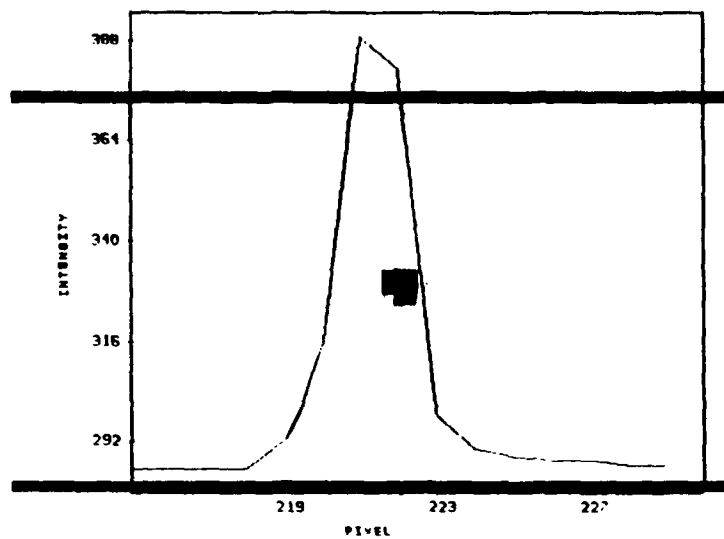


Figure C-8 Single Sonoluminescence Event Streak Camera Image
and Intensity Plot, File #9s1

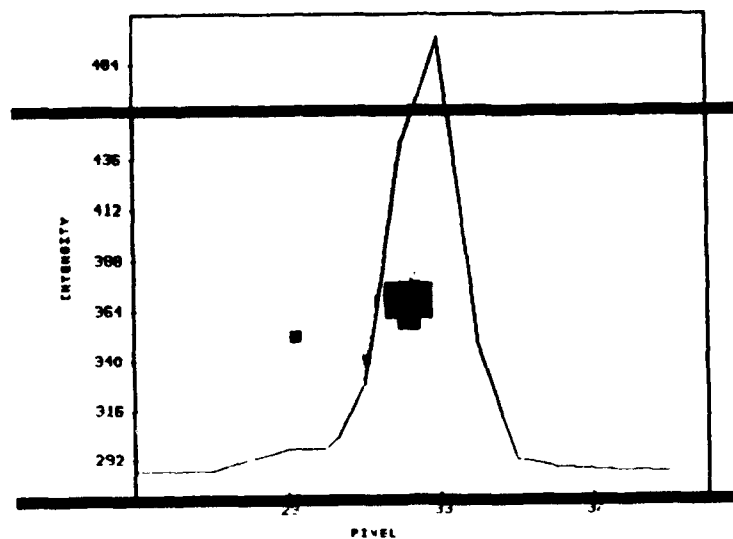


Figure C-9 Single Sonoluminescence Event Streak Camera Image
and Intensity Plot, File #9s4

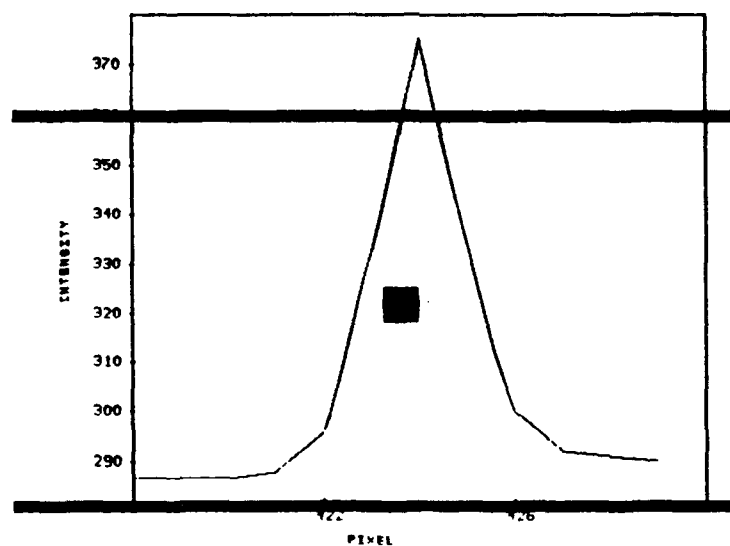


Figure C-10 Single Sonoluminescence Event Streak Camera Image
and Intensity Plot, File #9s5

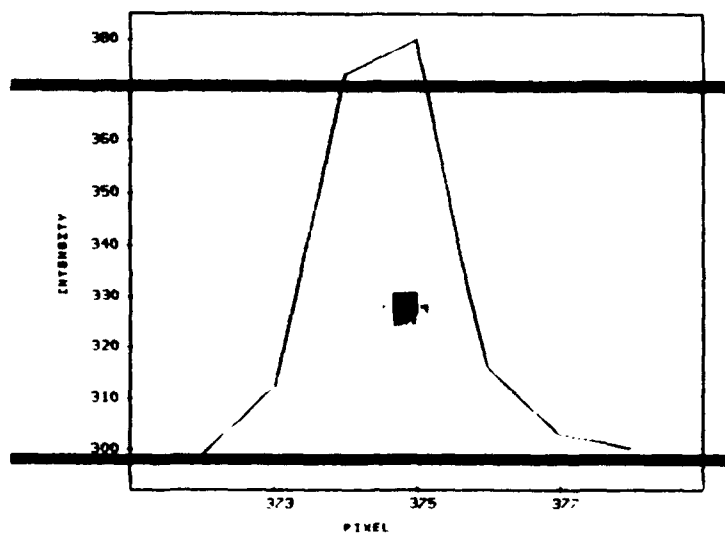


Figure C-11 Single Sonoluminescence Event Streak Camera Image
and Intensity Plot, File #95s1

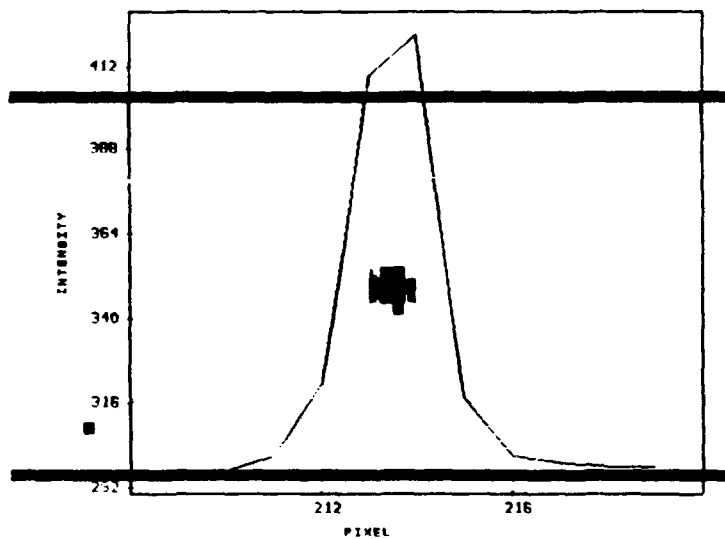


Figure C-12 Single Sonoluminescence Event Streak Camera Image
and Intensity Plot, File #96s1

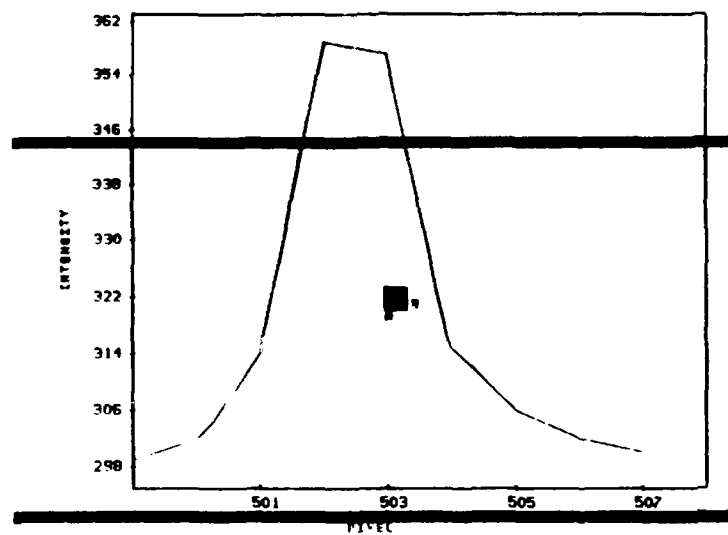


Figure C-13 Single Sonoluminescence Event Streak Camera Image
and Intensity Plot, File #96s2

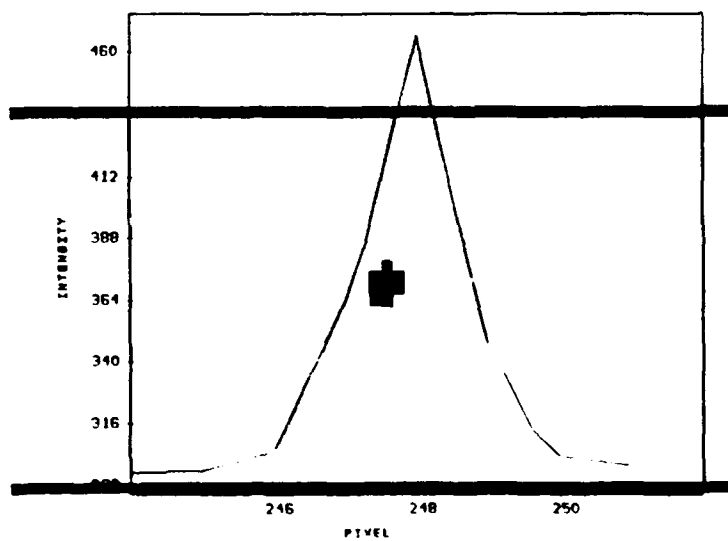


Figure C-14 Single Sonoluminescence Event Streak Camera Image
and Intensity Plot, File #97s1

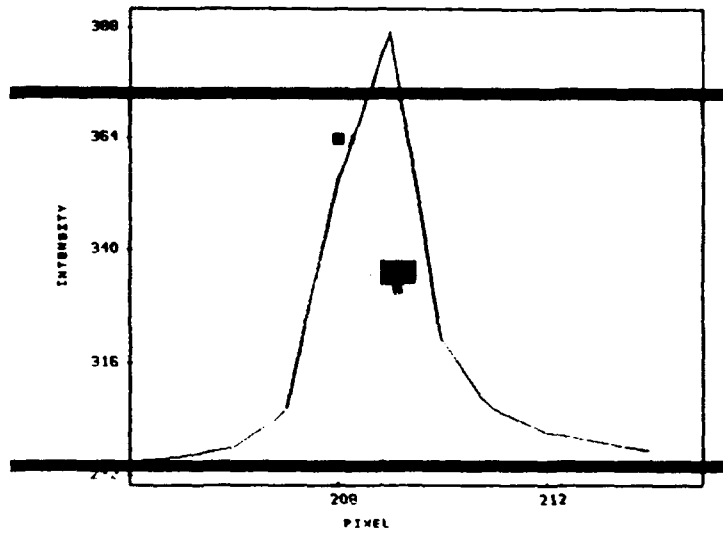


Figure C-15 Single Sonoluminescence Event Streak Camera Image
and Intensity Plot, File #97s2

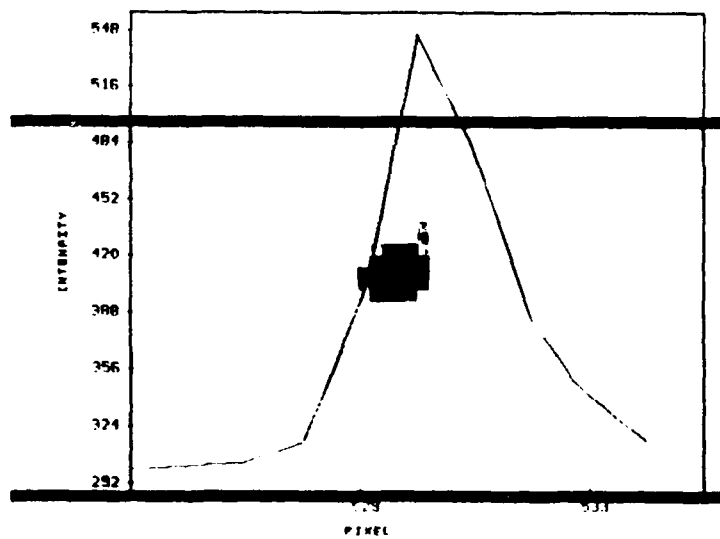


Figure C-16 Single Sonoluminescence Event Streak Camera Image
and Intensity Plot, File #97s3

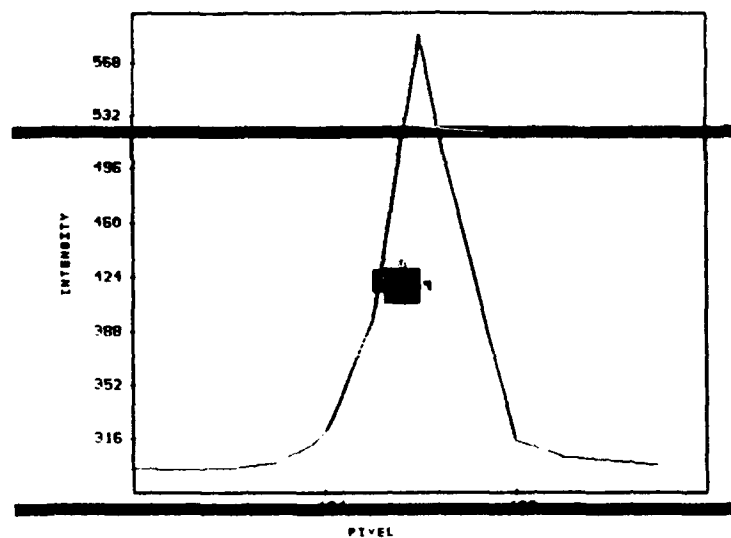


Figure C-17 Single Sonoluminescence Event Streak Camera Image
and Intensity Plot, File #98s1

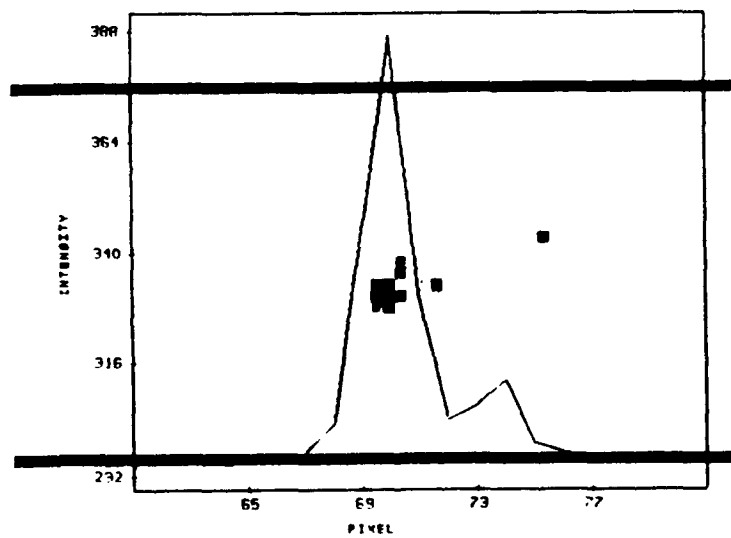


Figure C-18 Single Sonoluminescence Event Streak Camera Image
and Intensity Plot, File #98s2

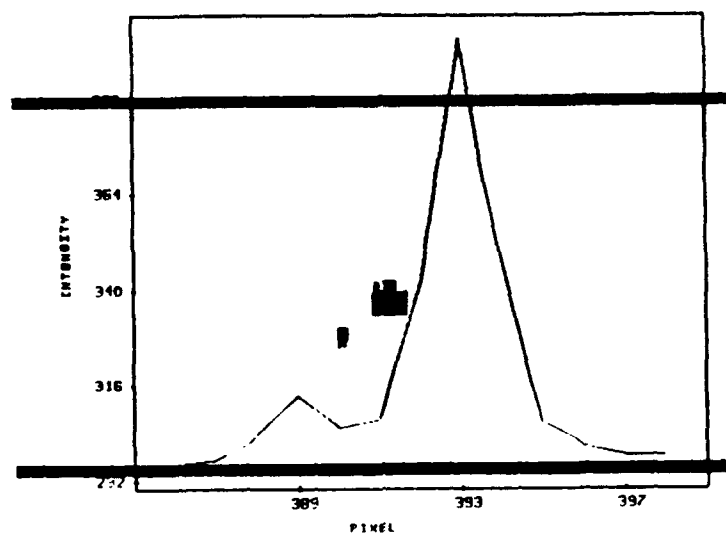


Figure C-19 Single Sonoluminescence Event Streak Camera Image
and Intensity Plot, File #98s3

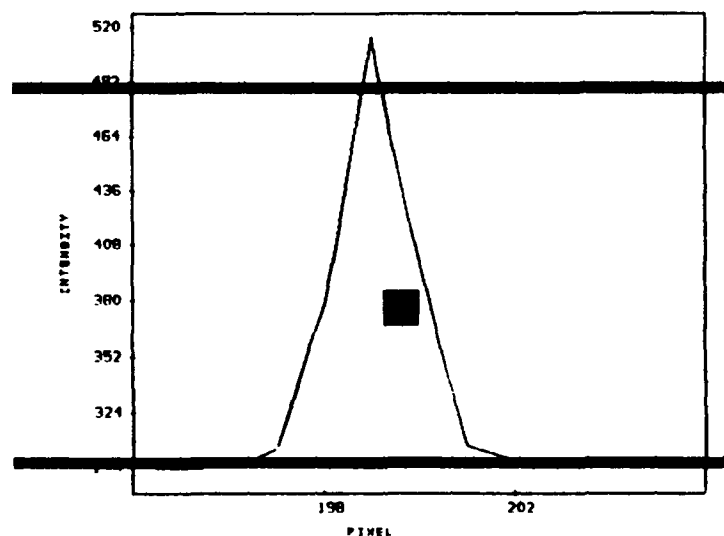


Figure C-20 Single Sonoluminescence Event Streak Camera Image
and Intensity Plot, File #99s1

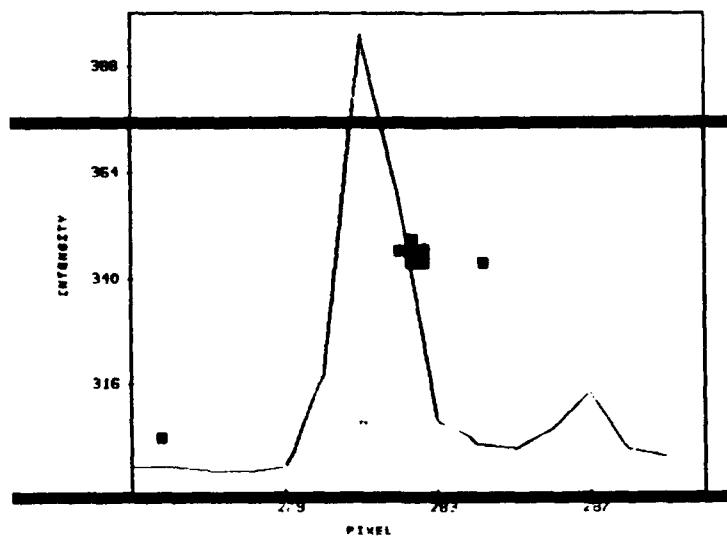


Figure C-21 Single Sonoluminescence Event Streak Camera Image
and Intensity Plot, File #99s3

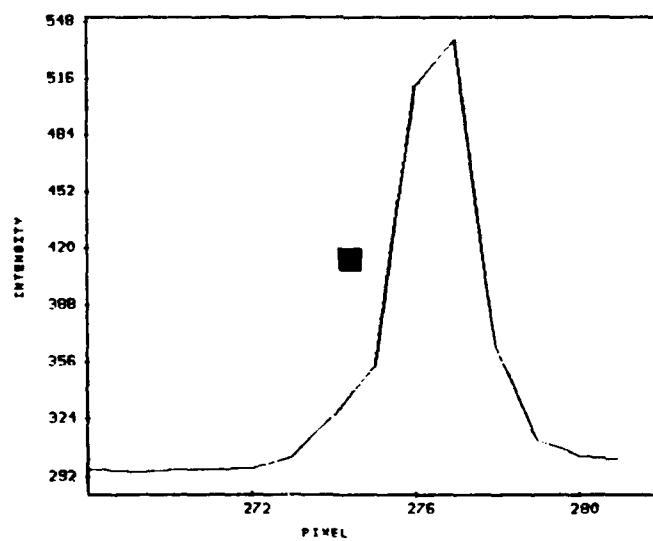


Figure C-22 Single Sonoluminescence Event Streak Camera Image
and Intensity Plot, File #99s4

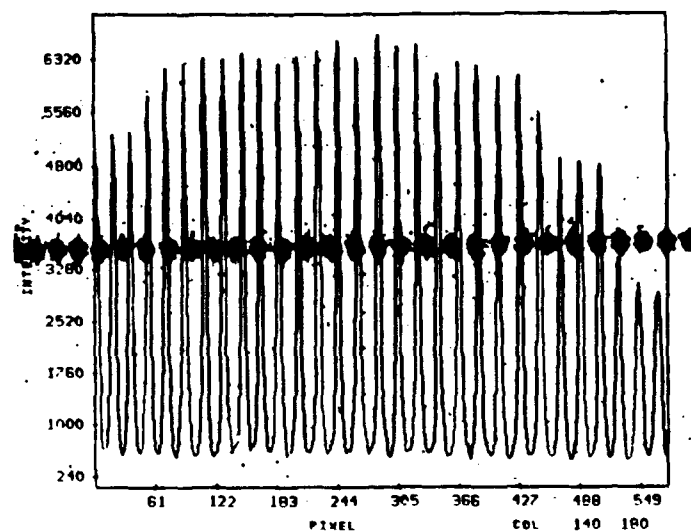


Figure C-23 3 GHz Comb Streak Camera Image and Intensity Plot, File #3GHz

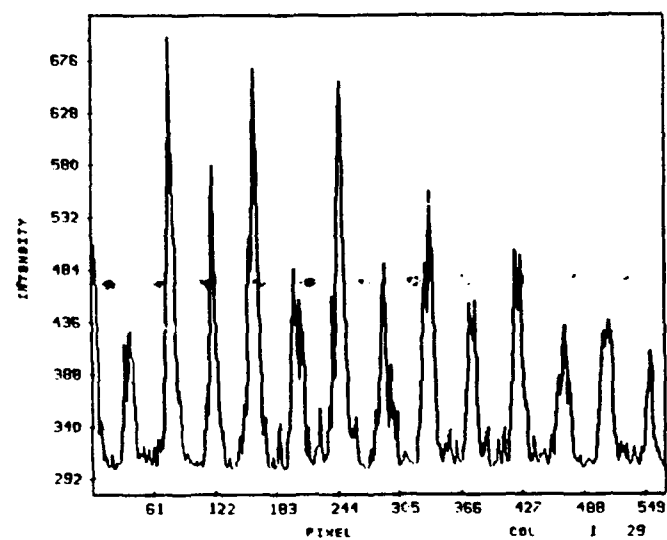


Figure C-24 6 GHz Comb Streak Camera Image and Intensity Plot, File #6GHz

Figure C-25 HeNe Streak Camera Image Normal Size, File #HeNe N

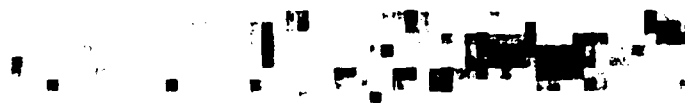


Figure C-26 HeNe Streak Camera Image Zoomed, File #HeNe Z

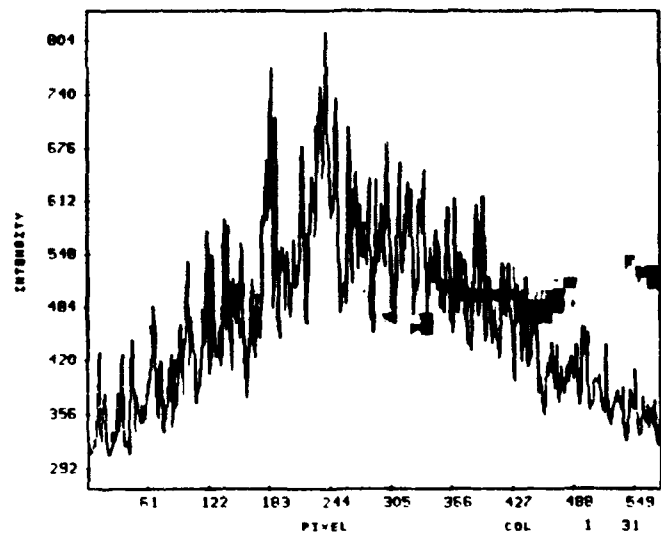


Figure C-27 HeNe Streak Camera Image Zoomed and Intensity Plot, File #HeNe G

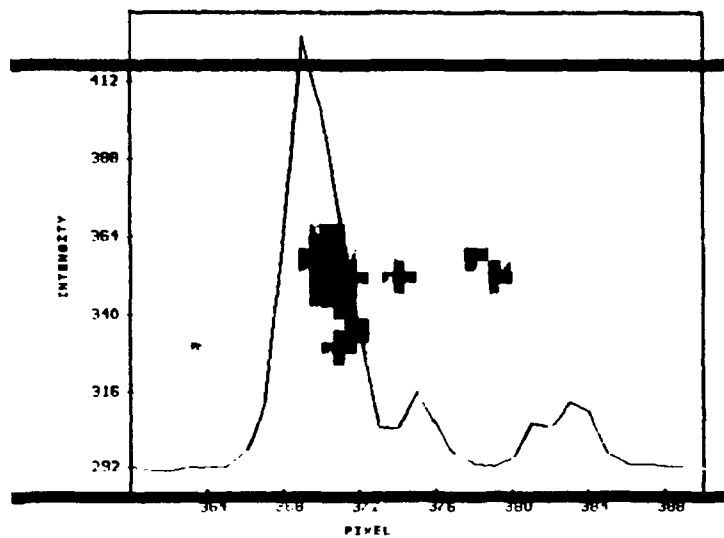


Figure C-28 13 ps Laser Pulser Streak Camera Image and Intensity Plot, File #p8

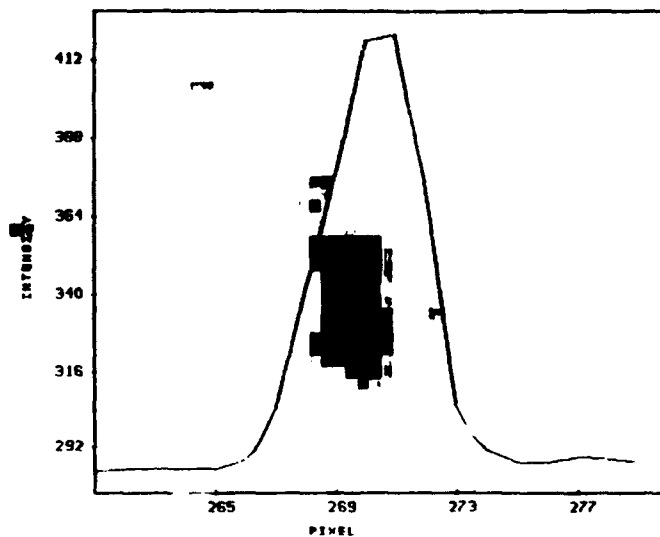


Figure C-29 Single Sonoluminescence Event Non-streaked Streak Camera Image
and Intensity Plot, File #1ns1

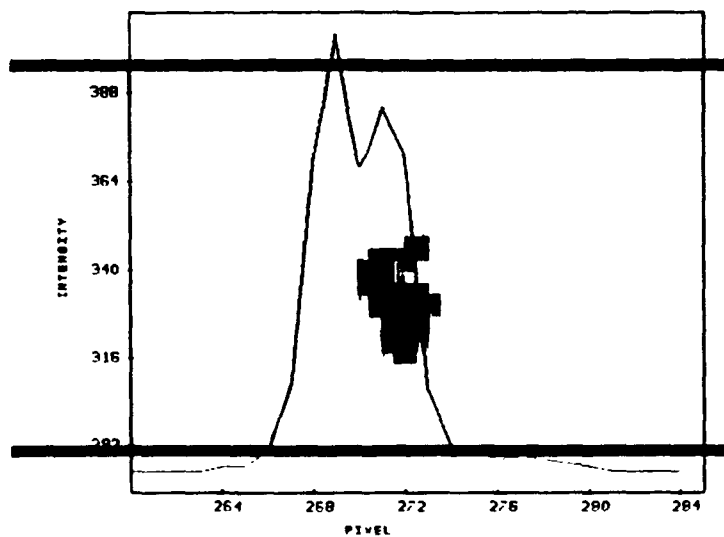


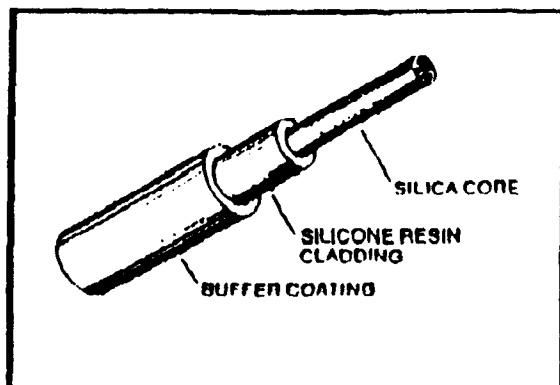
Figure C-30 Single Sonoluminescence Event Non-streaked Streak Camera Image
and Intensity Plot, File #4ns1

APPENDIX D. DATA SHEETS FOR EQUIPMENT

Figures D-1 through D-3 show the available data sheets for the equipment used.

Power-Core Fiber

PCS -- Plastic-Clad Silica



Plastic-Clad Silica Fiber Construction

Applications

- Laser Delivery Systems
 - Medical
 - Industrial
 - Ordnance Initiation
- Short-Haul Data and Video Communications
- Illumination Systems
- Sensing Systems
 - Medical
 - Industrial
 - Spectroscopy

Advantages

- Two cladding types available:
 - Non mechanically strippable clad fiber has a 35°C temperature capability and provides a stable termination with less pistoning. Recommended for crimp and cleave termination systems.
 - Mechanically strippable clad fiber has a 25°C temperature capability and provides easy cladding removal.
- Easy light coupling and low microbend loss due to high numerical aperture.
- Silicone-clad design provides low-cost UV performance superior to hard-clad polymer fibers.
- Both Low- and High-OH fiber designs available, providing a broad spectral transmission range from 220nm to 2400nm.
 - High-OH version provides superior radiation resistance in C₆₀ environments.
- Core, cladding and buffer are USP Class VI approved for non-toxicity and biocompatibility.
- Sterilizable (Radiation, EtO, Steam)
- Custom fiber sizes and coatings are available for specific applications.

Typical Spectral Response

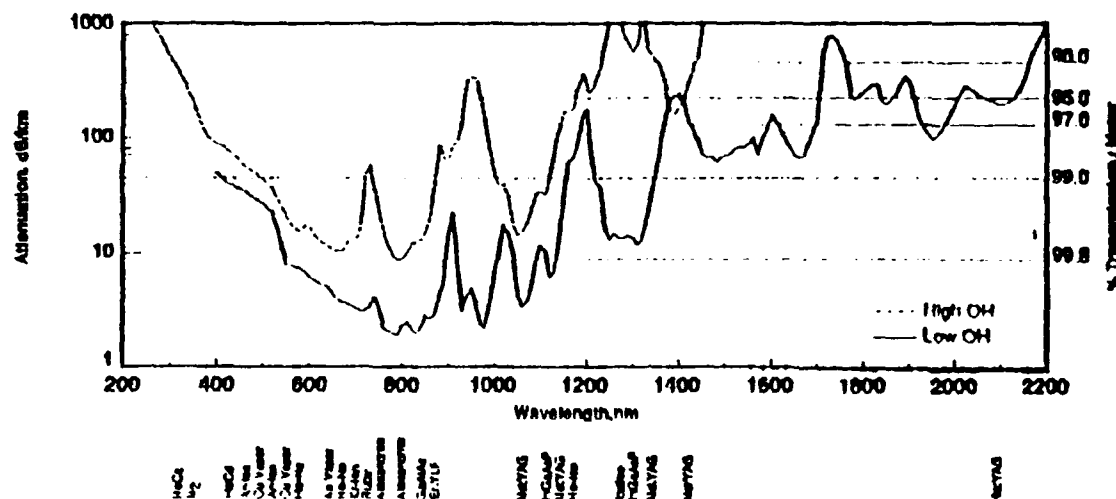


Figure D-1 Fiber Characteristic Data Sheet #1

PCS -- Plastic-Clad Silica

LOW-OH FIBER -- Designed for Visible to Near-IR Transmission

Part Number	Unit	FP-200-LMT	FP-400-LMT	FP-600-LMT	FP-100-LMT
Core Diameter	µm	200 ± 8	400 ± 8	600 ± 10	1000 ± 20
Clad Diameter	µm	380 ± 20	600 ± 30	830 ± 30	1400 ± 50
Buffer Diameter*	µm	600 ± 30	750 ± 30	1050 ± 30	1600 ± 50
Maximum Attenuation @ 820nm	dB/km	8	8	8	8
Bandwidth	MHz·km	20	13	8	—
Nominal Concentricity	%	95	95	95	90
Numerical Aperture†		0.40 ± 0.02	0.40 ± 0.02	0.40 ± 0.02	0.40 ± 0.02
Acceptance Angle (Full)	°	47°	47°	47°	47°
Peak Optical Power Capability‡	MW	1.8	6.3	14.0	64.3
Operating Temperature Range	°C	-35 to +150	-25 to +150	-25 to +150	-25 to +150
Proof Test Level	lpsl	50	40	25	—
Minimum Bend Radius					
— Recommended Short Term	mm	28	75	100†	150†
— Recommended Long Term	mm	40	100	140†	180
— Absolute Short Term§	mm	10	15	25	35
— Absolute Long Term§	mm	20	30	45	65
Standard Lengths	m	1100, 2200	500	300	50

HIGH-OH FIBER -- Designed for UV to Visible Transmission

Part Number	Unit	FP-200-HMT	FP-400-HMT	FP-600-HMT	FP-100-HMT
Core Diameter	µm	200 ± 8	400 ± 8	600 ± 10	1000 ± 20
Clad Diameter	µm	380 ± 20	600 ± 30	830 ± 30	1400 ± 50
Buffer Diameter*	µm	600 ± 30	750 ± 30	1050 ± 30	1600 ± 50
Maximum Attenuation @ 820nm	dB/km	12	12	12	12
Typical Attenuation @ 400nm	dB/km	40	40	40	40
Nominal Concentricity	%	95	95	95	90
Numerical Aperture†		0.40 ± 0.02	0.40 ± 0.02	0.40 ± 0.02	0.40 ± 0.02
Acceptance Angle (Full)	°	47°	47°	47°	47°
Peak Optical Power Capability‡	MW	1.8	6.3	14.0	64.3
Operating Temperature Range	°C	-25 to +150	-25 to +150	-25 to +150	-25 to +150
Proof Test Level	lpsl	50	40	25	—
Minimum Bend Radius					
— Recommended Short Term	mm	28	75	100†	150†
— Recommended Long Term	mm	40	100	140†	180
— Absolute Short Term§	mm	10	15	25	35
— Absolute Long Term§	mm	20	30	45	65
Standard Lengths	m	1100, 2200	500	300	50

* Standard buffer coating is Tefzel® 210
 † 2 meters 50% intensity

‡ Based on 8 GW/cm² for 100 fs laser with 10 ns pulse length.
 § Determined statistically for short gauge length.

Important Notice to Purchasers:

All statements, technical information and recommendations related to the Seller's products are based on information believed to be reliable, but the accuracy or completeness thereof is not guaranteed. Before utilizing the product, the user should determine the suitability of the product for its intended use. The user assumes all risks and liability whatsoever in connection with such use.

Any statements or recommendations of the Seller which are not contained in the Seller's current publications shall have no force or effect unless contained in an agreement signed by an authorized officer of the Seller. THE STATEMENTS CONTAINED HEREIN

ARE MADE IN LIEU OF ALL WARRANTIES, EXPRESS OR IMPLIED, INCLUDING BUT NOT LIMITED TO THE IMPLIED WARRANTIES OF MERCHANTABILITY AND FITNESS FOR A PARTICULAR PURPOSE WHICH WARRANTIES ARE HEREBY EXPLICITLY DISCLAIMED.

Seller shall not be liable to the user or any other person under any legal theory, including but not limited to negligence or strict liability, for any injury or for any direct or consequential damages sustained or incurred by reason of the use of any of the seller's products that were defective.

878 6900-1803 5 Rev. B
 ©1992 3M

Tefzel® is a registered trademark of E. I. DuPont de Nemours & Co.

3M Specialty Optical Fibers
 420 Frontage Road
 West Haven, CT 06516 4190 USA
 (203) 934-7901

3M

Figure D-2 Fiber Characteristic Data Sheet #2

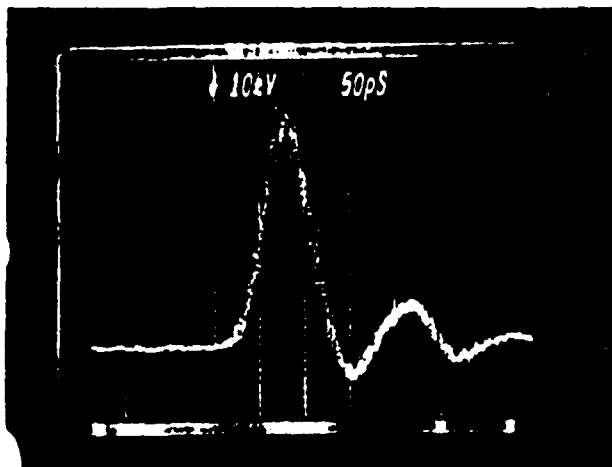
PICOSECOND LASER SYSTEM DATA SHEET

Model: PL-820F Head#: P8F11901 Controller#: P8F11901

Date: Aug 18/89

Sold To: L.L.N.L.

P.O.#: B097687



Oscilloscope Trace

Date tested: Aug 18/89

Oscilloscope: Tektronix 7704 with S4 sampling head (FWHM = 35 ps)

Detector: Antel Optonics AR-S3 coupled in through 30 cm length of 300 nm core fibre (FWHM = 45 ps)

Laser Controller Settings:

Bias Voltage: 250 V

Pretrigger: 75 ns

Repetition Rate: 25 kHz

Ambient Temperature: 21°C

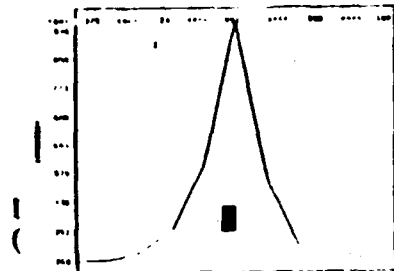
Laser Pulse Response:

Pulse width observed on oscilloscope trace (FWHM): 55 ps

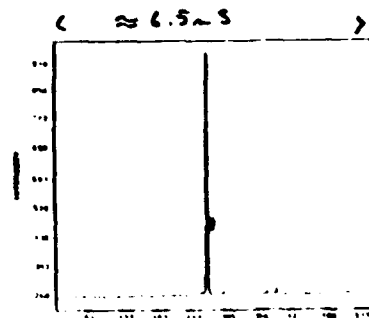
True (deconvoluted) pulsewidth (FWHM): 13 ps as measured by autocorrelator

Center wavelength: 820 nm

Pulse Peak Power (at laser window): 1000 mW



1.7 ps x 6.5 ps = 11 ps



P-14-89
Antel PL 820

Figure D-3 13 Picosecond Pulser Data Sheet

LIST OF REFERENCES

1. N. Marinesco and J.J. Trillat, C.R. Acad. Sci. Paris, V. 196, p. 858, (1933): as referenced by D. Felipe Gaitan, Lawrence A. Crum, Charles C. Church, and Ronald A. Roy, *Sonoluminescence and bubble dynamics for a single, stable, cavitation bubble*, J. Acoust. Soc. Am., V. 91(6), pp. 3166 - 83, 29 January 1992.
2. E. Newton Harvey, *Sonoluminescence and Sonic Chemiluminescence*, J. Am. Chem. Soc., V. 61, pp. 2392 - 8, September 1939.
3. D.F. Gaitan, *An Experimental Investigation of Acoustic Cavitation In Gaseous Liquids*, Ph.D. Dissertation, National Center for Physical Acoustics, University of Mississippi, September 1990.
4. Bradley P. Barber, Robert Hiller, Katsushi Arisaka, Harold Fetterman, and Seth Putterman, *Resolving the picosecond characteristics of synchronous sonoluminescence*, J. Acoust. Soc. Am., V. 91(5), pp. 3061 - 63, May 1992.
5. Figure prepared by Daren Sweider, Center for Microelectronics-Optoelectronics, Lawrence Livermore National Laboratory.
6. *Optical Multi-channel Analyzer*, Image Analysis Program, Marshall Long, LLNL, writer, 1989.
7. *Kaleidegraph*, Version 2.1.3, Data Analysis/Graphic Application Program, Synergy Software, April 1991.
8. E. Hecht, *OPTICS*, Second Edition, Bruce Spatz, editor, Addison-Wesley, p. 175, May 1990.
9. Ref. 8, p. 171.
10. Characteristic data sheet for fiber, 3-m Corporation.
11. Ref. 8, p. 268.
12. *American Institute of Physics Handbook*, Third Edition, Dwight E. Gray, editor, McGraw-Hill Book Company, p. 6-28, 1982 Reissue.

13. Test performed by Daren Sweider, Center for Microelectronics-Optoelectronics, Lawrence Livermore National Laboratory.
14. Figure prepared by Daren Sweider, Center for Microelectronics-Optoelectronics, Lawrence Livermore National Laboratory.
15. Figure prepared by Daren Sweider, Center for Microelectronics-Optoelectronics, Lawrence Livermore National Laboratory.
16. Figure prepared by Daren Sweider, Center for Microelectronics-Optoelectronics, Lawrence Livermore National Laboratory.
17. Figure prepared by Daren Sweider, Center for Microelectronics-Optoelectronics, Lawrence Livermore National Laboratory.
18. Phone conversation between Glenn Coles, 3-M Corporation, West Coast Regional Representative, and the author, 12 October 1993.
19. Figure prepared by Daren Sweider, Center for Microelectronics-Optoelectronics, Lawrence Livermore National Laboratory.
20. Characteristic transmission curve for the fiber used, 3-M Corporation.
21. Joseph T. Carlson, *Visible Spectrum of Stable Sonoluminescence*, Master's Thesis, Naval Postgraduate School, Monterey, California, December 1992.
22. Joseph T. Carlson, *Visible Spectrum of Stable Sonoluminescence*, Master's Thesis, Naval Postgraduate School, Monterey, California, December 1992.
23. Quantum Efficiency curve for the streak camera, given in Figure 14.
24. Ref. 8, p. 171.
25. *Handbook of Chemistry*, Fourth Edition, Lange, editor, Handbook Publishers, Inc., p. 867, 1941.
26. William C. Moss, Douglas B. Clarke, John W. White, *Hydrodynamic Simulations of Bubble Collapse and Picosecond Sonoluminescence*, Lawrence Livermore National Laboratory, UCRL-JC-114748, Preprint, September 1993.

INITIAL DISTRIBUTION LIST

- | | | |
|----|--|---|
| 1. | Defense Technical Information Center | 2 |
| | Cameron Station | |
| | Alexandria, Virginia 22304-6145 | |
| 2. | Library, Code 52 | 2 |
| | Naval Postgraduate School | |
| | Monterey, California 93943-5002 | |
| 3. | Professor William B. Colson, Code PH/Cw | 1 |
| | Chairman, Department of Physics | |
| | Naval Postgraduate School | |
| | Monterey, California 93943-5000 | |
| 4. | Professor Xavier K. Maruyama, Code PH/Mx | 5 |
| | Department of Physics | |
| | Naval Postgraduate School | |
| | Monterey, California 93943-5000 | |
| 5. | Professor Anthony A. Atchley, Code PH/Ay | 2 |
| | Naval Postgraduate School | |
| | Monterey, California 93943-5000 | |
| 6. | Professor D. Holland, Code PH/Ho | 1 |
| | Naval Postgraduate School | |
| | Monterey, California 93943-5000 | |
| 7. | Dr. D. F. Gaitan, Code PH/Gn | 1 |
| | Naval Postgraduate School | |
| | Monterey, California 93943-5000 | |

- | | | |
|------|--|---|
| 8. | Dr. Michael J. Moran
University of California
Lawrence Livermore National Laboratory
P. O. Box 808, L-41
Livermore, California 94551 | 1 |
|
 | | |
| 9. | Dr. Mark E. Lowry
University of California
Lawrence Livermore National Laboratory
P. O. Box 808, L-45
Livermore, California 94551 | 1 |
|
 | | |
| 10. | Ronald Haigh
University of California
Lawrence Livermore National Laboratory
P. O. Box 808, M/S, L-54
Livermore, California 94551 | 1 |
|
 | | |
| 11. | Daren R. Sweider
University of California
Lawrence Livermore National Laboratory
P. O. Box 808, L-44
Livermore, California 94551 | 2 |
|
 | | |
| 12. | William Moss
University of California
Lawrence Livermore National Laboratory
P. O. Box 808, L-200
Livermore, California 94551 | 1 |
|
 | | |
| 13. | Gary R. Abel
2103 Clydesdale Court
Fallston, Maryland 21047 | 1 |